Thesis for Degree of Doctor of Philosophy

Mass spectrometry based analysis of drugs, neurotransmitters and lipids in invertebrate model systems

Nhu Phan

UNIVERSITY OF GOTHENBURG

Department of Chemistry and Molecular Biology
University of Gothenburg
Gothenburg, Sweden
2015

Mass spectrometry based analysis of drugs, neurotransmitters and lipids in invertebrate model systems

Nhu Phan

Department of Chemistry and Molecular Biology
University of Gothenburg
SE-412 96 Göteborg
Sweden

Cover picture: Schematic of ionization process in SIMS for imaging Drosophila brain and C. elegans

ISBN: 978-91-628-9535-8
http://hdl.handle.net/2077/40045

Printed by Aidla Trading AB (Kompendiet AB)
Göteborg, Sweden, 2015

ABSTRACT

Mass spectrometry (MS) is one of the most universal analytical techniques due to its label-free detection principle and high chemical specificity, high selectivity, and sensitivity. MS is diverse with many different types of systems to meet different analytical demands from various research areas. MS can be used for bulk analysis, in particular when coupled with a separation tools such as capillary electrophoresis or liquid chromatography, provides highly accurate qualitative and quantitative information of sample compositions. Imaging mass spectrometry (IMS), on the other hand, allows for imaging the chemical structures in intact samples with impressive spatial resolution (< micron). In this thesis, MS is used for two main objectives. First, MS is used to investigate the concentration at the site of action of methylphenidate (MPH), and its neurological effects on the nervous system of *Drosophila melanogaster* (fruit fly). MPH, which is a common medical drug for attention deficit hyperactivity disorder and an alternative drug to replace cocaine during the process of quitting drug abuse, has a stimulant action similar to cocaine as it also binds to the dopamine transporter protein and thereby increases the concentration of extracellular dopamine, a neurotransmitter, in the mammalian nervous system. It has recently been evidence that MPH exhibits neurological impact in long-term use; however, the details of this disorder are not fully understood. *Drosophila* has been chosen as a model for these studies owing to its short life cycle, prolific reproduction, and highly conserved physiological effects with humans, especially in drug addiction. The second main objective of the thesis is to develop MSI methods for biomolecular imaging of tissue samples including *Drosophila* brain and *C. elegans*. Multimodal imaging with secondary ion mass spectrometry (SIMS) and laser desorption ionization mass spectrometry (LDI MS) of the fly brain provide complementary biomolecular information of the brain structure. The molecular signature of *C. elegans*, one of the primary biological models used today, is very useful for studies of cellular processes and can be related to behavior of the worm.

In paper I, the in vivo concentration of MPH in *Drosophila* brain after oral administration was determined by capillary electrophoresis mass spectrometry (CE-MS). The information was then applied to study the effects of methylphenidate treatment on the action of cocaine on dopamine uptake in vivo in *Drosophila*. In paper II, capillary electrophoresis mass spectrometry was extensively used for qualitative and quantitative analysis of orally administrated methylphenidate and metabolites as well as evaluation of the drug-dose dependency of neurotransmitter concentrations in the fly brain. In paper III, an imaging protocol for *Drosophila* brain with SIMS, including sample preparation, data treatment with image-based principle components analysis, and continuous imaging was developed. The imaging protocol was applied in paper IV to investigate lipid structural effects of MPH on *Drosophila* brain. The distribution and biological functions of biomolecules in the fly brain are studied using a combination of SIMS and SEM imaging. In addition, it is demonstrated that oral administration of MPH significantly alters the distribution

and abundance of various brain lipids. Paper V presents a multimodal imaging approach to *Drosophila* brain for lipid detection using matrix assisted laser desorption ionization (MALDI). Different surface modifications, including matrix sublimation and nanoparticle deposition, show specific detectable lipids and therefore can be used in a complementary fashion to profile biological samples. In paper VI, the chemical anatomy of *C. elegans* is studied using SIMS imaging. Two-dimensional and three-dimensional approaches are used for worm sections and the whole worm, respectively.

SAMMANDRAG

Masspektrometri (MS) är en av de mest universella analysteknikerna på grund av dess icke-riktade sätt, höga kemisk specificitet, höga selektivitet och känslighet. MS mångfacetterad teknik med många olika typer av system för att möta olika analytiska krav från olika forskningsområden. MS kan användas för bulkanalys kan sammankopplas med separationsverktyg såsom kapillärelektrofores eller vätskekromatografi, vilket ger mycket exakt kvalitativ och kvantitativ information av provkompositioner. Avbildande masspektrometri (IMS) kan användas för att avbilda den kemiska strukturen hos intakta prover med imponerande rumslig upplösning (<mikrometer). I denna avhandling är används MS för två huvudsyften; Först används MS för att undersöka koncentrationen vid verkningsplatsen för metylfenidat (MPH), och dess neurologiska effekter på nervsystemet hos *Drosophila* melanogaster (bananfluga). MPH, en vanlig behandlingsform för Attention Deficit Hyperactivity Disorder samt är ett alternativt läkemedel vid kokainabstinens, har en stimulerande verkan som liknar kokain eftersom det också binder till dopamintransportören och ökar extracellulärt dopamin, en signalsubstans i nervsystemet hos däggdjur. Det har nyligen bevisats att MPH uppvisar neurologiska effekter vid långvarig användning; dock är dessa effekter inte helt klarlagda. *Drosophila* har här valts som en modell för dessa studier på grund av sin korta livscykel, produktiva reproduktion, och högt-konserverade fysiologiska effekter likt människan, särskilt gällande narkotikamissbruk. Det andra syftet med avhandlingen är att utveckla IMS metoder för biomolekyläravbildning av vävnadsprover, inklusive *Drosophila* hjärna och *C. elegans*. MALDI-avbildning av flughjärnan ger kompletterande biomolekylär information om hjärnans struktur. Den molekylära profilen hos *C. elegans*, en av de främsta biologiska modeller som används i dag, är mycket användbart för studier av cellulära processer och kan vara direkt relaterade maskens beteende.

I artikel I, bestämdes in vivo koncentrationen av MPH i *Drosophila* hjärnan efter oral administrering genom kapillärelektrofores-masspektrometri (CE-MS). Koncentrationen applicerades sedan för att studera effekterna av hur metylfenidat-behandling influerar kokains påverkan på dopaminupptag in vivo i *Drosophila*. I artikel II, används kapillärelektrofores-masspektrometri för kvalitativ och kvantitativ analys av oralt administrerat metylfenidat och dess metaboliter samt utvärdering av läkemedel/dos-förhållandet i relation till neurotransmitterkoncentrationer i flughjärnan. I artikel III, utvecklades protokoll för avbildning av *Drosophila* hjärnan med sekundärjon-masspektrometri (SIMS) inkluderande provberedning, databehandling med bildbaserad principalkomponentanalys samt konsekutiv avbildning. Detta bildprotokoll tillämpades i artikel IV för att undersöka strukturella effekterna av MPH på lipider i *Drosophila* hjärnan. Distribution och biologiska funktioner biomolekyler i flughjärnan studeras med hjälp av en kombination av SIMS och svepelektronmikroskopavbildning. Dessutom visas att oral administrering av MPH avsevärt förändrar distributionen och förekomsten av olika lipider i hjärnan. Artikel V presenterar en multimodal avbildningsteknik av *Drosophila* hjärnan för att upptäcka lipider med hjälp av matris-assisterad laserdesorptions-jonisering(MALDI). Olika

ytmodifieringar inklusive matrissublimering och nanopartikeldeponering visar specifika detekterbara lipider och därför denna teknik kan användas på ett kompletterande sätt till SIMS för att profilera biologiska prover. I papper VI, studeras den kemiska anatomi *C. elegans* med hjälp SIMS avbildning. Två-dimensionella och tre-dimensionella metoder används för att studera snitt av masken samt masken i sin helhet.

TABLE OF CONTENTS

LIST OF PUBLICATIONS

Paper I. *Oral administration of methylphenidate blocks the effects of cocaine on uptake at the Drosophila dopamine transporter.* E. Carina Berglund, Monique A. Makos, Jacqueline D. Keighron, **Nhu T.N. Phan**, Michael L. Heien, and Andrew G. Ewing. ACS Chemical Neuroscience, 2013, 4 (4), 566-574. DOI: 10.1021/cn3002009.

Paper II. *Capillary electrophoresis-mass spectrometry-based detection of drugs and neurotransmitters in Drosophila brain*. **Nhu T. N. Phan**, Jörg Hanrieder, E. Carina Berglund, Andrew G. Ewing. Analytical Chemistry, 2013, 85 (17), 8448-8454. DOI: 10.1021/ac401920v.

Paper III. *ToF-SIMS imaging of lipids and lipid related compounds in Drosophila brain.* **Nhu T. N. Phan**, John S. Fletcher, Peter Sjövall, and Andrew G. Ewing. Surface Interface Analysis, 2014, (46), 123-126. DOI: 10.1002/sia.5547.

Paper IV. *Lipid structural effects of oral administration of methylphenidate in Drosophila brain by secondary ion mass spectrometry imaging*. **Nhu T. N. Phan**, John S. Fletcher, and Andrew G. Ewing. Analytical Chemistry, **2015**, *87* (8), 4063–4071. DOI: 10.1021/acs.analchem.5b00555.

Paper V. *Laser desorption/ionization mass spectrometry imaging of Drosophila brain using matrix sublimation versus modification with nanoparticles*. **Nhu T. N. Phan**, Amir S. Mohammadi, Masoumeh D. Pour, and Andrew G. Ewing. Submitted.

Paper VI. *Chemical anatomy of C. elegans with 2D and 3D imaging using ToF-SIMS*. **Nhu T. N. Phan**, Manish Rauthan, Marc Pilon, and John S. Fletcher. Manuscript in preparation.

RELATED PUBLICATIONS NOT INCLUDED IN THIS THESIS

Paper VII. *Mass spectrometry imaging of freeze-dried membrane phospholipids of dividing Tetrahymena pyriformis.* Ingela Lanekoff, **Nhu T. N. Phan**, Craig T. Van Bell, Nicholas Winograd, Peter Sjövall, and Andrew G. Ewing. Surface and Interface Analysis, 2013, 45 (1), 211-214. DOI: 10.1002/sia.5017.

Paper VIII. *Imaging mass spectrometry in neuroscience*. Jörg Hanrieder, **Nhu T. N. Phan**, Michael E. Kurczy, and Andrew G. Ewing. *ACS Chemical Neuroscience*, 2013, *4* (5), 666–679. DOI: 10.1021/cn400053c.

Paper IX. *Imaging mass spectrometry for single cell analysis*. **Nhu T. N. Phan**, John S. Fletcher, Andrew G. Ewing. Elsevier Reference Module in Chemistry, Molecular Sciences and Chemical Engineering. Waltham, MA: Elsevier 2014. DOI: 10.1016/B978-0-12-409547-2.11022-4.

Paper X. *Complementary lipid imaging and analysis of mouse brain samples using nanoparticle-laser desorption ionization and high energy argon cluster secondary ion mass spectrometry*. Amir Saeid Mohammadi, **Nhu T.N. Phan**, John S. Fletcher, and Andrew G. Ewing. Submitted.

CONTRIBUTION REPORT

Paper I. I was involved in planning the project and updating the progress of the project with Carina Berglund and Andrew Ewing. I took the main role in designing, performing mass spectrometric experiments and analyzing data with help from Ingela Lanekoff at the start. I participated in discussions and writing parts of the paper.

Paper II. I was involved in planning the project with collaborators. I discussed experimental issues with Jörg Hanrieder and performed the experiments. I was responsible for analyzing data and writing the paper.

Paper III. I was involved in planning and designing the project with collaborators. I performed experiments and analyzed data with help from John Fletcher. I was responsible for writing the paper.

Paper IV. I was involved in planning and designing the project with collaborators. I performed experiments with help from John Fletcher. I was responsible for analyzing data and writing the paper.

Paper V. I was involved in planning and designing the project with collaborators. I performed and coordinated experiments with Amir Mohammadi and Masoumeh Dowlatshahi Pour. I was responsible for analyzing data and writing a major part of the paper.

Paper VI. I was involved in planning and designing the project with collaborators. I performed experiments with help from Manish Rauthan on the culturing of *C. elegans*. I was responsible for analyzing data and writing the manuscript.

LIST OF ABBREVIATIONS

Abbreviations commonly used in the thesis:

AA - Arachidonic acid
ADHD - Attention deficit hyperactivity disorder
AuNP - Gold nanoparticle
CE - Capillary electrophoresis
CE-MS - Capillary electrophoresis mass spectrometry
CHCA - α-cyano-4-hydroxycinnamic acid
DAG - Diacylglycerol
DHB - Dihydroxybenzoic acid
EOF - Electroosmotic flow
ESI - Electrospray
GABA - γ-aminobutyric acid
GCIB - Gas cluster ion beam
HPLC - High performance liquid chromatography
IMS - Imaging mass spectrometry
LDI - Laser desorption ionization
LMIG - Liquid metal ion gun
MALDI - Matrix-assisted laser desorption ionization
MIMS - Multiple-isotope imaging mass spectrometry
MPH - Methylphenidate
MS - Mass spectrometry
NADA - N-acetyldopamine
NAOA - N-acetyloctopamine
NP - Nanoparticle
PC - Phosphatidylcholine
PE - Phosphatidylethanolamine
PI - Phosphatidylinositol
PLA - Phospholipase A
PLC - Phospholipase C
PLD - Phospholipase D
SALDI - Surface assisted laser desorption ionization
SEM - Scanning electron microscopy
SIMS - Secondary ion mass spectrometry
TAG - Triacylglycerides
TFA - Trifluoroacetic acid
ToF - Time of flight

CHAPTER 1. NEUROTRANSMITTERS, NEUROTRANSMISSION IN THE BRAIN, AND ACTIONS OF PHSYCHOSTIMULANTS IN THE NERVOUS SYSTEM

1.1. Neurons

The brain is the most complex organ and controls every part of the body, from the biological processes of a single cell to the functioning of an organelle, from physical motions to cognition processes, thought, perception, and emotion. In order to efficiently control the whole body, the brain possesses a very complicated communication network called the neuronal network. The human brain contains a billion neurons in this network. Within the network, one neuron can communicate with up to a thousand other neurons.[1] Two neurons typically connect to each other via a structure called a synapse, which is a gap of about 12-20 nm between the end of one neuron and the start of another.[2] A schematic of a neuron and the synaptic junction is shown in Figure 1. The synapse is a very important feature as it is the region where many molecular regulators localize to facilitate the selective and efficient transfer of a signal from one cell to the next. It is also the accessible region for exogenous compounds to alter the synaptic properties of the neuronal signaling.

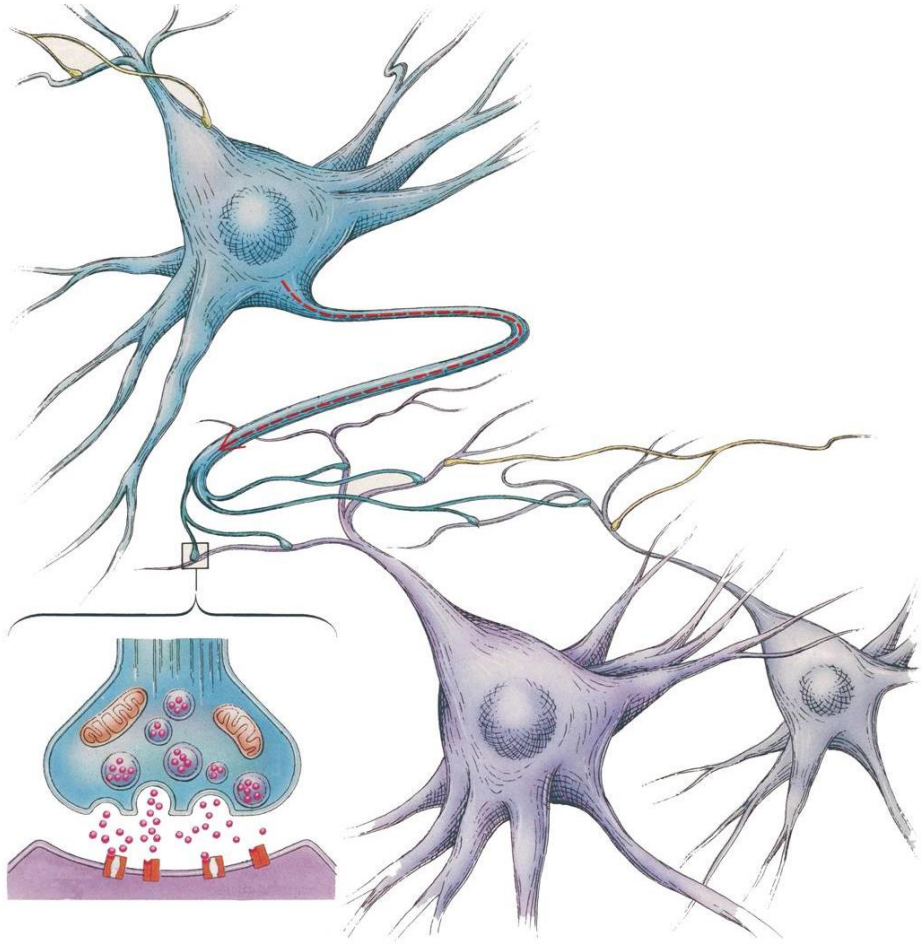

Figure 1. The neuron and synapse.[3]

Neurons come in many different shapes, typically consisting of three main parts: the dendrites, a cell body, and an axon with the axon terminals.[1] The cell body contains the nucleus and organelles to synthesize the neuronal materials such as proteins, and membrane lipids, as well as to develop organelles. The dendrites are typically, but not always, thought to receive signals and these are branched out to interact with the synapses from often many other cells. These dendrites then carry signals to the cell body. At the cell body, chemical signals received from presynaptic neurons and converted into small electrical impulses are integrated and form larger potentials called action potentials, which travel along the axon to the axon terminals to trigger exocytosis for further neuronal communication. The axon is a long extension from the cell body to other cells, often the dendrites of the next cells in the communication loop, and these are used to transmit the action potential. There is typically only one axon for a neuron. The axon can be either unmyelinated or myelinated- where the axon is periodically covered by a nonconductive myelin layer.[4] The myelination helps speed up the transmission of the action potential by up to 100 meters per second from the cell body to the terminal. Neurons with myelinated axons are found mainly in the peripheral and central nervous systems.

1.2. Neurotransmission

In the brain, neurons "talk" to each other on a millisecond time scale to transfer signals and responses between neurons and to other target cells. This communication process is called neurotransmission. In the terminal of a presynaptic neuron, chemicals called neurotransmitters are packed in small spherical packages made of lipid bilayers and integrated proteins called vesicles (see Figure 1 above). When the terminal of a cell receives an action potential, Ca^{2+} channels open to allow Ca^{2+} ions to diffuse from the outer into the inner part of the cell caused by depolarization of the presynaptic cell membrane and regulation of voltage gated calcium channels. The increase in calcium causes vesicles containing neurotransmitters that are close to the terminal to fuse with the cell membrane thereby releasing neurotransmitters. These transmitter substances diffuse into the synaptic space and subsequently bind to specific receptors on the postsynaptic neurons or target cells. The postsynaptic cells then generate (or inhibit) their own action potential leading to signal propagation from one neuron to the next, or a number of cellular processes in non-neuronal target cells. After transferring the signal, neurotransmitters detach from the receptors and are removed from the synapse by reuptake into presynaptic neurons, nearby cells, or are degraded by enzymatic reactions.

1.3. Neurotransmitters

Neurotransmitters are endogenous chemicals used to transfer the signals from presynaptic to postsynaptic cells. Neurotransmitters are like the "language" for neuronal communication. There are several common criteria to define neurotransmitters.[5-6] According to Purves *et al.*[5], a neurotransmitter is at first a substance that must be endogenous in the presynaptic neuron. Second, it is released from the presynaptic neuron in response to presynaptic electrical activation. Third, there is a specific receptor for this substance at the postsynaptic neurons or cells.

Neurotransmitters have two main effects on the receptor cell, excitatory or inhibitory. Some can have both effects depending on the kind of receptors.[7] The effect is excitatory if the membrane of the receptor cell decreases in potential to get closer to the threshold for generation of an

action potential to continue communication. The effect is inhibitory if the membrane potential is clamped at or increased above the resting potential so that the threshold potential is not attained and propagation of an action potential cannot take place. The resting and action potentials in a neuron are demonstrated in Figure 2.

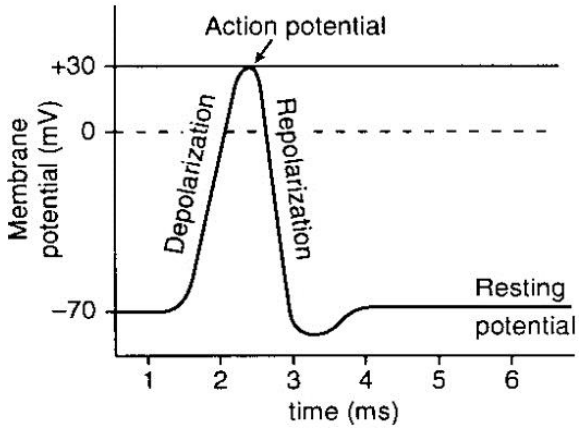

Figure 2. Resting and action potentials in a neuron

Like there are a variety of words or expressions used in human communication, neurons have many different neurotransmitters. The classification of neurotransmitters has been varied based on different aspects such as the size, postsynaptic actions, or chemical structure. According to Purves *et al.*,[5] there are two main categories based on the size of neurotransmitters, small molecule neurotransmitters and peptide neurotransmitters. Within the former one, there are several subgroups based on their chemical structure including acetylcholine, amino acids, biogenic amines, and purines. The classification of neurotransmitters is presented in more detail in Table 1.

Neurotransmitters play a crucial role in maintaining the proper functioning of the brain. Each of them is involved in regulating specific neurological and physiological processes in the nervous system. Imbalance of neurotransmitter levels in the brain is the main cause of a number of brain diseases and disorders, for instance the well-known Parkinson's disease, Alzheimer's disease, epilepsies, schizophrenia, depression, anxiety, sleep disorder, and drug addiction.[8]

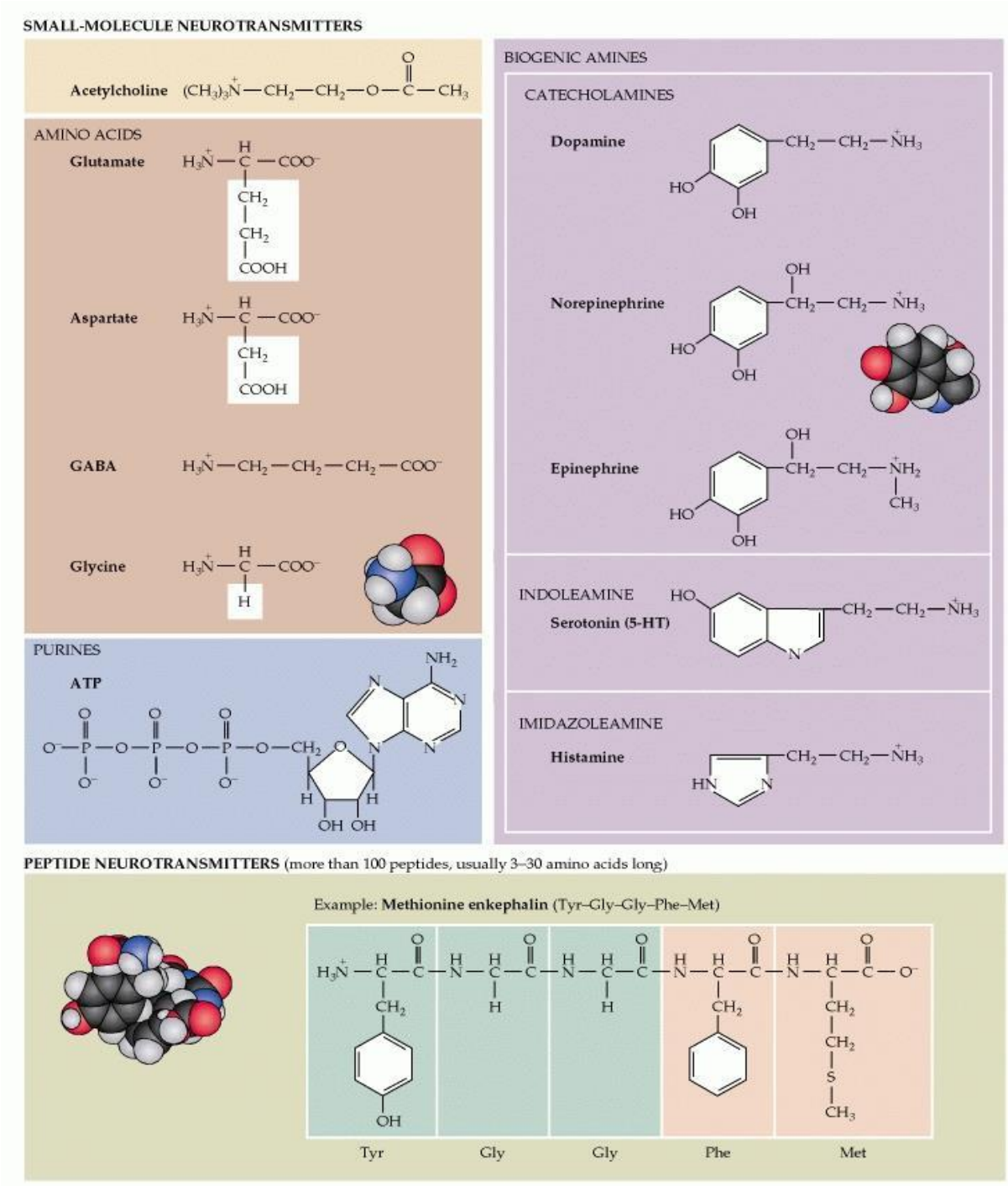

Table 1. Classification of neurotransmitters.[5]

1.3.1. Dopamine

The discovery and pioneering research of dopamine by Arvid Carlsson and Paul Greengard was awarded the Nobel Prize in Physiology and Medicine in 2000.[9] Dopamine is an important neurotransmitter belonging to the catecholamine group. This monoamine is involved in mediating motor function, olfactory processes, cognition, reward and reinforcement, learning and memory. There are around 400 000 dopaminergic neurons in the human brain localizing mainly in the substantia nigra.[10] Dopamine receptors are trans-membrane G-protein coupled protein receptors. There are five types of dopaminergic receptors classified into two main subgroups, D1-like, which includes D1 and D5; and D2-like, which includes D2, D3, and D4.[7]

The classification is based on the structure, biochemical and pharmacological properties of the receptors. Depending on the type of receptor, dopamine can exhibit excitatory or inhibitory effects. For instance phospholipase C (PLC), an enzyme for the hydrolysis of membrane lipid phosphatidylinositol 4,5-biphosphate to produce second messenger diacylglycerol (also known as diacylglyceride) and inositol 1,4,5,-triphosphate, was found to be activated by D1 receptors; however, it is inhibited by activation of the D5 receptor. Dopamine also exerts its effects on many different cellular processes by altering the properties of G-proteins, the activities of enzymes and ion channels. The biosynthesis of dopamine originates from the hydroxylation of tyrosine by the cytoplasmic enzyme tyrosine hydroxylase forming L-3,4-dihydroxyphenylalanine (L-DOPA). The product is then decarboxylated by cytoplasmic DOPA decarboxylase to produce dopamine prior to being packaged in transmitter vesicles via the vesicle monoamine transporter. After transmission, metabolism of dopamine is catalyzed by monoamine oxidase (MAO) or catechol-o-methyl transferase (COMT). Due to its widespread involvement in various signal transduction pathways, perturbation of dopamine level in the brain causes dramatic impact to various brain functions all leading or related to severe brain diseases and disorders, typically Parkinson's disease, schizophrenia, attention deficit hyperactivity disorder (ADHD), and addiction.[10-11] Pharmacological treatments utilizing different drugs to change the properties of the synthesis, release, metabolism and reuptake of dopamine, in order to restore the balance of this transmitter in the brain have been proposed; however, these have not been completely successful and there are many side effects of these treatments.

1.3.2. Serotonin

Serotonin (or 5-hydroxytryptamine, 5-HT) is an indoleamine neurotransmitter that regulates sleep, mood, behavior, diet, development, and cardiovascular function. Serotonin has fifteen types of receptors belonging to seven subgroups including 5-HT1-like, 5-HT2-like, and 5-HT3 to 5-HT7; the 5-HT1-like and 5-HT2-like receptors.[12] Like dopamine, serotonin can be either an excitatory or inhibitory transmitter. Serotonin has been shown to influence the dopaminergic system owing to the co-interaction of certain types of serotonergic and dopaminergic receptors,[7, 13] therefore it could also play a role in pharmacological treatments of diseases related to dopamine disturbance, for instance schizophrenia. This is a very complicated area and the knowledge of exact interactions here is not known.

Synthesis of serotonin begins with the amino acid substrate tryptophan. Tryptophan is hydroxylated by the enzyme tryptophan hydroxylase.[14] The product of this reaction, 5-hydroxytryptophan, is then decarboxylated by enzyme L-amino acid decarboxylase producing serotonin. The transmitter is subsequently oxidized by MAO_A to its primary metabolite 5-hydroxyindoleacetic acid (HIAA). Serotonin and a variety of receptors have been potential targets for therapeutic drugs which can be agonists - chemicals that bind to a receptor causing the action of a biological response - or antagonists - chemicals that block the action of agonists, selectively for particular types of receptors. The most common are antidepressant drugs, antipsychotics, drugs to treat anxiety, migraine, and to prevent nausea, and vomiting in cancer patients receiving chemotherapy.[15]

1.3.3. GABA

GABA (γ-aminobutyric acid) is the major inhibitory neurotransmitter. Several neurological disorders such as Huntington's disease, epilepsy, and anxiety are associated with the alteration of GABAergic neuron function.[16] GABA has both an ionotropic receptor ($GABA_A$), which regulates Cl^- across the cell membrane and clamps membrane potential (inhibitory), and a G-protein coupled receptor ($GABA_B$). The synthesis and metabolism of GABA is particularly different from the other transmitters in that it forms a closed cycle in which the transmitter is produced, released, re-uptaken, metabolized, and the metabolite product (glutamate), another transmitter, can be reused to generate GABA. The primary precursor for this cycle is glutamine.

1.3.4. Octopamine and tyramine

The physiological role of octopamine in synaptic transmission was discovered in 1973 whereas tyramine was considered to be a neurotransmitter from about 1990.[17-19] Octopamine and tyramine are the catecholamine neurotransmitters specific for invertebrates. They are the homologs of adrenaline and noradrenaline in vertebrates owing to similar chemical structure and physiological functions. These transmitters mediate aggression, the flight or fight response, motivation, and stress responses. Octopamine plays a role as a neurotransmitter, neurohormone, and neuromodulator. Octopamine, especially, has widespread influence on all the organs and activities of insects. It modulates signals in the peripheral, immune, sensory, and visual systems to the nervous system. It is involved in muscle tension and relaxation, respiration, heart rate, motor, and sleep behaviors.[20-21] The physiological role of tyramine in insects is not yet fully understood. The transmitter, however, is known to regulate different physiological and neurological aspects independently from octopamine such as locomotion, muscle performance, and pheromone biosynthesis.[22-23] Some studies have shown that tyramine and octopamine exhibit opposing effects on locomotion and activity of the enzyme adenylyl cyclase.[24] It also plays an important role in the sensitization of stimulant drugs in insects.[25]

The synthesis of tyramine and octopamine begins with tyrosine, the same precursor for dopamine synthesis. Tyramine is produced directly from the decarboxylation of tyrosine by the enzyme tyrosine decarboxylase. Tyramine is then hydroxylated by tyramine-β-hydroxylase producing octopamine. After it is released to interact with specific receptors, the transmitters are removed from the synapse by specialized transporters and subsequently tagged with an amine group through an N-acetylation or N-methylation reaction. As tyramine and octopamine are specialized for insects, they are good targets for pharmacological interventions, typically used for insecticides.

1.3.5. N-acetyldopamine and N-acetyloctopamine

N-acetyldopamine (NADA) and N-acetyloctopamine (NAOA) are the metabolites of dopamine and octopamine, respectively, from the N-acetylation reaction. This reaction is catalyzed by the enzyme N-acetyltransferase. N-acetylation is one of the major metabolic pathways for biogenic amines, beside the oxidation by MAO, commonly observed for dopamine, octopamine, tyramine, and serotonin. N-acetylated amines are most commonly present in the insect nervous system and MAO metabolites are found in mammals. NADA is mainly found in the cerebral ganglion, suboesophageal, thoracic and abdominal ganglia in coackroaches and other insects.

The metabolite NADA has been reported to exhibit antitumor activity in leukemia.[26] NAOA, on the other hand, has been suggested to be involved in controlling aggressive motivation in insects. [27]

1.4. Methylphenidate and its actions on the nervous system

Methylphenidate (MPH) or Ritalin has been a common and effective drug in the treatment of attention deficit hyperactivity disorder (ADHD) – a disorder characterized by inattention, hyperactivity, and impulsivity - in children and adolescents. MPH has been shown to positively affect these symptoms by enhancing attention, attentive allocation, focus, speed and accuracy of motor response processes. The clinically effective dose of MPH for children ranges between 0.3-1.0 mg/kg, which results in the apparent behavioral effects after about 2 hours of administration.[28] Despite the positive effects, it also has been demonstrated that the drug acts as a psychostimulant and causes drug addiction.[29] Having a similar chemical structure to cocaine and amphetamine, the action of MPH on the neurotransmitter transmission is also similar to these stimulants. MPH blocks the reuptake of neurotransmitters, typically dopamine, by binding to the dopamine transporter (Figure 3) leading to an increased dopamine level in the synapse. The elevation of synaptic dopamine is responsible for the euphoric feeling associated with the drug, reinforcing effects, and addiction in long-term use. The dopamine transporter is a 12 trans-membrane protein integrating into the cell membrane with extracellular and intracellular loops having N- and C- terminal groups inside the cell.[30] The reuptake of dopamine by the dopamine transporter occurs by the co-transport of two sodium ions and one chloride ion, which facilitates the conformational change of the dopamine transporter.[31] It has been suggested that dopamine binds to the binding site at the funnel-like tunnel segments 1, 3, 6, 8 and 10 of the dopamine transporter.[32] Thereafter, further conformational changes of the dopamine transporter take place, causing transport of dopamine to the intracellular presynaptic neuron. In the presence of stimulant drugs, such as cocaine and MPH, the drug binds to its selective binding sites on the dopamine transporter preventing the conformation changes needed for the transport of dopamine. [31, 33]

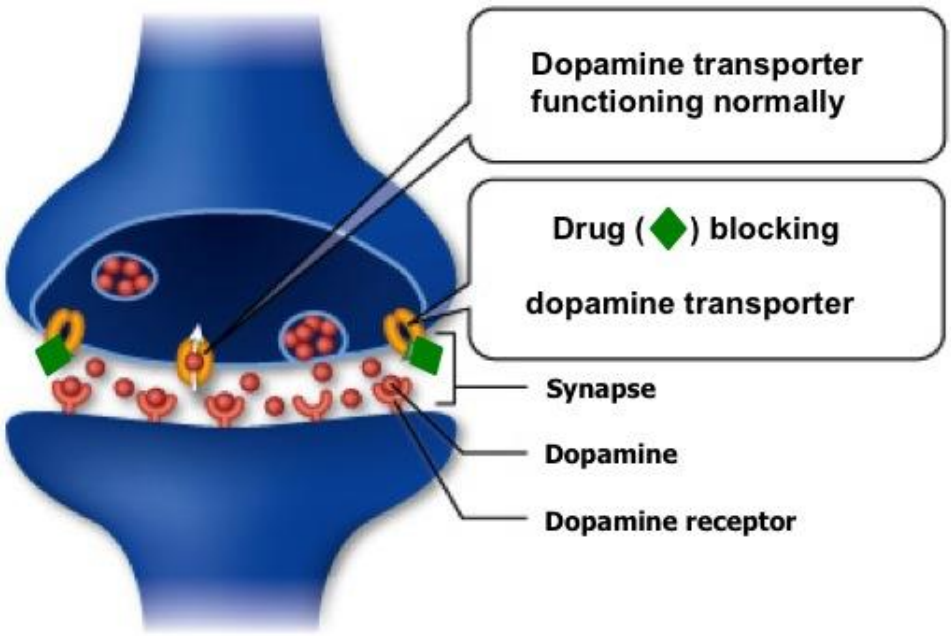

Figure 3. Function and disfunction of the dopamine transporter.[34]

In humans, MPH is less addictive than cocaine as the half-life of methylphenidate in the brain, based on the duration of dopamine transporter blockage, is longer than that of cocaine (60-90 min versus 15-25 min, respectively).[35] Since the clearance of the stimulant from the brain is necessary before it is possible for an individual to fully experience the reinforcing effects of the drug again, frequent repeated administration and overall abuse of MPH is limited compared to cocaine. The effect of the drug is also more spread out and less intense. If the mechanism of action is on the same part of the dopamine transporter, then these properties make MPH a possible candidate for the beginning stage of treatment of cocaine addiction. Replacement of cocaine with MPH might be a useful treatment as it produces less reinforcing effects compared to cocaine.[36]

As with many drugs, MPH can have an impact on the neurotransmitter system and functioning of the nervous system in other ways than affecting transmitter uptake. In addition to the neurotransmitter effects, the drug has been shown to affect various biomolecules in the brain and body. MPH induces significant changes in the lipid composition of the brain,[37] blood,[38] and plasma.[39] MPH administration also increases the reactive species formation that causes lipid peroxidation and protein damage in the prefrontal cortex of juvenile rats.[37] To date, detailed information about specific kinds of biomolecules as well as spatial distributions of the target molecules affected by the drug have not been provided. Due to its widespread use as a therapeutic drug, despite the mechanism of action of MPH on the nervous system not yet being fully clear, it is important to understand the molecular mechanism of MPH involved in neurological processes and the overall impacts of the drug on the chemical structure and function of the brain.

CHAPTER 2. BIOLOGICAL MODELS FOR MASS SPECTROMETRY

2.1. *Drosophila melanogaster*

2.1.1. Popularity of Drosophila as model system

For many years, *Drosophila melanogaster* (fruit fly) has been used as an important model organism in biological, pharmaceutical and medical research. *Drosophila* was first used by Thomas H. Morgan in genetic studies, for which he was awarded the Nobel Prize in 1933.[9] Since then, *Drosophila* has contributed enormously to investigations in genetic engineering, molecular biology, and physiology to provide fundamental knowledge for research on human development, diseases, and behaviors. *Drosophila* was the first complex organism to have its genome sequenced.[40] This enables genetic engineering to be fully annotated and has been used to manipulate the fly genome to produce tens of thousands of mutants. There are a remarkable variety of studies that have been modeled by *Drosophila*, for instance neurological disorders, cancer, diseases, drugs of abuse, and drug discoveries.[41] Several visibly distinguishable mutants are shown in Figure 4A.

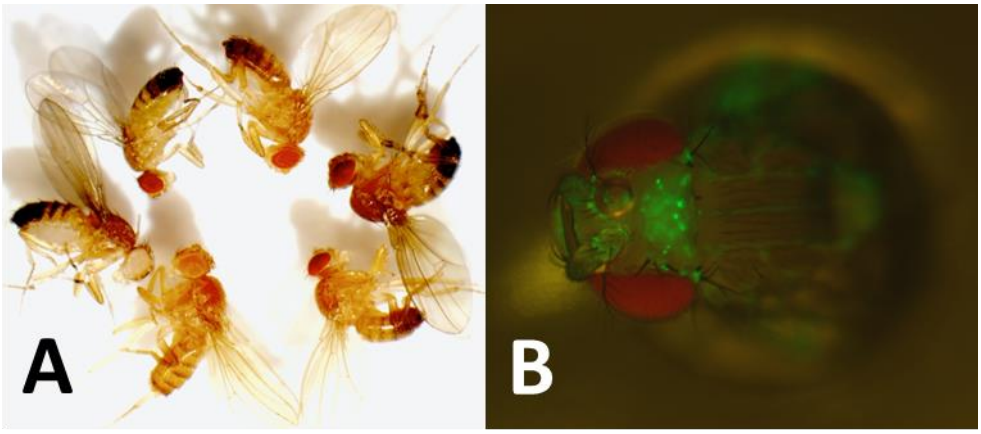

Figure 4. A: Fly mutants clockwise from left: white mutant followed by 5 other mutants in our stock in the lab. There are noticeable differences in color of the bodies, eyes, and wings. **B:** Green fluorescent protein labeled fly head immobilized in a Plexiglas block.

Drosophila has been used to study the mechanisms of neurological disorders such as epilepsy, Niemann-Pick disease, Parkinson's disease, and Alzheimer's disease.[40, 42-44] *Drosophila* has been used in studies of the blocking efficiency of orally administrated methylphenidate (MPH) on dopamine uptake and its effects on cocaine action on dopamine transporters as measured by fast scan cyclic voltammetry.[45] Studies have not been restricted to the neurotransmitter system and the flies have also been used to study the effects of the stimulant MPH on other brain biomolecules, particularly lipids and lipid related compounds, using mass spectrometry.[46-47] In addition, it has been used in a number of studies on the development of alcohol tolerance where it has been shown that the molecular mechanism of this process involves the functional integrity of various regions in the central brain especially the central complex and mushroom body; the octopaminergic system was mainly responsible for modulating the tolerance.[48]

Kevin White and coworkers have studied genome expression and corresponding protein-DNA interaction in *Drosophila* to investigate new regulating interactions in cancer, and they have discovered that the SPOP gene is involved in the signaling of tumor necrosis factor, a group of cytokines that induce cytotoxicity and necrosis of tumor cell lines.[41] Furthermore, *Drosophila* has been used successfully as a model for diabetes, aging, and oxidative stress as well as for testing the effects of therapeutic drugs before application on mammalian systems.[40, 49-51] One of the examples is that the *Drosophila* model of Huntington's disease has been used as an initial whole-animal validation of the candidate drug C2-8 for the inhibition of polyglutamine protein-mediated aggregation, the main cause of Huntington's disease. This was carried out after a high throughput drug screening approach on *in vitro* cell cultures. The results show that the drug reduces neurodegeneration in the flies. Based on these data, the drug has now been confidently tested on mammalian systems.[52]

2.1.2. Why is Drosophila a good model system?

Drosophila possesses many excellent properties well suited to a model organism. First, the flies have a short life cycle, which is about 2-3 weeks, allowing rapid manipulation of genes and phenotypes. Initially, a fly egg hatches to a larva after about half a day. The larva develops through three stages for 4-5 days and subsequently transforms to a pupa, which will become an adult fly after a week. An adult fly can live for about 2 weeks at 25 ^{o}C.[53] Second, the flies reproduce prolifically. A female fly can lay up to 100 eggs per day. Thus, *Drosophila* offers advantages for large population experiments, statistical analysis, and genetic studies where the observation and data of different generations are needed. Third, molecular mechanisms, for instance metabolism, organogenesis, and neural development, are conserved in *Drosophila* when compared to humans and mammals. A wide range of behaviors have been observed in flies such as learning and memory, sleep, courtship, stress, aggression, drug addiction and alcohol tolerance and all of these show sophisticated co-ordination of sensory inputs, cognitive processes, and motor systems. Finally, flies have a simple genome, which has been completely sequenced and annotated. The entire fly genome of 13 600 genes with 4 chromosomes has orthologs to aproxiamtely 60% of human genes.[54-55] There are well over 100 000 stocks of flies in various fly banks commercially available (over 63 000 in the Bloomington Flybase alone). Transgenic flies with markers such as green fluorescent protein (GFP) have been generated to visualize specific gene expression in the living flies at various developmental stages.[56] An example of a fly labeled with GFP to identify the dopamine regions (tyrosine hydroxylase) is shown in Figure 4B. Mutant flies with knockout genes are available to study the functions and expression of many specific genes.

2.1.3. Drosophila brain

The brain of *Drosophila*, with a volume of about 5 nL, has approximately 200 000 neurons, which form a complex connection circuit to conduct a variety of higher order neurological processes. The *Drosophila* nervous system shares many similarities to that of mammals, particularly the neurotransmitter system, complexity of the brain structure, and neurological functions of different regions of the brain. In *Drosophila* brain, neurotransmission involves complex activities of various types of molecules and organelles localizing at the presynaptic and postsynaptic neurons. In addition, when the flies are exposed to a drug of abuse such as cocaine,

MPH or nicotine, the blocking of the neurotransmitter transporters, that is stopping neurotransmitter re-uptake, by the drug is highly conserved between the fly and mammalian systems. Moreover, the flies also develop the same sensitization and desensitization responses to these drugs that lead to drug addiction in mammals. Altogether, *Drosophila* has a complex and high order brain structure and function, making it well suited for brain research.

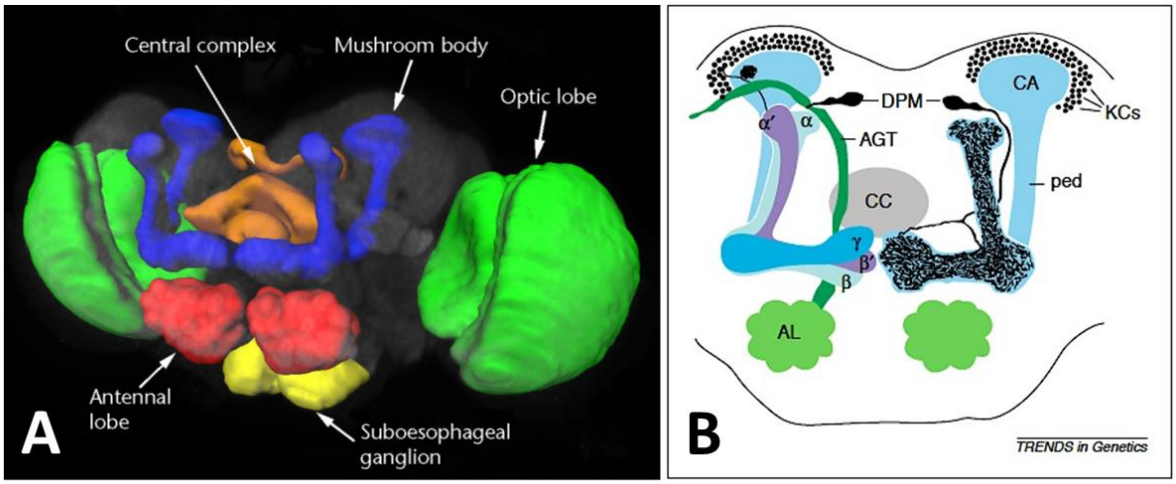

Figure 5. Schematics of *Drosophila* brain. **A:** Colored schematic of the important regions of the fly brain.[57] **B:** Frontal view of *Drosophila* central brain. KCs are Kenyon cells located on the mushroom body calyces (CA) projecting down to the pedunculus (ped) to the mushroom lobes α/β, α'/β', and γ. CC is the central complex, AL marks the antennal lobes, DPM is the dorsal paired medial cells innervating the mushroom body and stabilizing punitive and reward odor memories, AGT is the antenna glomerular tract relaying signals from the AL to the mushroom body.[58]

The *Drosophila* brain consists of two main parts, the central brain and the optical lobes (Figure 5A). The central brain or protocerebrum contains various distinct regions mediating different neurological processes. The most important part of the central brain is the mushroom body region, which is the center of olfactory learning and memory, and multisensory information processing. The mushroom body consists of the calyx neuropils, located posterior-dorsally in the protocerebrum (Figure 5B). About 2500 Kenyon cells, which are neurons involved in the learning and memory pathways of most insects, are situated in each mushroom body calyx and projected in parallel down the pedunculus to five lobes each containing three different kinds of neurons, α/β, α'/β', and γ.[58] Each kind of neuron has been suggested to exhibit a specific function, in particular, α/β and α'/β' neurons are important for long-term memory retrieval while γ neurons are crucial for olfactory memory.[59-60] Another important region is the central complex, situated along the midline of the protocerebrum.[61] It comprises four substructures, the protocerebral bridge, the fan shaped-body, the ellipsoid body, and the noduli. The central complex plays a key role in connecting many regions in the central brain, conducting and integrating various behaviors especially motor, locomotion, sensory, learning, and memory activities. There are two major types of neurons in the central complex, large-field and small-field neurons.[62] Large-field neurons only arborize within a substructure and connect it to one or two other regions of the central brain. Small-field neurons, on the other hand, mainly link different small areas of a substructure, or different substructures within the central complex. The antennal lobes make up the primary olfactory center and are located in the anterior region of the

brain. These lobes are comprised of glomeruli containing olfactory receptor neurons that are important for the flies to identify food, detect odors, and recognize partners and predators.[63] There are numerous glomeruli, each of which receives input from a specific type of olfactory receptor neuron. Besides receptor neurons, three groups of neurons are found in the antennal lobes. These are local neurons, projection neurons, and centrifugal neurons, and they connect the lobes to the mushroom body as well as other areas of the brain. These neurons also connect different domains within the lobes. Finally, the suboesophogael ganglia mediate gustatory activities. The sensory bristles in the proboscis, legs, and wings connect to the gustatory neurons, which in turn recognize the taste and produce an activating potential. The axons of the gustatory neurons carry the potential into projection neurons of the suboesophogael ganglia.[64]

The optical lobes, with approximately 60 000 neurons on each side, have three main neuropils, the lamina, medulla, and the lobula complex with the lobula plate.[65] Each compound eye, or ommatidium, contains eight photoreceptor cells R1-R8 surrounded by eye pigment. Photoreceptors R1-R6 are responsible for spatial vision being projected to the lamina, where the lamina neurons then project further into specific layers of the medulla columns. Photoreceptors R7 and R8 are responsible for color vision; however, these project directly to the medulla. The axons of medulla neurons terminate in the lobula complex and lobula plate. There are complex local interneurons connecting between the lobula complex and the lobula plate. From the lobula, various sets of neurons project to different regions of the central brain.

The major neurotransmitters in *Drosophila* brain, dopamine, serotonin, GABA, histamine, glutamate, and acetylcholine are found in mammals, including humans. In the fly brain, over a hundred dopaminergic neurons distribute in clusters mainly in the protocerebrum from which they project their axons into the mushroom body and central complex.[66-67] There are about 40 serotonergic neurons in each hemisphere of the fly brain. They arborize and innervate into all the major neuropils of the central nervous system. In addition, the GABAergic neurons are quite ubiquitous in the entire fly brain with concentrations about 1000 times higher than those of the monoamines in the same regions. It has been shown that the olfactory learning and odor-evoked responses in *Drosophila* are modulated by the inhibition of GABA.[16, 68-69]

The neurological and regulatory functions of these transmitters are also relevant to mammalian systems; however, the difference is that octopamine and tyramine in the fly brain replace epinephrine and norepinephrine in the mammalian brain, respectively. There are very few octopaminergic neurons in insect brains. In *Drosophila*, there are only about 100 octopaminergic neurons in the brain; however, the neurons have large arborization allowing them to innervate all the major neuropils of the brain and thoraco-abdominal nervous system.[21, 70] Among the thoraco-abdominal neurons, there are many that connect to the peripheral system and localize along the midline of the thoraco-abdominal ganglia and suboesophageal ganglia. These are classified into dorsal unpaired median (DUM), and ventral unpaired median (VUM) neurons as their cell bodies position along the dorsal and ventral of the midline, respectively. The DUM and VUM cells from suboesophageal ganglia arborize and send their axons to innervate almost every substructure of the mushroom body, central complex, and antennal lobes. The innervation of octopaminergic neurons also has been found in the medulla, lobula, and lobula plate of the optical lobes. The complex and dense arborization of octopaminergic neurons demonstrates the widespread action of the transmitter on the entire insect brain and body. The location of tyraminergic neurons has not been clearly defined yet. As tyramine is the precursor

of octopamine, highly overlapping localization of tyramine and octopamine is observed. Based on tyramine-like immunoreactivity, the transmitter has been found in the neurons of the brain, suboesophageal ganglia, and thoraco-abdominal ganglia. Among these areas, several do not contain octopamine.[23, 71] Tyramine is also found in non-neural tissue such as Malpighian tubules, digestive tract musculature, and ventral nerve cord.

The N-acetylated amine metabolite, NADA, has been reported to be present at 18 μM concentration in the *Drosophila* head.[72] The metabolite NADA also plays a role as a sclerotizing agent in hardening and darkening of the insect cuticle.[73] NAOA is present at a concentration of about 5 μM in *Drosophila* head.

In this thesis, *Drosophila* is targeted for mass spectrometry based analysis and imaging to study the chemical structure of the brain and the effect of the drug methylphenidate on the neurotransmitter composition and lipid anatomy.

2.2. *Caenorhabditis elegans* (*C. elegans*)

C. elegans has been widely used as a model organism in a variety of research areas especially cell biology, genetics, neuroscience, aging and pathology. It has been used as a primary model to study neural development, neural, metabolic and behavioral alteration due to changes of chemicals and temperature, molecular mechanism in relation to diseases and neurological disorders, genetics, cell biology and behaviors such as mating, aging and stress response to different living environments.[74-77] The small worm with simple anatomy and behavior has become a powerful tool to reveal different complex biological mechanisms at a molecular and cellular level that is extremely beneficial for research related to vertebrates and humans.

2.2.1. C. elegans as a model organism

C. elegans was first introduced to study animal development and behavior by the biologist Sydney Brenner in 1965 who was awarded the Nobel prize in 2002 together with Horvitz and Sulston for their work.[9, 74] Since then it has been widely used as a model organism. *C. elegans* is a free-living soil nematode having many features desirable in a model organism. First, the worm is small (1-1.5 mm in length), easy to cultivate in the lab by feeding with *E. coli* on a petri dish at a temperature of about 20 ºC. Second, the worm has a very short life cycle. From egg, developing to adult worm, to reproductive age takes about 3 days. The lifespan of the worm is about 2 to 3 weeks depending on living conditions. This reduces experiment cycle time and speeds up the study of different generations. Third, the worm reproduces very rapidly and prolifically. The worm has two sexes, hermaphrodite and male. A hermaphrodite lays 300-350 eggs following self-fertilization and even more when mated with a male. Therefore, large numbers of samples can be easily obtained for statistical analysis. In addition, crossing with a male results in different phenotypes useful for genetic research. Fourth, the worm has a simple nervous system comprising of 302 neurons in the hermaphrodite and 381 neurons in the male. This makes it easy to study detailed function and regulation of specific neurons, as well as their connections in the neuron network. Fifth, although the worm looks like it has very simple morphology and behaviors with less than 1000 cells totally, these cells form many different tissues and complicated structures. In addition, they are persistent in number and localization in the animal body. The worm also has a transparent body. These characteristics enable observation inside a living worm in order to track cell development, differentiation, and migration. Moreover with the aid of fluorescence markers, molecular and cellular processes can

be easily observed and studied. Sixth, the worm has a simple genome containing about 19 000 genes with 6 chromosomes.[78] Similar to *Drosophila*, the genome has been completely sequenced and mutants are available for various studies on molecular mechanisms and diseases. Several mutants with morphological defects on the body and tails are shown in Figure 6. Finally, it was discovered that the molecular and cellular processes between the worm and human are also highly conserved. The worm genome has about 60-80% homologues when compared to the human genome.[79] Many human diseases have been found to have similar pathways in the worm.

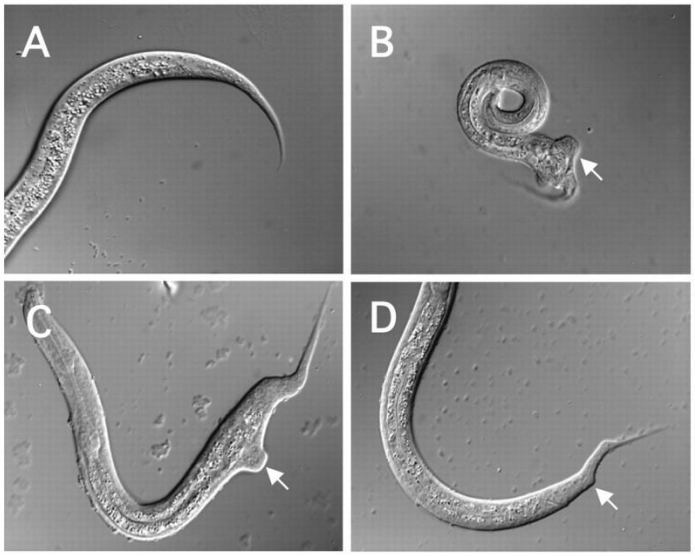

Figure 6. Body and tail of different *C. elegans* mutants. Tail of wild type larval worm (A) and morphological defects in the body and tail of mutants of hlh-14- a protein promotes neurogenesis *via* asymmetric cell division (B, C, D).[80]

2.2.2. Anatomy of C. elegans

The detailed anatomy of *C. elegans* is comprehensively reviewed in the literature.[74] Briefly, the worm body is cylindrical in shape comprising two concentric tubes separated by a space filled with fluid. The worm body is maintained by internal hydrostatic pressure. The body is protected by a collagenous cuticle, which covers the outer tube. In the outer tube, attaching to the cuticle are four musculatures running along the length of the body that enable the worm to move forward and backward in a sigmoidal movement. The outer tube also contains the hypodermis, nervous system, immune and hepatic organs coelomocytes, and excretory system (anus). The inner tube, on the other hand, contains the ingestion organ (pharynx), intestine, and reproductive gland (gonad). The pharynx in the head pumps food from outside, grinds, filters and transports it to the intestine at the central lumen and to the anus located near the tail. Neurons are located around the pharynx forming a ring along the ventral midline and in the tail. The nerve ring makes the connection between the entire nervous system from the sensory organ at the head tip to the central nerve cord and to the tail.

The reproduction organ of the worm is the gonad, which has anterior and posterior arms to produce egg and sperm cells in hermaphrodite. These two arms have a common uterus co-locating with a vulva at the ventral center of the worm body. Eggs in the gonad arms are fertilized with sperm and move towards the uterus to be subsequently laid outside through the

vulva. The male gonad, however, contains only a single anterior arm to produce sperm cells. The anatomical structure of *C. elegans* is shown in Figure 7.

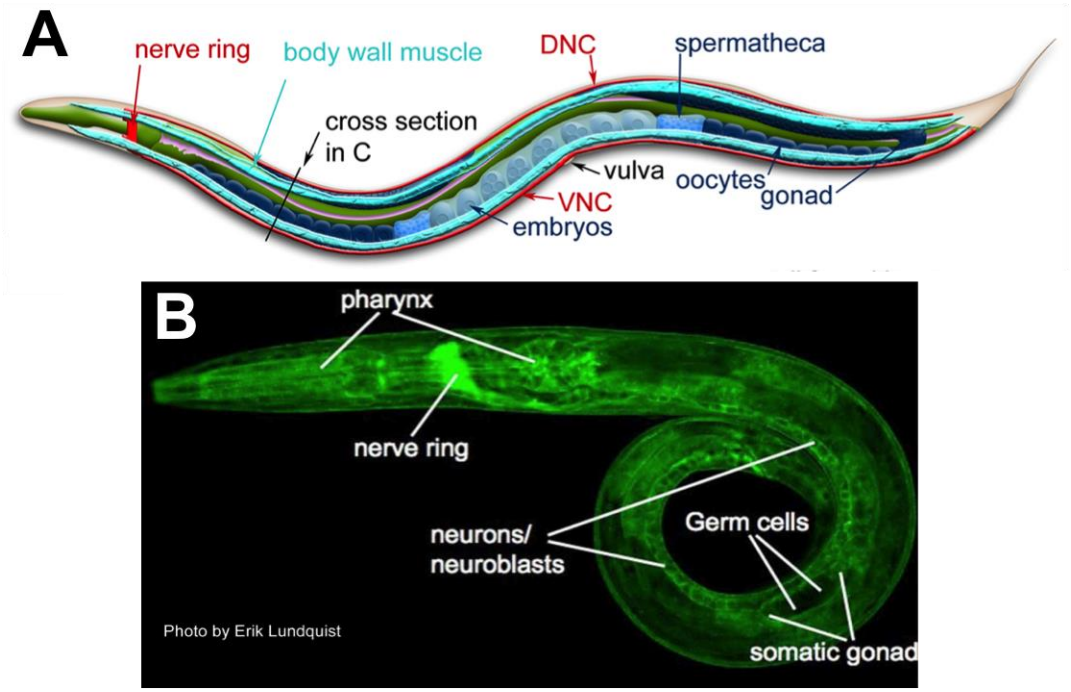

Figure 7. Anatomical structure of *C. elegans*. **A:** Animation image. DNC is dorsal nerve cord, and VNC is ventral nerve cord. **B:** Green fluorescent protein labeled *C. elegans*.[81-82]

The anatomy of the worm has been completely described based on electron microscopy; however, a detailed chemical architecture of the worm has not been fully worked out. In this thesis, *C. elegans* is targeted for SIMS imaging to study the chemical structure of the worm. Studies like these should provide very useful anatomical information from a chemical basis to facilitate further use of imaging mass spectrometry (IMS) using these model organisms.

CHAPTER 3. LIPIDS AND BIOLOGICAL FUNCTIONS OF LIPIDS

Lipids are naturally occurring molecules with both hydrophilic and hydrophobic properties. They are small molecules with masses typically up to about 1000 Da. Lipids are a very important group of biomolecules playing different functions in biological systems. The major functions of lipids include formation of lipid bilayers in the cell membrane, storage of energy, and serving as reservoirs of second messengers for cellular signaling. There are more than 1000 lipid species in an eukaryotic cell.[83] Lipids are classified into eight main groups, including fatty acids, glycerolipids, glycerophospholipids, sphingolipids, sterol lipids, prenol lipids, saccharolipids, and polyketides, based on the hydrophobic and hydrophilic structures constituting the lipid molecules.[84] Each group contains several subgroups.

3.1. Biological functions of lipids

3.1.1. Lipids as components of cell membranes

Among the different lipid groups, glycerophospholipids are the main component of the lipid bilayers of cell membranes beside cholesterol. Over 400 glycerophospholipids with different structures have been identified in a single cell.[85] In brain tissue, glycerophospholipids comprise about 20-25% of the dry weight.[86] Glycerophospholipids are structurally characterized by two hydrophobic fatty acyl tails and a hydrophilic phosphate headgroup connected by the three hydroxyl groups of a glycerol backbone. The oxygen on the phosphate group can link to different hydrocarbon groups whose structure affects the size of the headgroup. The geometry of the lipid is determined by the sizes and shapes of the polar headgroup and hydrophobic tails. The lamellar shaped lipids such as phosphatidylcholine (PC) have a polar headgroup that has similar size compared to the hydrophobic tails, whereas the conical shaped lipids such as phosphatidylethanolamine (PE) and phosphatidylinositol (PI) have headgroups that are smaller than the tail groups. Due to their geometries, the lamellar shaped lipids such as PC and sphingomyelin are highly localized in the outer leaflet of cell membranes, whereas PE, PI and phosphatidylserine (PS) are mainly distributed in the inner leaflet of membranes.[87] Most importantly, the highly complex composition of lipids in the plasma membranes and their geometries play important regulatory roles in different cellular processes.

***Lipids in Exocytosis*.** Lipid geometry allows the membrane the flexibility to facilitate exocytosis - the process of membrane fusion between a vesicle and plasma membrane of the presynaptic neuron to release neurotransmitters. To promote this fusion, glycerophospholipids rearrange their localization in the membrane in such a manner that conically shaped lipids, typically PE and PI, accumulate in the high curvature fusing site and lamellar shaped lipids, especially PC, are dominant in the low curvature regions (Figure 8). Therefore the lipid structure of the cell membrane alters during this process. There have been several pieces of evidence supporting this hypothesis. The cylindrical shaped lipid PC is excluded and the conical shaped lipid 2-aminoethylphosphonolipid is highly localized in fusion pores during the mating of *Tetrahymena thermophila*.[88] In another supporting study the conically shaped lipid phosphatidylinositol-4, 5-

bisphosphate - a derivative from PI - has been shown to play a regulatory role in the synaptic fusion of vesicles.[89]

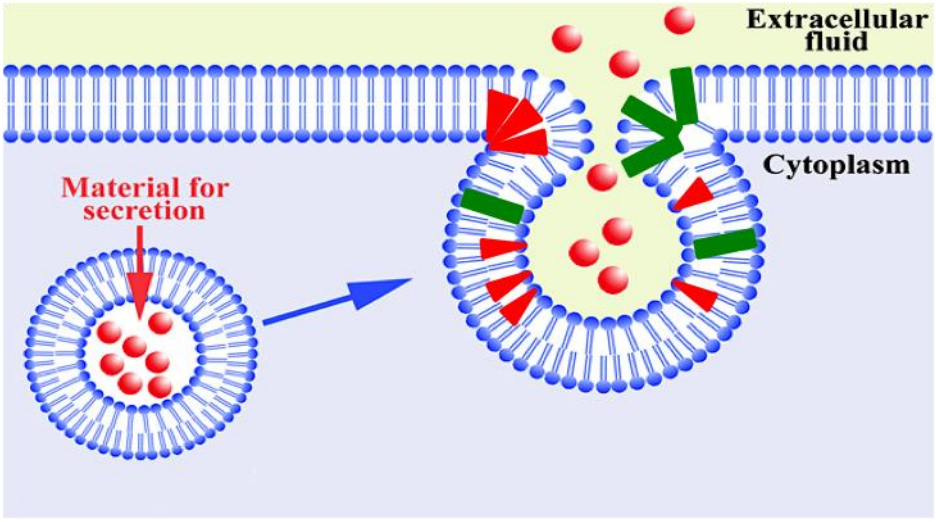

Figure 8. Distribution of glycerophospholipids in the plasma membrane and their rearrangement in the membrane fusion process of exocytosis. Red balls are molecules to be secreted; green bars are cylindrical lipids like PC; red triangles are conical lipids like PE and PI.

Lipid rafts. Lipids, mainly sphingolipids and cholesterol, cluster in the plasma membrane to form microdomains called lipid rafts. These rafts have been suggested to be the residential sites of transmembrane proteins and ion channels.[90] Lipids serve as protein anchors attaching proteins to the cell membrane as well as to regulate protein activities. In addition, activities of ion channels, particularly K^+, Ca^{2+} ion channels, are affected by lipids and fatty acids such as arachidonic acid.

3.1.2. Lipids as reservoirs of energy storage

Lipids, particularly fatty acids (FA) and triacylglycerols (TAG), are the main reservoirs of energy for biological systems. FAs and TAGs are efficiently reduced thus they can be used to generate higher energy compared to the other energy sources such as carbohydrates and proteins. The complete oxidation of FAs produces 38 kJ/g, whereas that of carbohydrates and proteins produces 17 kJ/g.[91] In addition, due to the hydrophobic properties of lipids, they are present in anhydrous forms and therefore provide highly concentrated energy storage for biological reactions. TAGs are typically accumulated in adipose cells, commonly called fat cells, from which they are transported to different tissues of the body by the blood. Lipids are generally taken into the body by diet, but some are synthesized.

3.1.3. Lipids as reservoirs of second messengers

Via biosynthetic and metabolic reactions with different enzymes, lipids generate a variety of compounds that play a role as second messengers for cellular signaling (Figure 9). The generation of second messengers is complex and diverse. One second messenger can be produced *via* different catalytic mechanisms from different precursors. In addition, a relation among these biochemical reactions exists such that a single biochemical pathway influences a sequence of related signaling pathways.

One of the most important lipid-based second messengers is arachidonic acid (AA), a 20 carbon

polyunsaturated fatty acid generated by the hydrolysis of glycerophospholipids by enzyme phospholipase A2 (PLA2). AA is also a product of a serial metabolic reactions in which the converted form of phosphatidylinositol - phosphatidylinositol 4,5-biphosphate (PI-4,5P_2) - is hydrolyzed to DAG which is then further hydrolyzed by enzyme phospholipase C (PLC).[86, 92] AA is known to modulate Ca^{2+}, K^+ ion channels, the N-methyl-D-aspartate (NMDA) receptor, activities of protein kinase C, and monoamine transporters by inhibiting glutamate uptake.[87, 93-94] AA is metabolized to eicosanoids, for instance it is oxygenated by the enzyme cyclooxygenase generating different types of prostaglandins, which are the important mediators in synaptic transmission and plasticity.[95]

Diacylglycerols (DAGs) are another major group of second messengers. DAG is abundantly produced from the catalytic cleavage of glycerophospholipids, particularly PI by the enzyme PLC, and PC and PE by enzyme phospholipase D (PLD).[86] DAG is the main effector of protein kinase C and protein kinase D, which in turn alter other enzyme activities. On the other hand, it is also a precursor of second messengers such as AA and phosphatidic acid.

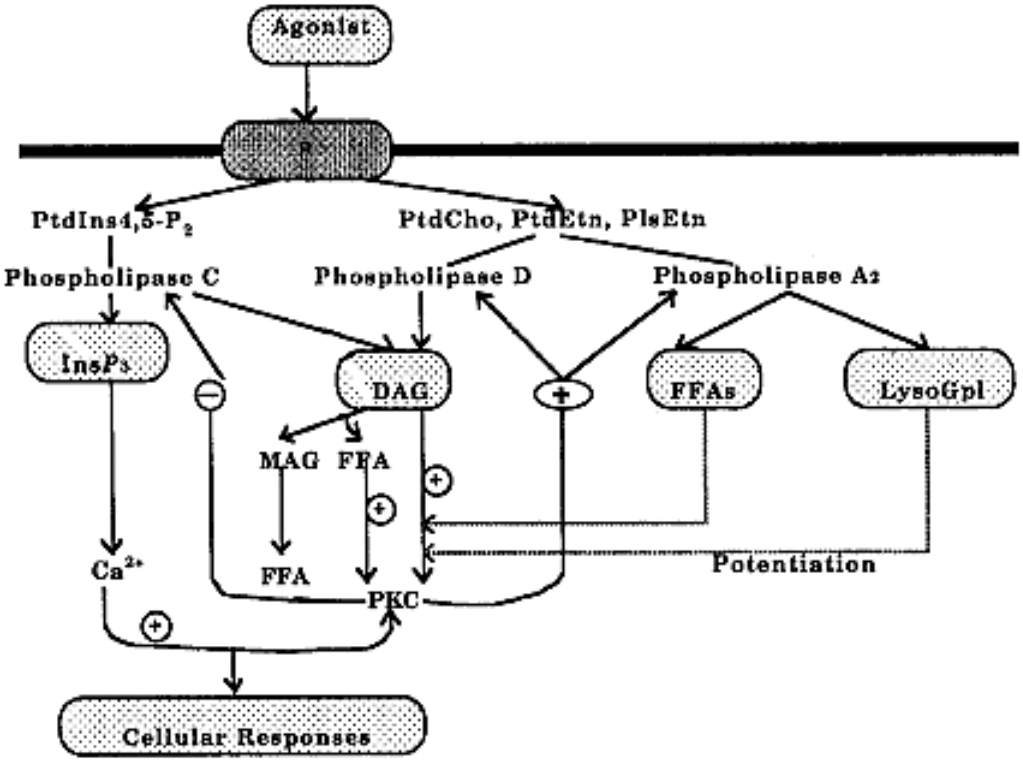

Figure 9. Biosynthetic and metabolic pathways of glycerophospholipids as a reservoir of second messengers.[86]

Ceramides are metabolites produced from the hydrolysis of sphingomyelin by sphingomyelinase.[96] These lipids attributes their regulatory roles to a variety of cellular functions especially the cellular response to stress and injury. Stimuli inducing apoptosis such as tumor necrosis factor and chemotherapy agents result in increasing levels of ceramides in the cell leading to an inflammation response and cell death. The typical targets of ceramide effects are ceramide-activated protein kinase (CAPK), ceramide-activated protein phosphatase (CAPP), protein kinase C, and phospholipase D. Generally, ceramides cause dephosphorylation of phosphoproteins altering cell functions. One example is that ceramides have been shown to dephosphorylate and inhibit the activity of Akt - a kinase responsible for insulin signaling and

mitogenesis.[97] In addition, *via* protein phosphatase 1, ceramides cause dephosphorylation of retinoblastoma gene products, that then affects the cell cycle.

3.2. Biosynthesis and metabolism of lipids

The biosynthesis and metabolism of lipids are a series of reactions catalyzed by different enzymes. There are complex relations between the biosynthetic and metabolic pathways of lipids, as the intermediates and products of a single synthetic pathway can be the precursors of other synthetic or metabolic ones. Exogenous or endogenous interferences of a particular pathway will consequently interfere the others.

The biosynthesis of PC comprises three pathways, the base-exchange from free choline, the citidine diphosphocholine (CDP)-choline pathway, and conversion of phosphatidylethanolamine catalyzed by methyltransferase.[98] The main materials involved in the synthesis of PC are choline, diacylglycerols and pre-existing phospholipids. On the other hand, the biosynthetic pathways for PE synthesis include the decarboxylation of phosphatidylserine by phosphatidylserine decarboxylase, the CDP-ethanolamine pathway, and Ca^{2+}-dependent base-exchange of ethanolamine with pre-existing phospholipids.[99] Among these, the CDP-choline and CDP-ethanolamine are the main synthetic pathways for PC and PE with the rate-limiting intracellular enzyme cytidylyltransferase.[100] It has been shown that citidylyltransferase is highly localized in the brain implicating an active involvement of this enzyme in the synthesis of PC and PE in nervous tissue.[101]

PI is synthesized from the reaction of CDP-diacylglyrerols and inositol catalyzed by PI synthase. Phosphatidic acids and inositol are the primary substrates. PI is then a starting precursor for seven different phosphorylated forms of PI.[102-103] The major phosphorylated forms in mammalian cells are phosphatidylinositol 4-monophosphate (PI-4P) and PI-4, $5P_{2,}$ which form a source of second messengers, substrate for hormones, and modulators of enzyme and proteins such as PLD and actin regulatory proteins. The materials for the biosynthesis of these lipids including particular headgroups, diacylglycerol backbones, fatty acids, and pre-existing phospholipids are tightly connected together in one or the other of the reactions for all the lipids.[104]

The metabolism of the glycerophospholipids occurs in the presence of a group of phospholipases mainly including phospholipase A1 (PLA-1), phospholipase A2 (PLA-2), phospholipase C (PLC), and phospholipase D (PLD); each has different sites of action on the glycerophospholipid molecules (Figure 10).[86] PLA-1 catalyzes the hydrolysis of glycerophospholipids at the sn-1 bond to release free fatty acid and 2-acyl lysophospholipid, whereas PLA-2 acts on sn-2 bonds producing fatty acids and 1-acyl lysophospholipids. The lysophospholipid can then be used as recycling material for glycerophospholipids or be further metabolized by lysophospholipase. PLC hydrolyzes the sn-3 phosphodiester bond of the PI and its phosphorylated forms to generate DAG and noncyclic or cyclic inositol phosphates. In *Drosophila* heads, the isoforms PLC-B - a group of phosphoinositide specific enzymes coupled to guanine-nucleotides (G proteins)- were discovered.[105] Finally, PLD catalyzes the cleavage of glycerophospholipids, typically PC, into phosphatidic acid and a free base. It is clear that the activities of the enzymes involved in lipid biosynthetic and metabolic pathways heavily influence cell signaling and other processes, and moreover it implicates the relationship between these enzymes in regulating signaling in the cell.

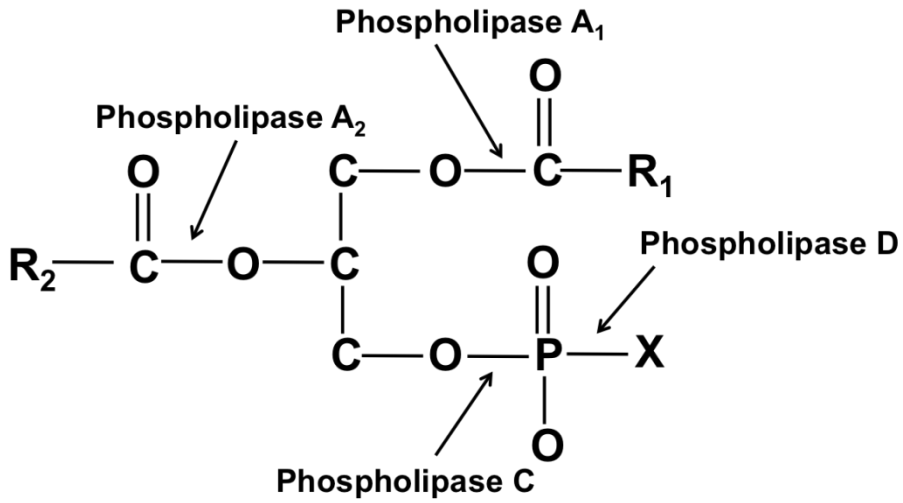

Figure 10. Metabolic action of enzyme phospholipases on glycerophospholipids. X: Choline, ethanolamine, inositol, or serine.[86]

3.3. Lipids involved in neurological disorders and brain diseases

Due to the widespread involvement of lipids in all cellular processes and the close relationship between their synthetic and metabolic pathways, perturbation of a particular lipid not only influences its second messenger signaling or a particular mediating protein but also influences the entire signaling network, neural plasticity, and normal biological functions. Numerous studies have been done to show that lipids are involved in various neurological disorders and diseases.

The ratio of PC to PE has been shown to play an important role in maintaining the integrity of cell membranes and the decrease of this ratio might promote the development of steatohepatitis and liver damage in mice.[106] The decrease of the PC to PE ratio leads to a decrease in membrane potential that might initiate cell inflammation. In addition, changes in lipid composition alter membrane structure as well as the activities of different cell membrane proteins, and ion channels. These changes might significantly affect the processes of exocytosis and endocytosis.

Lipid perturbation has been found to cause cell death. Decrease in PC synthesis has been studied in different cell lines such as PC12 and MT58 cells and induces cell death.[107] Several hypotheses for the relation between the change in PC and apoptosis have been suggested. It might be that the PC-binding protein acts as a sensor of intracellular PC levels and activates the signal for apoptosis. Alternatively, a decrease in PC might induce changes in subcellular structure, which is vital to cell survival.

Schizophrenia is a mental disorder characterized by abnormal social behavior with hallucinations and delusions. It has generally been hypothesized that schizophrenia is caused by a malfunction of neurotransmitter regulation, which decreases synaptic plasticity. However, several studies have shown that there is an abnormal concentration and distribution of PC, ceramides and fatty acids in the brains of schizophrenic patients.[108] The levels of PC and PE plasmalogen are found dramatically reduced in schizophrenia patients suggesting that there is an impaired structure and function of the cell membrane.[109] Matsumono *et al.*[110] employed matrix-assisted laser desorption ionization (MALDI) imaging mass spectrometry (IMS) and direct microregion analysis on the postmortem brains of schizophrenia patients and found significant changes in phospholipid distribution. Particularly, PC (diacyl-16:0/20:4) increases in

concentration in the frontal cortex, whereas PC (diacyl-16:0/18:1) decreases its level in the frontal and occipital cortex. From these results, the authors suggest that the abnormalities of regional lipid metabolism in the patient brains are important in schizophrenia.

Lipids have also been found to be significantly different in ADHD patients. Fatty acids have been suggested to be possibly involved in ADHD owing to observations that several syndromes of ADHD are similar to those of essential fatty acid deficiency.[111] Alpha-linoleic acid (omega-3) and linoleic acid (omega-6) are two of the most important essential fatty acids supplied by diet. These acids are the materials used to synthesize longer polyunsaturated lipids to maintain cell membrane structure and cellular functions. In ADHD patients, a decrease in omega-3 level, and an increase in the ratio of AA and eicosapentaenoic acid in red blood cells has been observed. An increasing number of studies are focusing on using omega-3 as a clinical treatment for mental disorders including ADHD.[112-113] Germano *et al.*[114] analyzed fatty acid levels in the blood and red blood cells of ADHD patients following omega-3 supplementation and evaluated its clinically beneficial aspects for the disorder. It has been shown that after the supplementation, the ratio of omega-3 and omega-6 increases together with a significant increase in the ratio of phospholipids, especially PC and PE, and cholesterol. Omega-3 supplementation therefore appears to lead to improvement in inattention and hyperactivity behaviors of ADHD patients.

Ischemic stroke is another disorder characterized by lipid disfunction, in this case causing lipid changes and cell death. This is characterized by a critical reduction of blood circulation to a certain brain region causing loss of neurological functions and brain injury. Ischemic stroke is caused by low oxygen and glucose supply transported by blood, which inhibits ATP production and activates the release of glutamate.[115] This elevated glutamate results in increased intracellular Ca^{2+} and activities of phospholipases, the major enzymes of glycerophospholipid metabolism. High levels of second messengers produced from glycerophospholipid metabolism might activate the pathways of cell inflammation and apoptosis.[116] Studies have shown that lipid perturbation occurs in rat brain following ischemic stroke. In more detail, the potassium ion adduct of PC is present at lower concentration, whereas the sodium ion adduct of PC is distributed at higher concentration in the ischemic brain region. Furthermore, significantly high levels of lysoglycerophospholipids, sphingomyelin, and DAGs are accumulated in the injured brain indicating that the metabolic pathways of lipids are altered in the inflammatory cellular response.

A major disease of the brain worldwide is Alzheimer's disease (AD). This is a neurodegenerative disease that is identified by progressive loss of memory and cognitive functions. Significant alterations in lipids including cholesterol, glycerophospholipids, ceramides, and sulfatides have been found in Alzheimer's patients.[117-118] The levels of lipids in AD brain appear to decrease due to lipid peroxidation, which has been suggested to be one of the main molecular mechanisms causing AD. Polyunsaturated fatty acids as well as PE and PI are reduced in different regions of AD brains. PE-plasmalogen in the gray matter of AD brain is also diminished. This might account for the elevated activity of the enzyme PLA_2 and thereby induce oxidative stress. Changes in membrane lipid composition might cause neural membrane defects and consequently impaired signal transduction and synaptic function in AD brains.

In summary, owing to their ubiquity in cellular membranes and involvement in various biological functions such as signaling, lipids plays a central role in maintaining the proper functioning of single cells in biological systems. Perturbation in composition and distribution of

lipids is certainly a cause and consequence of different types of disorders, injuries, and diseases especially in the nervous system. Understanding the molecular mechanisms of how lipids change and affect these disorders and diseases will be of great benefit to biology and pharmacology where lipids and lipid affecting drugs might be used as clinical treatments.

CHAPTER 4. CAPILLARY ELECTROPHORESIS MASS SPECTROMETRY

Capillary electrophoresis (CE) is a very powerful separation technique widely used in analytical chemistry and life science. The first use of electrophoresis was reported by Tiselius who was awarded the Nobel prize in 1948.[9] In 1981, Jorgenson and Lukacs used a fused silica capillary to separate ionic species to demonstrate the advantageous resolving power of capillary zone electrophoresis (CZE) that brought the technique widespread recognition and applications in many different areas. Since then, CE has been developed and modified continuously to become one of the main liquid phase separation techniques besides high performance liquid chromatography (HPLC). A number of applications of CE have been found in various areas such as environment, food, biology, clinical and pharmaceuticals to separate inorganic ionic species, small organic compounds, drugs, and biomolecules.[119-120] Particularly in neuroscience, CE is commonly used to separate many signaling molecules such as neurotransmitters, metabolites, neuropeptides, and proteins.

CE possesses several unique features that make it a valuable separation technique. First, the separation is based on the difference in mass, charge, and structure of the analytes, which results in different electrophoretic mobilities. This is very useful for separating the analytes from interferences in samples, especially in biological samples where complex matrices are present. Second, CE offers high separation efficiency with 10^5-10^7 theoretical plates due to its characteristic plug flow profile.[121] Third, the required amount of sample is extremely small with the injection volume typically in the nL range. For that reason, the technique is the best choice when sample quantity is limited such as small size samples and single cell analysis. In neuroscience, CE has been successfully used to separate and quantify biogenic amine neurotransmitters in the regional brain and whole brain of *Drosophila*, and to determine the content of vesicles at zeptomole concentration levels.[122-123] In those experiments, CE was coupled to electrochemical detection. Also, the amino acids in the hemolymph of *Drosophila* larvae, and the glial fibrillary acidic protein - a major filament protein of astrocytes acting as an indicator for neurodegeneration induced by the neurotoxin 1-methyl-4-methyl-1, 2, 3, 6-tetrahydropyridine in mouse brain, were detected by CE coupled to laser-induced fluorescence detection.[124] Fourth, CE can be coupled with different detectors such as UV, electrochemistry, and mass spectrometry. Offline and online analysis can be performed with a simple and flexible setup. CE connected to microdialysis sampling allows continuous measurement of the unbound chemicals in the brain or other tissues in a living biological body.[125] Finally, CE instruments are relatively inexpensive compared to the other separation instruments and therefore affordable in most labs.

Among many detectors used with CE, mass spectrometry is one of the most preferable due to its high accuracy in structural identification based on the m/z of analytes and fragment m/z values when tandem MS is employed. CE coupled to MALDI, electrospray ionization (ESI), atmospheric pressure chemical ionization (APCI), and inductively coupled plasma (ICP) mass spectrometry are commonly found. For MALDI-MS, CE eluent can be spotted on a conductive substrate for offline analysis. Online coupling with different MS interfaces is also possible.

A method using CE coupled to ESI-MS was developed to separate 352 metabolite standards and applied to determine 1692 metabolites extracted from *Bacillus subtilis*.[126] The identities of

cationic, anionic metabolites and nucleotides were determined in separate measurements with specific optimized conditions.

CE-MALDI ToF and ToF/ToF MS were applied to analyze complex peptide mixtures from protein digests with concentrations between 1-1000 nM.[127] With this offline configuration, the separation time is decoupled from the MALDI-MS analysis. Peptide identification and quantification with MALDI-MS can be done before MS/MS analysis in order to focus on the interested peptides. In addition, the sensitivity for MS/MS signals can be improved by using a longer sampling time for the precursors. This is usually restricted by the separation window when online analysis is used.

ICP-MS is a very sensitive method for elemental analysis with detection limit in a range of pgL^{-1}-ngL^{-1}.[128] Coupling of CE and ICP-MS is an attractive approach to analyze trace elements in biomolecules like metalloproteins. An example of this method is the analysis of sulfur and the trace elements cadmium, nickel, manganese, and zinc in metallothionein-like proteins extracted from bream liver.[129] The method can be used to separate and quantify these trace elements with high sensitivity, about 1 μgL^{-1} for S, and 300-500 ngL^{-1} for the other elements.

CE-ESI-MS is one of the analytical methods extensively used in peptidomics and proteomics. For example in clinical microbiological studies, CE-ESI-MS is a sensitive and unbiased analytical platform to identify antibiotic resistance in miroorganisms.[130] Carbapenemases are common enzymes in multi-drug resistant gram-negative bacteria producing resistance to β-lactam. To detect the enzyme, the cells were digested with trypsin followed by CE-MS analysis and identification based on bacterial protein databases. The results indicate the presence of particular carbapenemases to discriminate clearly resistant and susceptible bacterial strains.

4.1. Principle of capillary zone electrophoresis

CE can be used to separate analytes in ionic form based on their different migration velocity in a specific electrolyte buffer through a capillary. The migration velocity depends on the size, structure and charge of the ions at a given pH. Basically, two reservoirs of electrolyte buffer are in contact with two ends of a capillary. A high potential (typically 20-30 kV) is applied across the ends of the capillary through the electrolyte buffer, a more negative potential is typically applied to the entrance (cathode) and a more positive potential to the exit (anode). The entrance when sampling is placed in the sample reservoir. After injection, it is placed in the buffer reservoir for analysis. The exit of the capillary is coupled to a detector. The sample injected into the capillary might contain negative, positive or neutral species, depending on the pH of the electrolyte buffer. In a high electric field, the ionic species migrate towards the end with opposite polarity, whereas the neutral species do not move. This is called electrophoretic migration caused by the electrical attraction of ions in high electric field. However, if only an electrophoretic force is present, the neutrals and the anions migrating backwards to capillary entrance will not be detected.

Most capillaries are made of fused silica containing silanol groups (SiOH) on the capillary surface. This group becomes negatively charged, SiO^-, in buffers with pH above about 2. At the interface between the capillary wall and buffer solution, the negatively charged surface of the capillary attracts positive ions from buffer solution to form an electric double layer, the inner Hemholtz layer and outer Hemholtz layer where positive ions are solvated. The solvated positive ions tend to migrate towards the cathode creating a driving force for the bulk solution.

The movement of the solvated ions and buffer solution is called electroosmotic flow (EOF). The potential that exists at the shear plane of the double layer is called the zeta potential. Zeta potentials depend on the amount of negatively charged silanol groups as well as the concentration of cations in solution, and therefore these potentials depend on the pH of buffer solution. In the presence of EOF, the migration of ionic species is not only driven by electrophoretic force but also the EOF. As the EOF is towards the anode and its magnitude is usually larger than the electrophoretic movement, all species including negative, positive and neutral ones move towards the exit of the capillary, however, at different velocities. Positive ions move fastest followed by neutral species and subsequently negative ions. Among positive ions, ions with smaller size or more positive charges move faster than the ones with larger size or less positive charges. A similar pattern is observed among negative ions, however, with the opposite effect from migration speed. Neutrals cannot separate from each other as they all have the same velocity caused by EOF. Consequently, all analytes arrive at the detector at different times, except neutral species. The principle of operation for CE and the relative migrations of EOF and ions are shown in Figure 11.

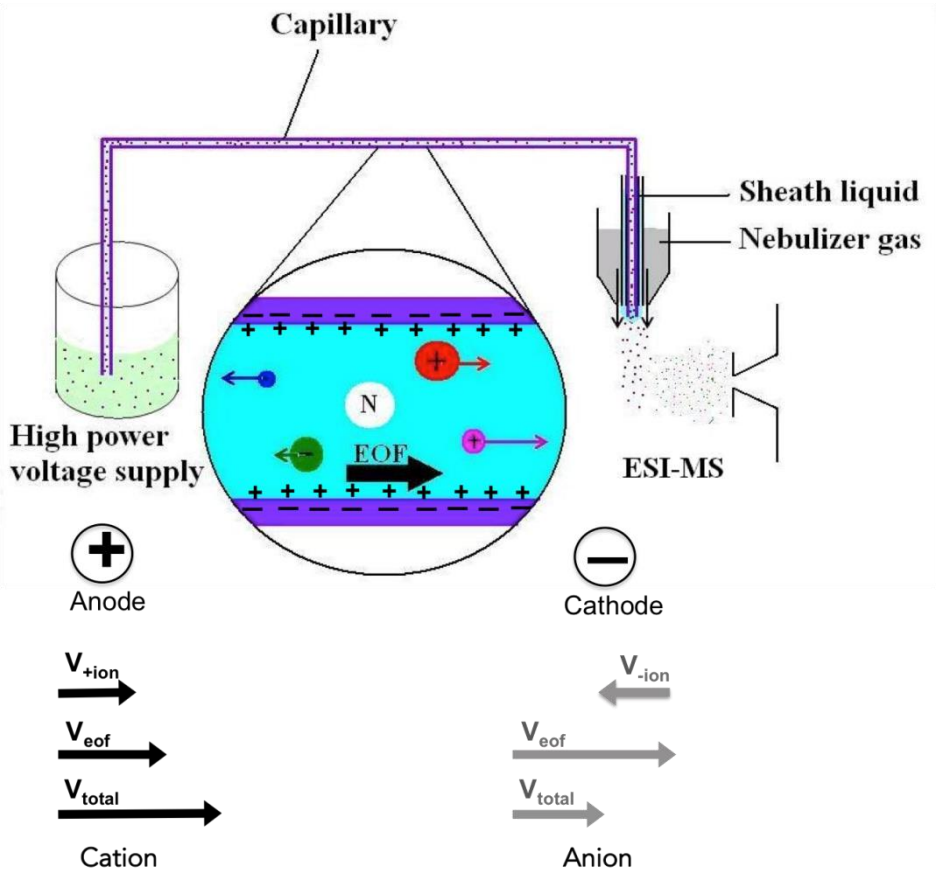

Figure 11. Schematic operation of CE-MS with an ESI interface and an illustrative explanation of EOF and electrophoretic velocities.

The velocity of bulk solution caused by EOF, v_{EOF}, is presented in equation 1:

$$v_{EOF} = \frac{\epsilon\zeta}{4\pi\eta} E = \mu_{EOF} E \qquad (1)$$

Where: **ε** is dielectric constant of solution, ζ is zeta potential, η is viscosity of solution, μ_{EOF} is electroosmotic mobility, and E is the electric field strength.

The velocity of the analyte with spherical shape caused by electrophoretic flow (EPF), v_{EPF}, is presented in equation 2:

$$v_{EPF} = \frac{q}{6\pi\eta r}E = \mu_{EPF}E \qquad (2)$$

Where q is the charge of the analyte, r is the radius of the analyte, μ_{EPF} is electrophoretic mobility.

As a result, the total velocity of the analyte is the sum of these velocities as in equation 3:

$$v_{total} = v_{EOF} + v_{EPF} = (\mu_{EOF} + \mu_{EPF})E \qquad (3)$$

There are several modes of CE depending on the analytes to be separated and samples, including capillary zone electrophoresis (CZE), capillary gel electrophoresis (CGE), capillary electrochromatography (CEC), micellar electrokinetic capillary chromatography (MECK), and capillary isotachophoresis (CITP). Each has a particular modification to the characteristics of the electrolyte buffer or the capillary in order to improve separation of specific groups of analytes. CZE, however, is the most common due to its universal application, simplicity, and ease of manipulation. CZE is compatible with MS detection because the materials used for electrolyte buffer and capillary in CZE are "chemically friendly" to MS compared to the other modes of separation.

4.2. CE in comparison to HPLC

In comparison to HPLC, the other major liquid phase separation technique, CE provides several advantages.[120] First, using an open tubular capillary without a stationary phase, CE exhibits no eddy diffusion, which is present in packed columns in HPLC. In addition, a flat plug flow profile is obtained in CE driven by EOF that is different from the parabolic flow profile in HPLC driven by pressure. These factors contribute to peak broadening and therefore lower separation efficiency in HPLC compared to CE. Characteristic flow profiles in CE and HPLC are shown in Figure 12. Second, CE is better suited for analysis of small size samples as the sample volume required is much smaller (nL) than HPLC (typically µL), although recently developed ultra-HPLC can decrease the volume to low µL level. In addition, the volume of buffer consumed by CE is microliters to milliliters whereas HPLC can use liters of solvent. Another advantage of CE is that instrumentation is simpler and less expensive.

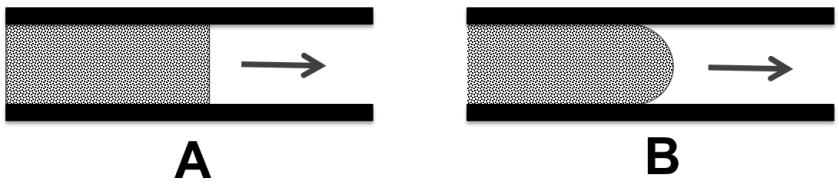

Figure 12. Characteristic flow profiles in CE and HPLC. **A.** Plug flow profile in CE. **B.** Parabolic flow profile in HPLC.

4.3. Electrospray ionization mass spectrometry (ESI-MS)

Online coupling of CE and MS has been established as a powerful analytical tool combining highly efficient separations and a highly accurate identification and quantification approach. One of the critical factors determining the performance of CE-MS is the efficient transfer of the analytes from the capillary to the mass spectrometer without affecting resolving power. It is

facilitated by using an optimized interface. There are several types of CE-MS interfaces suitable for different ionization methods such as fast atom bombardment, thermospray, ESI, APCI, and inductively coupled plasma. ESI is the most preferred choice at present since it transfers the analytes directly from the capillary to MS at close to atmospheric pressure. This makes the instrumental setup simple and convenient for operation. In addition, ESI provides a stable spray of solvent, facilitating stable ionization and transfer of analytes to the MS. This results in high reproducibility of the measurements. Moreover, multi-charged ions can be obtained by ESI enabling detection of large molecules like proteins.

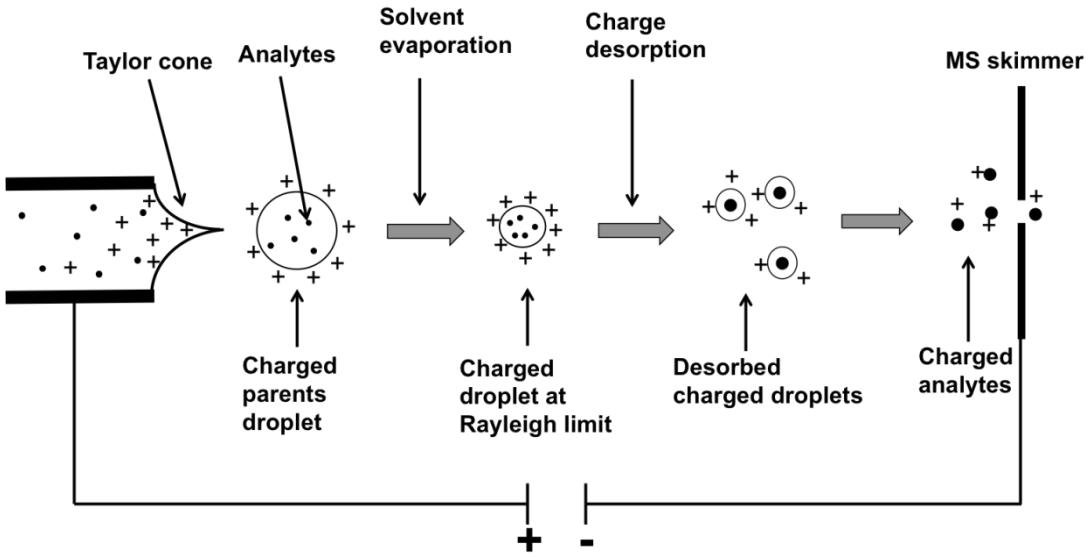

Figure 13. Operational principle of ESI.

The operational principle of ESI is shown in Figure 13. The exit of the capillary is connected to an electrically conductive base where a potential of about 3-6 kV is applied with respect to a skimmer that acts as the MS inlet.[131] A coaxial sheath flow of solvent is supplied to the end of the capillary. When buffer solution containing the analytes arrives at the exit of the capillary, in the presence of high electric field 10^6 V/m, a Taylor cone is produced at the tip of the capillary as a result of electrical attraction on the ions of opposite polarity in the buffer solution towards the skimmer. The sheath flow provides a constant flow in order to maintain the stability of the Taylor cone. Ions continue to accumulate on the liquid surface of the Taylor cone, which then will break to produce charged droplets. On the way to the skimmer cone, the solvent in the charged droplets evaporates leading to an increase in surface charge density and a decrease in droplet size. At the time when the electric field strength within the charged droplet exceeds the surface tension of the droplet (Rayleigh limit), the ions are desorbed from the droplet to become free ions in the gas phase. The gaseous ions are then extracted by the skimmer and separated in the mass analyzer according to their mass to charge (m/z) ratio. Sheathless interfaces are also available, yet usually give poor reproducibility although offer somewhat better sensitivity.
In this thesis, CE-MS was used in papers 1 and 2 for analysis of the concentration of the stimulant drug methylphenidate and its metabolites as well as to quantify neurotransmitter levels in *Drosophila* heads.

CHAPTER 5. BIOLOGICAL IMAGING MASS SPECTROMETRY

Imaging mass spectrometry is a powerful imaging technique for visualizing the spatial distribution of chemical components in samples, from inorganic and organic materials to biological tissues and single cells. IMS is distinguished from other imaging techniques such as immunohistochemical imaging, chemical staining, and fluorescence microscopy owing to its unique characteristics, especially the label-free and non-targeted detection, high chemical specificity, high accuracy for structural elucidation, and sufficient sensitivity for single cell analysis. IMS, particularly secondary ion mass spectrometry (SIMS) and MALDI, has been rapidly and continuously developing to meet the expectations and needs of various research areas. For biological, medical and pharmaceutical research, IMS has been increasingly recognized as a very useful approach for studying biological processes, biomarkers of diseases, and pharmacology.

5.1. ToF-SIMS imaging

5.1.1. Principles of SIMS

Secondary ion mass spectrometry is a powerful imaging technique providing chemical information with high spatial resolution (< 50 nm). The spatial resolution ultimately depends on the spot size of the primary ion beam, but in reality is often limited by the available signal in each pixel. However, current developments in primary ion sources and matrix assisted SIMS have improved signal levels and, hence, the spatial resolution as well as the detectable mass range of the technique. SIMS typically allows the detection of biological molecules up to around 1500 Da, such as intact lipids, metabolites, lipid fragments, and elements.

Beside the advantages of being label-free and having molecular specificity, that are also obtained with any other mass spectrometric imaging techniques, SIMS provides chemical information potentially at submicron spatial resolution. In addition, it is versatile and capable of ionizing chemical species from almost all kinds of materials. Additional modification of the sample surface with matrices is not necessary in most cases and can be detrimental to image resolution. The surface sensitivity of the technique can be an advantage for some applications but extreme care must be taken during sample preparation to prevent any possible contamination.

The chemical ejection and ionization process of SIMS is shown in Figure 14. In brief, a focused ion beam, typically with energy between 5 keV and 40 keV, impacts the sample surface resulting in the ejection of secondary species (positive, negative, and neutral), the charged portion of which can be extracted and mass analyzed. The mass analyzers can be time-of-flight (ToF), ion trap, and magnetic sector; however, the most commonly used analyzer for biological analysis is the ToF due to its capability to rapidly carry out parallel mass detection with good mass resolution and mass range.

Insights into the generation of secondary ions under the impact of primary ion beams have been provided by collision cascade theory and by using a combination of molecular dynamic computer simulation and experimental work.[132-134]

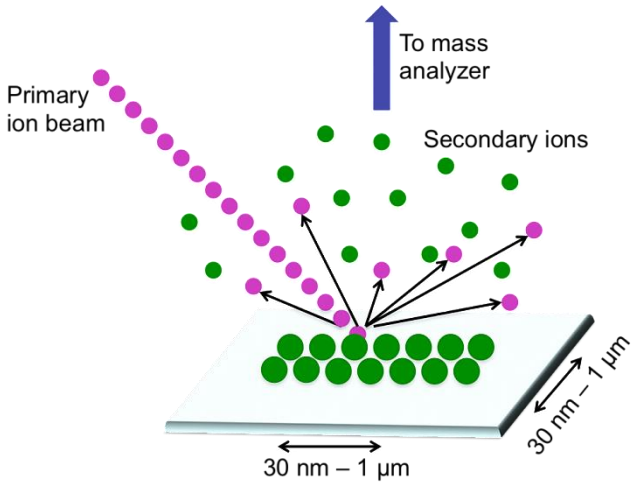

Figure 14. Ion ejection process in SIMS. Analytes are shown in green. Achievable spatial resolution is from 30 nm to 1 µm.

Collision cascade. As the primary ions impact a sample surface, they penetrate into the sample and transfer energy to sample molecules causing fragmentation and motion of the molecules. The transferred energy depends on the kinetic energy of the incident ions, typically ranging from 5 to 40 keV. As the transferred energy is much higher than the bond energies in the molecules, extensive fragmentation occurs within the impacted area where primary ions directly collide with the sample molecules. Further away from the impacted spot where the sample molecules collide with nearby energetic molecules, they receive less energy increasing the chance of ejecting molecular particles. This phenomenon is called a collision-induced cascade. Most of the ejected particles are neutral and often only 0.1% are ionized to positive or negative ions depending on the electronic configuration of the molecules.

Parameters influencing secondary ion yield.
The basic SIMS equation is:[134]

$$I_m = I_p Y_m \alpha_m^{\pm} \theta_m \eta \qquad (4)$$

Here, I_m is the secondary ion current, I_p is the primary ion current, Y_m is the sputter yield of secondary species including ions and neutral, $\alpha_m^{\pm}$ is the ionization probability, θ_m is the fractional surface concentration of analyte m, and η is the transmission of instrument.
There are several important factors affecting the generation of secondary ions in SIMS including the mass and size of primary ions, the kinetic energy of primary ions, the angle of incidence, and the properties and composition of the target material. A number of simulation studies on different primary ion sources with a variety of target materials have been carried out. Postawa and co-workers[135] performed a study on the ejection from a Ag [111] surface covered with three layers of benzene using 15 keV Ga^+ and C_{60}^+ incident ions. They showed that the atomic Ga^+ projectile only loses 3 % of the original kinetic energy (15 keV) when impacting benzene layers. This is because the collision surface between a Ga^+ ion and benzene molecules is small producing a lower damage cross section, the measure of the surface area being damaged by a primary ion, than the C_{60}^+ ion. Consequently, the remaining high kinetic energy Ga^+ ion can penetrate easily through the organic layers to the Ag substrate therefore resulting in a high

damage depth - the thickness of the sample being damaged by primary ions. The C_{60}^+, or bucky ball, on the other hand undergoes different mechanism when impacting as a primary ion. C_{60}^+ transfers its energy much more efficiently to the benzene layers on the surface compared to Ga^+ due to the larger interaction surface. For C_{60}^+ they found that 60 % of the energy was transferred for a 15 keV source. A 15 keV C_{60}^+ ion comprises 60 carbon atoms, each possessing 250 eV. Due to its low remaining kinetic energy after collision with the benzene surface, the C atoms do not penetrate deeply into the Ag substrate, but rather deposit their energy in a shallow layer on the sample resulting in a lower damage depth. The damage cross section, however, is higher with C_{60}^+. The secondary ion yield - the number of secondary ions ejected by incident primary ions - particularly for molecular ions is higher with C_{60}^+ than Ga^+. In general, the increased mass and size of primary ions provides improvement in secondary ion yield of molecular ions, less damage in depth, but a significant increase in damage cross section. These characteristics of the primary ions bring different advantages. Large size projectiles are well suited as etching beams, whereas the smaller size ones are commonly used as analysis beam for the benefit of spatial resolution as they are often formed from liquid metal ion sources.

To examine the effect of kinetic energy of the primary ions, Rzeznik *et al.*[136] created a model with a monolayer of benzene deposited on Ag crystal substrate and irradiated by Ar_{2953}^+ cluster projectiles with kinetic energies ranging from 0.1 to 20 eV/atom. The sputtering yield- the number of secondary species (ions and neutrals) ejected by each incident primary ion- of benzene was shown to increase linearly with increased kinetic energy when the energy exceeded a threshold value. At higher energy, the yield reached saturation. The results agreed with the findings from practical experiments carried out by Fletcher *et al.*.[137] In his work, the variation of secondary ion yield versus increasing impact energy of the primary ions C_{60}^+ was investigated for a variety of sample materials such as metals, antioxidants, biopolymers, phospholipids, and peptides. The results showed that the secondary ion yield was generally enhanced with increasing impact energy of the projectile on the different materials. Moreover, the linearity for high mass particles can be extended with higher energy. For instance, a 20 keV or 40 keV C_{60}^+ beam produces maximum yield for low mass secondary ions, m/z 50-200, whereas an 80 keV beam is optimum for ions of m/z 200-400. In the analysis of biological samples where high mass molecular ions are of particular interest, high energetic projectiles are preferably used in order to produce more molecular ions. It should be also noted that highly energetic projectiles can cause severe sub-surface damage as the primary ions can penetrate to many sample sub-layers.

The incident angle of the primary ions is also an important parameter affecting the secondary ion yield and sample damage. It has been demonstrated that there is an optimum incidence angle to obtain the highest secondary ion yield.[138] The optimum angle may vary with the projectile properties or sample materials. From the simulation of low energy Cs^+ irradiation on semiconductors (Si, Ge, InP) with incidence angles ranging from 0^o to 85^o, the highest yield is obtained at 65-75^o. The experimental work on cholesterol films deposited on Si substrates and bombarded by a 40 keV C_{60}^+ beam at the impact angle 40^o and 73^o showed that the 40^o angle is more beneficial for the sputtering yield.[139] Another modeling approach using solid benzene impacted by 14.75 keV Ar clusters, Ar_{366}^+ and Ar_{2953}^+, has been performed.[140] Although different sizes of cluster ions lead to different ejection processes, the optimum incidence angle is not significantly different between 40^o-45^o for different cluster sizes. The yield increases as the

angle increases from 0 to the optimum degree because the kinetic energy of the primary ions deposits closer to the surface with larger angle. This results in more efficient ejection of molecules on the top surface layers. Above this angle, the energy starts to be reflected, leading to decreased yield. However, from the damage viewpoint, the optimum angle is different. The optimum angle for secondary ion yield can lead to increased damage cross section while a glancing angle can limit damage depth.

5.1.2. Primary ion sources for SIMS

Development of new primary ion sources is one of the main thrusts in modern instrumental development of SIMS. The ultimate goal is to obtain spatial resolution as low as a few nanometers while minimizing the sample damage. The goal is to improve the ion beam efficiency, which is the ratio of secondary ion yield and the damage cross section. With continuous development, various primary ion sources have been made available in the field. Reactive atomic ion sources (Cs^+, O_2^+) can be focused to very small probe sizes (< 50 nm for Cs^+) and increase ionization by inducing fragmentation and altering the electronic state of the sample surface. Due to the high fragmentation, molecular information is typically lost. These ion sources are primarily used in dynamic SIMS experiments which use high ion dose densities to erode the sample, leading to high signal and sample degradation.

Liquid metal ion guns (LMIG) have ultrahigh brightness and produce extremely focused ion beams. These beams, when used at low doses (static SIMS), are capable of creating molecular ions; however, the relatively low availability of the molecular ions limits the useful size of the probe and increasing doses create higher damage. Materials used for LMIG have a low melting point, low volatility, low surface free energy and good wetting.[141] Ga^+ was the first candidate as it is a liquid at room temperature. Indium is a little easier to focus and the ion is larger. Metal cluster sources such as Au_n^+, Bi_n^+ are more recent common LIMGs with possible beam size ~100 nm. Metal clusters deposit energy slightly closer to the surface than atomic projectiles, leading to a slight decrease in damage. Moreover, they produce overlapping collision cascades resulting in high action/high yield events as identified by Delcorte and Garrison in molecular dynamic simulation studies.[142]

Cluster ion or polyatomic ion sources have received wide recognition since the observation that a SF_6^+ beam resulted in high secondary ion yield although damage cross section was only slightly higher compared to the Cs^+ beam.[143] The study inspired a significant amount of later research on the performance of this cluster beam and further investigation of other larger cluster sources. Kollmer[144] compared the performance of several atomic and polyatomic ion sources including Ga^+, Au_n^+, Bi_n^+, C_{60}^+ on the organic sample, Irganox 1010, and on the pharmaceutical, Salbutamol. They found that a significant increase of secondary ion yield occurred when the beam was changed from atomic Ga^+ to Au^+ and finally to polyatomic C_{60}^+. The damage cross section followed the same tendency, however, less significant. Therefore, C_{60}^+ provided the highest efficiency of secondary ion generation in that work. Another study performed by Touboul[145] compared the imaging capability of Bi_n^+ and Au_n^+ ion beams on rat brain samples. Different cluster sizes from the same projectile Bi_n were examined as well as similar size clusters of different materials. From the results, secondary ion yield efficiency increased 5 times from Bi^+ to Bi_3^+. In addition, Au_3^+ and Bi_3^+ showed very similar properties in terms of secondary ion yield and damage cross section as they have similar size and mass. However, the Bi_3^+ beam had higher current than the Au_3^+ beam resulting in shorter image acquisition times.

The reason for this is the lower ionization potential and lower melting point of Bi compared to Au. These properties indicate that the Bi_3^+ beam has the benefit of more efficient ionization and allows one to run the Bi_3^+ gun at very low emission currents to produce a low energy spread. The spot sizes obtained with 50 keV Bi_3^{2+} and 25 keV Au_3^+ sources are about 100 nm and 200 nm, respectively.[144] All together, the Bi_n^+ LMIG is well suited as a primary ion source for high spatial resolution imaging with static SIMS due to its advantage in spot size, secondary ion yield, and reasonable analysis time compared to other LMIGs. The C_{60}^+ source, due to its high secondary ion yield and low subsurface damage, is another main primary ion beam not only in dynamic SIMS for depth profiling but also in static SIMS for surface imaging when spatial resolution at submicron scale is not required. In addition, the C_{60}^+ source can function as an etching beam, thus enabling the possibility of 3D molecular imaging. The spot size of the C_{60}^+ beam is typically ~1 μm although it has been reported to focus to better than 200 nm on some systems.[146] Current investigations of the mega size gas cluster ion beams (GCIB) such as Ar_n^+ and $(H_2O)_n^+$ have attracted huge interest since they provide remarkably reduced fragmentation of the secondary ions due to softer sputtering by the clusters and minimal subsurface damage, although spatial resolution suffers. Simulations of the Ar_n GCIB have been performed. Cluster Ar_n^+ ion beams with an energy < 200 eV per constituent atom have been shown to be superior to C_{60}^+ beams in several aspects, particularly the degree of damage and fragmentation. Therefore, it appears to be an excellent etching beam in 3D imaging or depth profiling.[147] Matsuo, a pioneer in developing Ar cluster GCIB sources, examined the fragmentation degree for the amino acid arginine and the tripeptide gly-gly-gly under the incidence of atomic and cluster Ar ions with various sizes, Ar_{300}^+, Ar_{700}^+, Ar_{1000}^+, and Ar_{1750}^+.[148] The fragmentation was shown to depend on both energy and cluster size. In particular, low energy and large size resulted in higher molecular ion signals and cleaner spectra due to less fragmentation. In addition, when sputtering with a 5.5 keV Ar_{700}^+ ion beam onto polymer films, damage was significantly reduced. In addition to use as etching beams, cluster GCIBs have been used as primary analysis beams in several current studies. A water cluster ion gun, 10 keV $(H_2O)_{1000}^+$, has been developed by the Vickerman group to increase the ion yield for analysis by an enhanced proton mediated reaction.[149] The gun showed a 10 times improvement in the ion yield when applied to lipid standard samples. More recently, the Fletcher group has examined the performance of a high energy 40 keV Ar GCIB. They compared the imaging parameters between the 40 keV C_{60}^+, 20 keV Ar_{4000}^+, and 40 keV Ar_{4000}^+ guns on brain tissues and human hair samples.[150] The 40 keV Ar_{4000}^+ produced the highest signal relative to the other guns at m/z values above 500 Da and a spatial resolution of < 3 μm was obtained. GCIBs clearly have great potential as analysis beams, as well as etching beams, for imaging lipid and lipid related compounds in biological samples.

5.1.3. Acquisition modes in SIMS

There are two approaches for image acquisition by the primary ion beam in IMS, microprobe and microscope.[151-152]

Microprobe. In SIMS imaging the most common approach to obtain chemical information from a material is the microprobe mode in which a focused primary ion beam is used to continuously raster the surface spot by spot or pixel by pixel. When the primary ion beam sputters a pixel, the secondary ions generated are extracted and separated by the mass analyzer to produce a mass

spectrum of this pixel. The beam then continues to sputter a new spot to produce a spectrum until the whole surface is scanned. The relative position of the primary ion beam spot is recorded and is used to reconstruct the spatial localization of the secondary ions on the sample. Consequently, an ion image in which the signal intensities of the ions are displayed using a color scale to indicate intensity is constructed for specific ions from all the spectra as a function of position. In the microprobe mode, spatial resolution is determined by a combination of the beam size and the abundance of the ions detectable within the spot. The primary ion beam in SIMS can be normally focused to submicron diameters, and this can define the spatial resolution if the sensitivity is sufficient. The microprobe mode is mainly used in static SIMS for the advantages of spatial resolution, sensitivity, and data transfer rate limitations in ToF measurements.

Microscope. Alternatively but less commonly, a position-sensitive detector can be used, introducing another concept of imaging acquisition, the microscope mode. The commercial CAMECA IMS instrument is operated with this microscopic acquisition approach and much of the early work in dynamic SIMS imaging was carried out this way. In this mode, an unfocused primary ion beam is used to sputter a large area of the sample surface. The desorbed ions keep their original spatial position relative to their origin on the sample while they travel through the ion optics to the detector. The spatial resolution does not depend on the beam size but on the quality of the ion optics and the detector. This approach is well suited for dynamic SIMS for profiling as often spatial resolution is not a very strict requirement. Moreover, larger areas can be measured thus helping to reduce the number of pixels and analysis time compared to microprobe mode.

5.1.4. Static versus dynamic SIMS

Sensitivity and spatial resolution are the major challenges in any imaging technique especially for biological applications. SIMS accommodates these needs by two methodological regimes, static SIMS and dynamic SIMS.

In static SIMS, a primary ion beam impacts the surface at a dose density below a certain level called the static limit, typically taken as 10^{13} ions/cm^2,[134] although this can be much lower for organic samples. Ideally, only 1 % the material on the surface is sputtered ensuring that secondary ions represent the chemistry of the pristine sample. Because a focused primary ion beam is used, chemical information from the surface can be highly spatially resolved. This regime is used when the chemical composition on the sample surface is of particular interest or when increased primary ion dose density results in chemical damage in the sample sub-surface. Static SIMS has been increasingly applied in biological studies to map the distribution of biomolecular ions below 1500 Da such as atomic species, amino acids, fatty acids and intact lipids. Due to the restricted primary ion dose, static SIMS faces a major challenge in sensitivity. The developments in primary ion sources, described above have been in progress with the aim to enhance the secondary ion yield while maintaining or improving the spatial resolution.

In contrast to static SIMS, dynamic SIMS utilizes a high dose density of primary ions (above the 10^{13} ions/cm^2 limit) to erode the sample. In dynamic SIMS instruments, quadrupole or magnetic sector mass analyzers are commonly utilized as they are compatible with a continuous, d.c., primary ion beam. Typically, reactive primary ion beams using ions such as O_2^+ and Cs^+ are used giving high secondary ion yield to enhance sensitivity, however, these also result in higher fragmentation. The regime therefore is mainly used to analyze atomic and small fragmented

ions. To extract molecular information, isotopic labeling strategies have been developed. Multiple-isotope imaging mass spectrometry (MIMS) allows imaging of several molecular species using dynamic SIMS.[153] Furthermore, a high primary ion dose erodes the sample and gives the third dimension or three-dimensional (3D) imaging. Due to abundant signal in a very small pixel, dynamic SIMS can provide very high resolution for imaging (< 50 nm).

3D imaging has been an emerging label-free imaging modality attracting huge interest in the biological and medical communities. This modality provides a three dimensional distribution of the molecular species within an organism. As discussed above, various primary ion sources have been introduced for SIMS. Since the introduction of polyatomic ion guns, especially C_{60}^+, conventional ToF-SIMS instruments have utilized a combination of static and dynamic SIMS for 3D imaging. In this approach, a finely focused analysis beam commonly, an LMIG, is used to statically image the sample, then a non-focused etching beam such as a polyatomic ion gun is used to dynamically remove the damaged layer to prepare a fresh new surface for the next cycle. The analysis can be continued effectively etching through the sample and chemical images of all the layers can be stacked together to create a 3-dimensional chemical image. Dual beams or a single beam can be used for both analyzing and etching. The most recently developed instrument for this approach, the *J105-3D Chemical Imager* from Ionoptika Ltd; however, employs a C_{60}^+ ion gun to dynamically erode the sample and 2D images are recorded along the depth of the sample. Unlike with the other dynamic SIMS instruments, the J105 uses a ToF mass analyzer and the use of the C_{60}^+ gun enables detection of molecular ions up to about m/z 1000 Da. The 3D analysis regime has opened up numerous biological applications for SIMS as it allows simultaneous mapping of biomolecules inside bio-systems without any further chemical labeling.[154-155]

5.1.5. SIMS imaging with the J105-3D Chemical Imager

There are various designs of SIMS instruments; the most common for organic sample analysis utilizes a pulsed primary ion beam for sputtering the sample and a ToF mass analyzer to ensure high mass resolution and allow parallel mass detection capability. The most recently developed ToF-SIMS instrument, the *J105-3D Chemical Imager*, with a special design provides different capabilities and advantages for SIMS analysis.[156] A schematic of the J105 is shown in Figure 15.

In the J105, a continuous d.c. primary ion beam is used and the secondary ion beam from the sample is pulsed by a buncher placed in front of the ToF analyzer. In this instrument, the continuous stream of secondary ions ejected from the sample first enters into an rf-only quadrupole where the energy of the ions is removed by collision with a gas. The ions are then filtered through an electrostatic analyzer before entering the buncher.

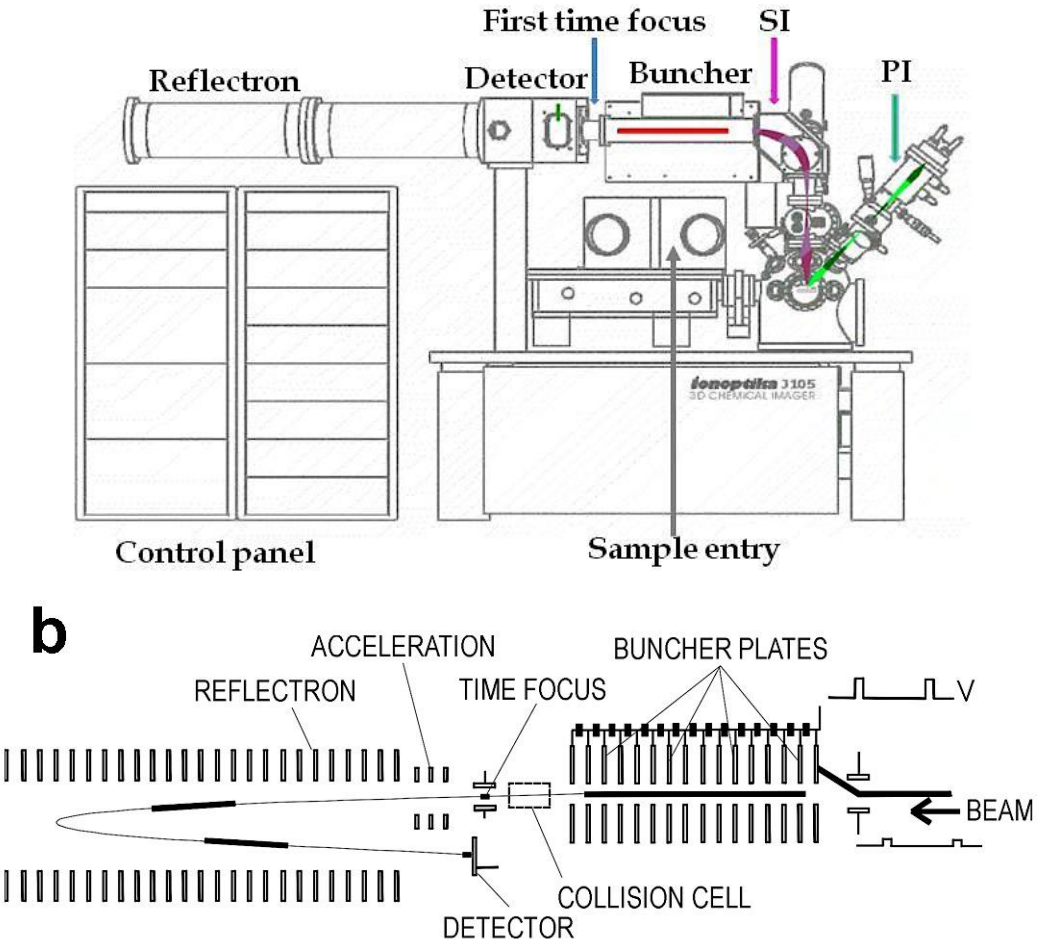

Figure 15. Schematic of the J105-*3D Chemical Imager* (A), and operation of the buncher and harmonic field ToF reflectron (B).[156]

In the buncher, the ions are squeezed into short pulses using accelerating voltages applied between the entrance and the exit of the buncher. The energy spread of the bunched ions after the buncher is about 6 keV. By using a continuous primary ion beam, the duty cycle increases significantly therefore shorter analysis time is obtained compared on the same sample analyzed with a conventional instrument. All of the sample material is used for analysis thus helping to increase the sensitivity. In addition, unlike conventional ToF-SIMS instruments, the mass resolution is independent from the sputtering process and sample topography that causes a mass shift due to a variable travel time of the secondary ions. As a result, compromise between mass resolution and spatial resolution is not required, and mass calibration is not needed for every spectrum. The J105 in our laboratory is equipped with a 40 keV C_{60}^+ primary gun and a high energy 40 keV Ar GCIB both of which can be used as either etching or analysis beams. The mass resolution of the instrument ~7000 for m/z 700-800 can be readily obtained for biological samples. Spatial resolution is less than 1 μm and 3 μm for the C_{60}^+ and Ar_{4000}^+ GCIB, respectively.

The J105 uses a harmonic field ToF reflectron. Conventional ToF-SIMS instruments utilize field free ToF where the flight time of the ions with equal kinetic energy are separated based on their different m/z. However, such analyzers are incompatible with the large energy spread produced in the secondary ion bunching process. In the harmonic field ToF, the ions travel in a quadratic field that allows the independence of time of flight from initial energy of the ions. A

useful feature of the strategy of the J105 analyzer is that it allows tandem MS to elucidate secondary ion structure. Secondary ions are dissociated by collision at high energy (1-6 keV as the collision occurs after the ions have left the buncher) with a gas such as N_2 or Ar in a collision cell located between the buncher and ToF analyser. After colliding, the parents and fragmented ions of choice are selected using a timed ion gate before traveling in the ToF analyzer.

Finally, the instrument is equipped with a glove box to facilitate sample handling. The glove box can be filled with Ar gas so that the sample is kept away from moisture. This is very useful and especially important for frozen samples to prevent an ice layer from being deposited on the sample surface and hindering the analysis. This is also beneficial for samples sensitive to moisture.

5.1.6. Sample preparation for SIMS imaging

To acquire relevant chemical and spatial images of a sample, especially heterogeneous biological samples, one of the most important and sometimes difficult issues is choosing a suitable sample preparation method. The main challenge here is how to preserve the morphology and chemical information of a sample while exposing it to high vacuum conditions. A number of sample preparation protocols suitable for particular applications have been developed, each with their own advantages and limitations.[157-159] The main protocols that have been widely used are freeze-drying, fixation, freeze fracture, frozen hydrated analysis, etching by temperature or etching with a defocused etching gun such as C_{60}^+ or low energy Ar GCIB.

The most common and convenient method is freeze-drying. Briefly, freshly obtained biological tissue is plunge frozen. The plunge freezing minimizes the ice crystallization in the sample. Frozen tissue is then cryosectioned, typically at -20 ^oC, into 10-25 µm slices. The tissue slices are then mounted onto a conductive substrate and subsequently inserted into a vacuum of ~10^{-3} mbar where the water from the samples is sublimated slowly to dryness. Cellular samples may undergo a similar procedure in which the cells can be sectioned by an ultracryostat producing slices with thickness down to several µm. Alternatively, cells can also be freeze dried directly after plunge freezing. Freeze drying enables analysis at room temperature making it simple and easy to handle the samples. The method is well suited for tissue imaging; however when subcellular distribution is of interest, freeze-drying induces a risk of morphological change of the sample and chemical migration can occur during the drying process causing artifacts in analysis.[160]

Freeze fracture and frozen hydrated sample preparation have been considered the ideal methods for maintaining chemical and structural information for subcellular biological imaging.[158] Typically after plunge freezing, samples are kept frozen during the analysis. In freeze fracture, tissue or cellular samples are plunge frozen in a sandwich assembly, which is opened in the instrument under vacuum. The sample surface is exposed to provide intact chemical information. The protocol protects the sample from possible environmental contamination and produces a thin layer of condensed water, which enhances molecular ion signals.[161] In addition, the method can also be used to fracture the inner compartments of the cells for subcellular analysis. There is an issue with obtaining a suitable, reproducible fracture plane. Also, rough surfaces and buried samples often hinder the analysis.

In order to overcome the topographic problems in freeze fracture, etching by slightly elevated temperature or cluster ion gun can be employed to remove the top ice layer of the sample without damaging the subsurface, and also helps flatten the sample surface eliminating topographic problems. When etching by temperature the temperature is increased to a critical point so that the top overlayer of condensed water slowly sublimates exposing the biological sample below. Alternatively, sputtering with the C_{60}^+ gun or Ar GCIB can also be used to remove the water overlayer from the sample. These strategies maintain sample morphology and prevent contamination; however, the sample handling is elaborate and time consuming.

5.1.7. Applications of SIMS in biological samples

The contribution of SIMS to biological studies has been significantly increasing especially for tissue samples such as brain, heart, hair, intestine mucosa, spinal cord.[150, 162-165] Due to great improvements that have been made concerning practical spatial resolution due to improved signal levels, single cell analysis has also become an attractive area although it is still somewhat challenging.

To study lipid domains during membrane fusion, an important process in exocytosis, Ostrowski *et al.* used SIMS to image membrane lipids on mating *Tetrahymena thermophile* as a model of the high curvature in lipid fusion.[88] Two complementary cell strains were induced to mate and were prepared for analysis using the freeze fracture and frozen hydrated methods. In the intact plasma membranes of tightly bound *Tetrahymena*, the concentration of the lamellar shaped lipid PC (represented by the headgroup ion with m/z 184) diminished in the mating junction, whereas that of conically shaped 2-aminoethylyphospholipid (2-AEP) (represented by the headgroup ion with m/z 126) was more intense. In a later study, changes in the membrane domains observed previously were now examined as a function of the junction stability and it was concluded that the cell membranes formed junctions prior to changes in lipid composition.[166] SIMS images of mating *Tetrahymena* are shown in Figure 16A-C.

SIMS is not only capable of 2D imaging of single cells; applications of SIMS for 3D imaging of single cells have also been reported although these are still sparse in the literature.[155, 167-168] Fletcher *et al*.[167] performed 3D imaging on Hela cells using the J105 with single beam 40 keV C_{60}^+. The authors examined sample preparation approaches including fixing with formalin, freeze-drying, and non-fixing, and frozen-hydrated samples (Figure 16D-E). For frozen-hydrated sample preparation, a freeze fracture device called a *mousetrap* was used to fracture the sample apart exposing clean cells for analysis. The C_{60}^+ beam was used to obtain a series of images with the ion fluence exceeding the static limit. The frozen-hydrated method preserved the localization of many cellular components. Specific cellular markers, the headgroup of the membrane lipid phosphotidylcholine at m/z 184 and the DNA base adenine at m/z 136, were used for 3D image reconstruction. Subcellular compartments such as nuclei and endoplasmic reticulum were clearly visualized.

Another example is the 3D imaging of Hela cells using the ION-TOF instrument with dual beams; a 25 keV Bi_3^+ as the analysis beam and a 10 keV C_{60}^+ ion source as the etching beam.[168] The cells were incubated with a nuclear marker bromodeoxyuridine (BrdU), fixed with paraformaldehyde, then washed and air dried before analysis. The etching step with C_{60}^+ proved very useful to remove the damage or smearing during air-drying sample preparation. Different acquisition modes were checked with regard to the ion image qualities. The burst mode, in which the primary analysis beam is fired in a burst of short pulses of primary ions, was used as

it showed good compromise between spatial resolution and mass resolution. The data showed clearly that the location of nuclei marked with BrdU and other subcellular regions represented by cellular markers like CN^-, CNO^- and $C_xH_yO_z$ could be distinguished in 3D.

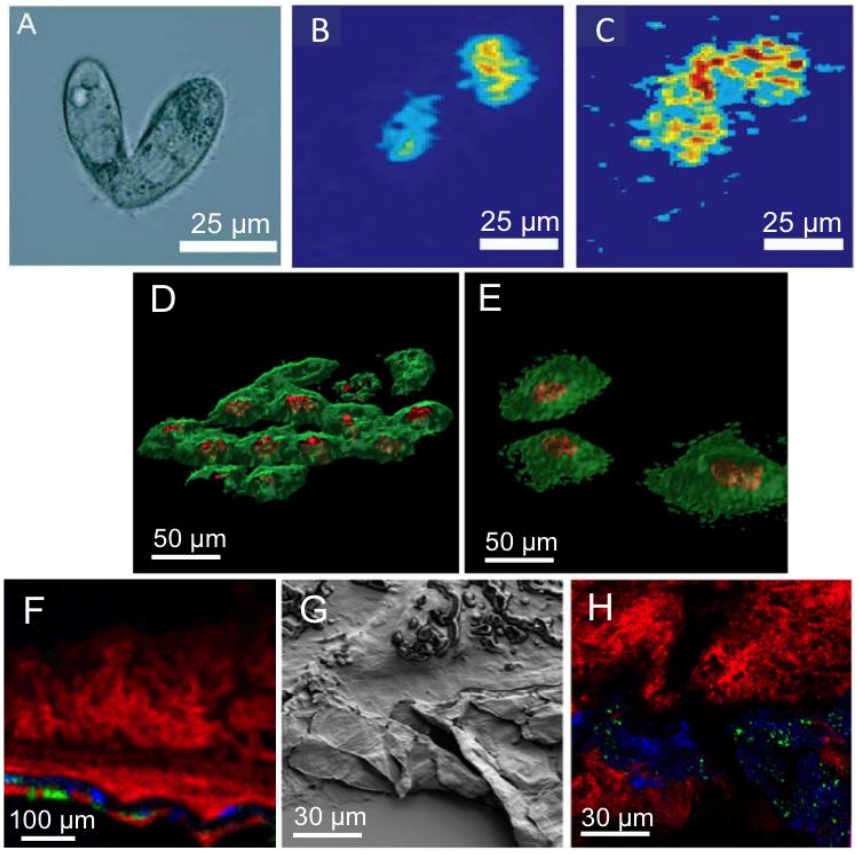

Figure 16. Some biological applications of SIMS IMS. (A-C) Imaging of a mating *Tetrahymena* cell pair. (A) Microscopic image, (B-C) SIMS selected ion images, (B) PC m/z 184, (C) 2-AEP m/z 126. Scale bars are 25 µm; (D-E) 3D imaging of Hela cell membrane, (D) Frozen hydrated cells, membrane (m/z 184) in green, nucleus (adenine at m/z 136) in red, (E) Fixed freeze-dried cells, membrane (m/z 184) in green, nucleus (guanine at m/z 152 and tryptophan at m/z 130) in red; (F-H), Chemical distribution of the cross section of mouse ear topically treated with drug roflumilast, (F) SIMS image: roflumilast in green, ceramide fragment in blue, PC in red, (G) SEM imaging of cross section of mouse ear, (H) High resolution SIMS image: roflumilast in green, phospholipids PO_2^- in blue, fatty acid (C24:0) at m/z 367 in red.[166-167, 169]

The potential of SIMS for subcellular imaging has been enhanced by the development of MIMS applied in dynamic SIMS. Several prominent examples of this technique include tracking and quantifying stem cell division in mammalian intestine, lipid metabolism in individual lipid droplets which presents the abundance of enterocytes in *Drosophila* intestine, quantifying the protein synthesis in hair-cell stereocilia of the inner ear of frogs and mice in *vivo*.[170-171] MIMS was used to investigate the mechanism and the sites of action of the drugs at subcellular level. Multimodal imaging of the distribution of the ^{15}N labeled platinum-based anticancer drug cisplatin in human colon cancer cells was performed using MIMS and fluorescence microscopy.[172] Monolayers of colon cancer cells were adhered on the substrate where they were treated with ^{15}N labeled cisplatin. The cells were then embedded in resin and subsequently

sectioned for MIMS analysis. Different cellular compartments were identified based on different atomic secondary ion images including the cytoplasm, nucleus, nucleolus, and chromatin. Cisplatin was found to accumulate in sulfur-rich and phosphorous-rich aggregates inside the cytoplasm and nucleolus, where the drug was believed to bind to S-ligands and DNA. In addition, the drug also had high affinity to N-ligands and acidic environments. The affinity of the drug towards S-rich, N-rich, and acidic organelles could be the basis for the mechanism of action of the drug and the cell resistance mechanism.

In order to obtain good treatment of dermatological diseases, it is important to understand the penetration properties of the topically applied drugs into the skin. ToF-SIMS with 25 keV Bi_3^+ LMIG was used to image the skin cross sections of inflammatory mouse ears topically treated with the active pharmaceuticals ingredients (Figure 16F-H).[169] In addition, SEM microscopy was also used in correlation with SIMS imaging in order to observe the structure of different skin layers and the distribution of the drugs in the skin. The frozen samples were sectioned then dried before they were analyzed at room temperature. From the analysis, various lipids were detected such as ceramides, phospholipids, sphingolipids, cholesterol, cholesterol sulfate, fatty acids and TAGs, and all had heterogeneous distribution across the skin section. Particularly, fatty acid (C24:0) and cholesterol sulfate localized in stratum corneum, whereas ceramide was excluded from this region. On the other hand, some PE, PI, and sphingomyelin species showed homogeneous distribution. All the drugs were shown to distribute heterogeneously on the skin surface and within stratum corneum except roflumilast, which penetrated further into the inner epidermis layer. The detection limit of the drugs based on signal to noise in the spectra of the control and drug treated sections was 1-2 mM. ToF-SIMS together with SEM can be a very good imaging approach to map drug delivery in a biological body and might be highly valuable for clinical and pharmaceutical studies.

Osteoarthritis is a common rheumatic disease characterized by the loss of cartilage caused by the disorder in lipid metabolism and ion regulation in the chondrocytes, cells that form cartilage. To study the alteration in chemical composition and structure, particularly lipid and elements caused by osteoarthritis, Cillero-Pastor *et al.* used ToF-SIMS with a Au^+ primary ion gun to observe the difference between healthy and diseased cartilage.[173] Principal component analysis and discriminant function analysis were utilized to reveal the biomarkers for osteoarthritis, which included the fragments of vitamin D_3, prostaglandins, glycerolipids, and fatty acids. There was significant accumulation of cholesterol and fatty acids in the superficial area of the osteoarthritis cartilage. Vitamin E also increased in the cholesterol rich area. Moreover, Ca^{2+}, PO_2^-, PO_3^- ions were highly localized in the diseased cartilage, whereas CN^- representing protein content decreased. The study shows that the synthesis and metabolism of lipids are closely involved in the pathological effects of osteoarthritis.

In a final example, the recently developed Ar cluster GCIB has been used for biological analysis in terms of molecular signal enhancement. Gas cluster ions (20 keV Ar_n^+, n=1-6000) were used to map the distribution of intact lipids in a mouse brain section.[174] In addition to the signal intensities obtained using pure Ar clusters, Ar clusters doped with less than 5% CH_4, and the 40 keV C_{60}^+ gun were compared. The use of Ar_{1700}^+ produced significantly higher lipid signals in the mass range between 600-850 compared to the use of C_{60}^+. Within this mass range, various observed lipids distributed differently across the mouse brain, especially lipids and cholesterol, which had complementary localizations. For instance, the $[M+H]^+$ pseudomolecular ion and K^+ and Na^+ adducts of PC (32:0) localized mainly in the hippocampus and inner cerebellum,

whereas cholesterol was abundant in the white matter surrounding the hippocampus and cerebellum. Glucosyl ceramide (d18:1/16:0) on the other hand distributed within the corpus callosum. Finally, another important point of the study is that a small amount of CH_4 (1.1 %) incorporated into the Ar clusters in the beam further enhanced the signal intensity of intact lipids by two times. The beam size of the Ar cluster gun in this case was 4 μm.

5.2. MALDI imaging

5.2.1. Principles of MALDI imaging

Matrix-assisted laser desorption ionization imaging mass spectrometry has played an important part in the imaging technologies for organic compounds in biological, pharmaceutical, and medical science. The technique provides spatially resolved information of the analyzed ions over a mass range from several hundred to several tens of thousands of Da, which covers a variety of biomolecules including intact lipids, peptides, proteins, and polymers. The principle of MALDI is illustrated in Figure 17.

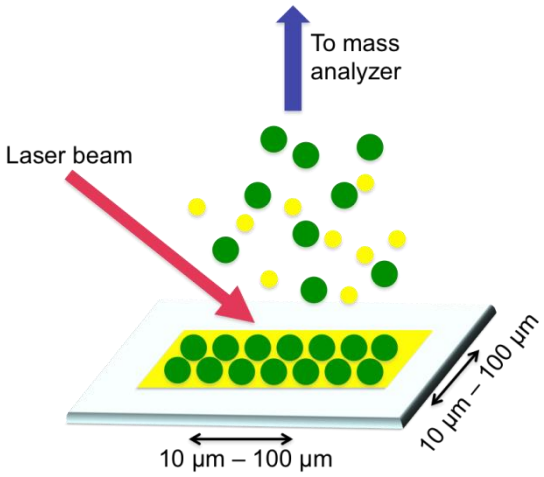

Figure 17. Principle of MALDI ionization. Analytes are in green, matrix is in yellow. Laser spot size is typically from 10 to 100 μm.

Typically in a MALDI imaging experiment, a sample is coated with a thin homogeneous layer of organic matrix solution before analysis. The role of the matrix solution is important for the soft ionization of the analyzed biomolecules. The matrix solution helps extract the biomolecules from the sample surface to mix and co-crystalize with the matrix molecules when the solution evaporates. The matrix then resonantly absorbs the energy from the irradiated laser to become excited matrix molecules.[175] The amount of the energy deposited per unit volume increases causing perturbation of the solid-state structure of the matrix and analytes. As the deposited energy reaches an appropriate level, disintegration of the solid phase occurs. The desorption of ions thereafter occurs within the expanding phase of matrix and analyte molecules. Analytes can also be ionized *via* protonation by the resonantly absorbing matrix. MALDI is a soft ionization technique in that there is little fragmentation of molecules during ion formation. Ions are normally singly charged. The lasers used in MALDI are UV or IR lasers, most common are the N_2 at wavelength 337 nm, and the frequency tripled Nd:YAG at 355 nm.

5.2.2. Spatial resolution in MALDI imaging

Spatial resolution is one of the biggest challenges in MALDI IMS for biological imaging. Generally the achievable spatial resolution on a commercial MALDI instrument is about 20 µm (although some are quoted at 10 µm), which is the smallest spot size of the laser. Spatial resolution is primarily dependent on laser beam size and matrix crystal size. Modifying either of these factors should improve the spatial resolution. There have been various ways to narrow the beam size. With a given laser on a commercial MALDI, oversampling can be used.[176] The laser completely ablates the overlapping part of two adjacent spots therefore significant signal only comes from the fresh adjacent area which is smaller than the spot size. This strategy has a long analysis time; however, as it requires complete ablation of material. An alternative is the use of the microscope acquisition mode with a position-sensitive detector like that used in SIMS although this is not commercially available.[177] Another approach is an instrumental development where the optical geometry is altered so the laser irradiates from the back side of the sample placed on a transparent substrate.[178] With this geometry, the beam size can be focused down to 1-2 µm. Spengler has used an atmospheric MALDI interface to produce a co-axial laser/ion extraction system where the laser focal length can be greatly reduced for improved spatial resolution.[179]

5.2.3. Sample preparation for MALDI imaging

Good sample preparation is again a critical requirement in MALDI imaging in order to maintain the spatial information and natural abundance of the analytes on the sample from the time of sample collection until analysis. It influences the sensitivity, reproducibility, and accuracy of the imaging. In MALDI, depending on the sample and the biomolecules of interest, sample preparation can include several or all the following steps: sample collection, storage, sectioning into thin slices, thawing and drying, washing, on tissue digestion, surface modification and matrix deposition. For tissue samples, sectioning with a cryo-microtome is carried out to obtain thin slices within the 10-25 µm thickness range. The sections are then placed onto a conducting substrate for example indium tin oxide (ITO) coated glass and freeze-dried before further surface modification and matrix deposition.

Sample washing. Washing is recommended to remove unwanted and easily diffusible molecules like salts from the sample surface so that they do not affect the measurement. Ion suppression is usually observed in samples having high salt content and this obscures the signals from the analytes of interest. In addition, the crystallization process is also influenced by the presence of salts.[180] Washing procedures vary depending on the molecular group of interest. A common washing procedure to remove salts is to use ethanol, 70 %, followed by 90 % ethanol, which helps temporarily fix the sample. For lipid analysis on high salt containing samples, very mild and quick washing with a low concentration (5-10 mM) of a MS friendly salt like ammonium formate can be helpful to partially remove the salt content. For analysis of high mass species such as peptides and proteins, removal of high lipid content can be carried out with an organic solvent such as chloroform or xylene.[181] Cold washing can also be used to minimize the delocalization of the biomolecules while removing the interferences.

Matrix deposition. Matrix deposition is one of the most important steps in sample preparation for MALDI. A matrix solution typically comprises three components, an organic solution such

as ethanol, methanol or acetonitrile, an organic matrix material, and trifluoroacetic acid (TFA). Choosing the suitable matrix material and solution compositions are critical tasks, not only to obtain high quality spectra but also to preserve spatial distribution of the molecules of interest in the samples. In addition, the quality of ion images is also affected by these parameters. Different matrices have different crystal sizes, for example crystals of 2,5-dihydroxybenzoic acid (DHB) are larger than those of α-cyano-4-hydroxycinnamic acid (CHCA), thus this restricts the minimum achievable spatial resolution in MALDI imaging. Various matrix materials have been investigated for different target groups of molecules in the mass range from several hundred Da to several hundred kDa. Sinapinic acid (3,5-dimethoxy-4-hydroxycinnamic acid, SA) is a common matrix for high mass molecules like proteins while CHCA and DHB have been widely used for detection of intact lipids, metabolites, and small peptides in positive ion mode.[181] The use of 9-aminoacridine, on the other hand, provides a suitable matrix for detection of lipids and metabolites in negative mode.[182] The ratio of matrix to organic solvent combination, the concentration of matrix, and the concentration of TFA can also be manipulated to improve the integration of the matrix with the analytes of interest as well as the crystallization process. In the matrix, the organic solvent is used to extract the molecules from the sample and it quickly evaporates enabling matrix crystallization. The percentage of solvent depends on the hydrophobicity of the molecules of interest. The ratios 50:50 of acetonitrile/water and 50:50 of ethanol/water are common solutions for various tissue samples.[181] The concentration of organic matrix should be sufficient to produce homogeneous matrix coverage on all sample surfaces ensuring homogeneous ionization. For common matrices such as CHCA, DHB, and SA, concentrations generally range between 10-30 mg/mL. Moreover, the acid, TFA, plays a role as a source of protons facilitating the protonation of the analytes. A typical concentration of TFA for most MALDI analyses is 0.1 %.

Various methods of matrix application have been developed for both manual and automatic deposition. A good matrix application method should provide homogeneous coverage of matrix on the sample surface and increase the extraction of the molecules while limiting their delocalization. The choice of matrix deposition method is determined by the requirement of spatial resolution for imaging and the abundance of the analytes in the sample. The most commonly used method is spotting. Here, sample is delivered as nano- or micro-droplets of matrix solution covering the surface. Another method is spraying, where the sample is sprayed with a matrix mist resulting in a thin coating of matrix on the surface. Spraying offers smaller matrix droplets, or better spatial resolution, compared to spotting; however, it is less reproducible due to a risk of chemical delocalization if the sample gets too wet during spraying. Manual matrix deposition methods can be performed with a micropipette and airbrush for spotting and spraying, respectively.[183] Automatic devices such as inkjet printers, acoustic dispensers for spotting, and automatic pneumatic sprayers, vibrational sprayers for spraying are commercially available.[184]

Besides wet matrix application, solvent free approaches have been developed for matrix deposition. One of these is sublimation, in which the matrix is sublimed and deposited on sample surface in a vacuum. The method limits the diffusion of molecules usually caused by wet deposition as well as decreasing the matrix crystal size. As a result, spatial resolution is improved. Crystal sizes for DHB and CHCA matrices are generally in a range between 5 to 20 μm when spraying deposition is used. Sublimation, however, produces matrix crystals

generally from 1 to 3 μm in size.[185-186] Sublimation, however, might not be very efficient in extracting the analytes due to the lack of an organic solvent. Re-wetting of sample surface with a solvent or TFA after sublimation has been suggested in order to improve co-crystallization of molecules and matrix.[185]

Nanoparticles as an alternative to the organic matrix. Investigation of surface modification, noticeably with nanoparticles (NPs), as an alternative to standard organic matrices has been extensively carried out.[187] This surface modification falls into a new technical platform - surface assisted laser desorption ionization (SALDI). Nanoparticles of various materials with diameters from 2 nm up to 100 nm have been shown to efficiently absorb the laser energy, which then assists the ejection and ionization of biomolecules. The nano size of these particles offers the possibility to obtain high spatial resolution potentially for submicron analysis if a sufficiently small laser beam spot is used and there is sufficient sensitivity to detect extremely small numbers of biomolecules. In addition, NPs eliminate the formation of heterogeneous matrix crystals, which usually occurs using organic matrix deposition. Moreover, SALDI analysis using NPs as the matrix is less dependent on the irradiation wavelength as it has a broad absorption window including UV and IR wavelength. Modification with NPs offers selective ionization of biomolecules that provides better selectivity compared to organic matrixes.[188] Among different nanoparticle materials, gold nanoparticles (AuNPs), in particular, have been increasingly used in SALDI to analyze small biomolecules such as glutathione, glycosphingolipids, triacylglycerides, and carbohydrates.[189-192] Owing to their surface plasmon resonance properties, AuNPs serve as an efficient reservoir for photon energy deposition as well as an energy transfer media for analytes *via* the thermal propagation process.[188, 193] This results in significantly enhanced ionization of the analytes. When compared to MALDI, NPs are potentially highly useful matrix materials for laser desorption ionization (LDI) as they offer the capability of imaging at submicron spatial resolution as well as providing complementary chemical information to the organic matrices used on biological samples.

CHAPTER 6. CONCLUDING REMARKS AND FUTURE PERSPECTIVES

Mass spectrometry is a powerful, sensitive and selective analytical technique. The high separation efficiency combined with high identification capability of CE-MS makes it well suited for various applications in life science research. MSI, on the other hand, possesses unique properties with high chemical specificity and possible subcellular spatial resolution opening up a number of possibilities for imaging in biological, pathological, clinical and pharmaceutical studies. In this thesis, using CE-MS and MSI, I first quantify the *in vivo* concentration of methylphenidate and its metabolite at the site of action, *Drosophila* brain. Moreover, I provide evidence for the significant neurological effects of stimulant drug methylphenidate on the chemical structure and compositions of *Drosophila* brains. Drug dose dependent concentration of neurotransmitters is observed, and the sensitization reaches the saturation at the dose 20-25 mM of methylphenidate. In addition, distribution and abundance of other biomolecules change substantially following methylphenidate administration, especially a significant decrease in intensity of PC whereas there is a dramatic increase in the abundance of DAG, PE and PI. Furthermore, I also developed an alternative imaging technique LDI MS for fly brain imaging with the purpose to obtain complementary lipid information with SIMS. The work provided comprehensive comparison of the pros and cons in lipid imaging of each sample preparation method, including automatic matrix spraying, matrix sublimation and nanoparticle surface modification. From that work, experimental conditions can be selected for fly brain imaging of the interested group of molecules. Finally, I introduce a map of chemical anatomy of *C. elegans* obtained by SIMS imaging with 40 keV C_{60} and Ar cluster ion beams. The information from this work will be very useful for further studies on the molecular basis of cellular processes and behaviors of the worm. The establishment of the developed methods and the data obtained open up several possibilities for future studies.

From the observation that methylphenidate strongly alters the neurotransmitter system of the fly brain, further work can be carried out to fully characterize the effect of the drug. Examination of the neurotransmitter levels after removing the administration of methylphenidate would be interesting. It would show whether the drug effect is reversible and can be altered as they return to the original concentration or if it is a permanent effect. Absolute quantification of saturated concentrations of neurotransmitters could also be carried out. In addition, experiments with cocaine administration should be useful to compare with methylphenidate in terms of the dependence tendency of neurotransmitter levels on cocaine, and the saturated sensitization dose.

By exploring the neurological effect of methylphenidate on other biomolecules, especially lipids, several potential studies can be proposed. First, it would be very useful to be able to map the localization of co-neurotransmitters as well as methylphenidate in the fly brain with the lipids. From this, the sites of action of the drug inside the brain would be mapped out and the mechanism of its involvement on other cellular processes might be worked out. On the other hand, the distribution of methylphenidate in the brain as well as in different parts of the fly body could provide a more thorough understanding of drug distribution, drug targets, and its metabolic pathways in the entire fly body. The method is a powerful chemical imaging tool for visualizing and tracking distribution of different targets such as drugs in pharmaceutical and

clinical research. The study of recovery of brain lipids after drug removal should also be helpful to evaluate the reversibility of neurodegenerative impacts of the drug. Another interesting feature is that under the effects of methylphenidate, it is likely the concentrations of lamellar shaped lipids PC decrease, whereas the intensities of the conical shaped lipids PE, and PI increase. This might implicate the morphological shape of lipids as relating to their particular molecular mechanism in the neurological disorder that is treated with methylphenidate. One of the possibilities is that their regulating mechanism in synaptic exocytosis and endocytosis is altering the synaptic activities. Methylphenidate could change the lipid structure of the neural membrane and thus change the characteristics of synaptic behavior. Alternatively, methylphenidate could change the synaptic activity leading to alteration in lipid compositions of neural membrane that subsequently affects lipid synthetic and metabolic pathways and thus blocking or remediating the neurological disorder. Further work to confirm the role of lipids in the neurological effects induced by methylphenidate might involve supplementation of PC during or after methylphenidate administration in order to compensate for the change of lipid ratios caused by the drug. Neurotransmitter levels as well as the abundance and distribution of lipids PC, PE, PI, should be compared with the data obtained with only drug administration. If lipid supplementation causes recovery of the balance of neurotransmitters and lipids in the brain, this might be the basis for understanding the mechanism of the ADHD neurological disorder. Finally, further studies could be carried out on other psychostimulants such as cocaine and methamphetamine to observe the similarities and differences in neurological chemical effects of stimulant drugs.

The LDI MS imaging protocols developed could be potentially used on fly brain following methylphenidate administration in order to obtain complementary molecular information to SIMS. The next objective with MALDI imaging would be to study the effects of methylphenidate on larger molecules, particularly neuropeptides and proteins. With this, a complete profile of the neurological effects of methylphenidate on *Drosophila* brain would be obtained for clinical and pharmaceutical research on this drug in particular, and psychostimulants in general.

In conclusion, the mass spectrometric methods developed and the results obtained in this thesis offer multiple potential future studies and further insights into the neurological disorders treated by methylphenidate and the mechanism of action of this stimulant and other psychostimulants.

SUMMARY OF PAPERS

The general aim of this thesis has been to develop mass spectrometry methods including CE-MS and imaging MS to apply on small systems used extensively in biology and biochemistry. The focus here has been on *Drosophila melanogaster* (fruit fly) and *C. elegans* (small worm). The overreaching goal has been to further our knowledge of the effects of the neuro-stimulant methylphenidate on the brain, and another main focus has been to examine lipid composition across the brain and its change with the drug. The thesis has two main parts using two methods, CE-MS and imaging MS. In papers I, II and IV, the focus is on measuring methylphenidate and its effect on lipid composition in the brain as well as a little bit on the amine neurotransmitters. In papers III-VI, the focus is on the biomolecular composition of the brains of both organisms with imaging MS. In particular, two different kinds of imaging MS that are SIMS imaging in papers III, IV, and VI, and laser desorption in paper V. In addition to these papers, I list four papers not included in the body of the thesis. Two of these are reviews, papers VIII and IX. Paper VII followed some earlier work with SIMS analysis on the single cell organism, *Tetrahymena pyriformis*. However, instead of mating *Tetrahymena* used in earlier work, in paper VII, dividing *Tetrahymena* was imaged and the freeze dried approach was found to lead to masking of the desired lipid signal by the cell cilia. In paper X, I worked with others to use a multi-modal approach to imaging the mouse brain with MS. The following is a short summary of each of the six papers included in the body of the thesis.

In paper I, *Drosophila melanogaster* was used as a model system with *in vivo* electrochemistry to quantify the effects of oral methylphenidate on dopamine uptake during direct cocaine exposure to the fly CNS. The effect of methylphenidate on the dopamine transporter was explored by measuring the uptake of exogenously applied dopamine solution. First it was found that oral consumption of methylphenidate inhibits the *Drosophila* dopamine transporter and the inhibition is concentration dependent. Then, following cocaine administration to untreated flies, the electrochemical peak height from dopamine exposure increased to 150 % of the control as cocaine blocked the dopamine transporter. This similar experiment resulted in only a 110 % increase for methylphenidate-treated flies. Thus, the dopamine transporter is mostly inhibited for the methylphenidate-treated flies and blocks most of the action of cocaine. In addition to peak height, the rate of the clearance of dopamine was measured by amperometry. For untreated flies the rate of clearance changes 40 % when the dopamine transporter is inhibited with cocaine, and for treated flies the rate changes only 10 %. This is very consistent with the peak height measurements. The main part of this work that I carried out was to use CE-MS to determine the *in vivo* concentration of methylphenidate and this was explored in more detail in paper II. In paper I found that when flies were fed for three days with methylphenidate in doses of 5, 10, and 15 mM, the methylphenidate concentration *in vivo* was 80, 206, and 242 μM in the brain, respectively. Therapeutic doses of oral methylphenidate that induce significant blockade of the dopamine transporter (50 to 75 %) in the human brain are in the range of 0.25 to 1 mg/kg. The *in vivo* doses to the methylphenidate-fed flies correspond to administered doses of 1.9, 4.8, and 5.6 mg/kg which is within the range of the doses (0.75 to 10 mg/kg) used for pharmacokinetics and bioavailability of oral methylphenidate examined in rats.

In paper II, capillary electrophoresis coupled to mass spectrometry was explored in more detail to determine the *in vivo* concentrations of methylphenidate over a wider range, and to determine a major metabolite of this drug in the heads of *Drosophila melanogaster*. These concentrations, evaluated at the site of action, the brain, have been correlated with orally administrated methylphenidate. This is a significant advance as most work in the area of *in vivo* measurements compares the administered dose and it is difficult to obtain *in vivo* concentrations at the site of action. As discussed above for Paper I, methylphenidate might be used to mediate cocaine addiction due to its lower pharmacokinetics, which results in fewer addictive and reinforcing effects than cocaine. The effects of the drug on the nervous system, however, have not been fully understood. In addition to measurements of drug concentration, in paper II the method was used to examine drug dose dependence on the levels of several primary biogenic amines. I found that the *in vivo* concentration of methylphenidate increased with increasing feeding doses up to 25 mM methylphenidate. Furthermore, administrated methylphenidate increased drug metabolism activity and some neurotransmitter levels; however, this increase appeared to saturate at a feeding dose of about 20 mM. This method, developed for the fruit fly, provides a new tool to evaluate the concentration of administered drug at the site of action and provides information concerning the effects of methylphenidate on the nervous system.

In paper III, I developed an imaging protocol using ToF-SIMS to study the spatial distribution of biomolecules in *Drosophila* brain. Fly brains were analyzed frozen to prevent molecular redistribution prior to analysis. Different molecules were found to distribute differently in the tissue, particularly the eye pigments, diacylglycerides, and phospholipids were noticeably different, and this is thought to reflect their biological functions in the brain. In addition, a new variation of principal components analysis for comparison of images was introduced. Principal components analysis is applied to ToF-SIMS images which contain a huge number of spectra, and each spectrum corresponds to a pixel. By mapping the score values onto a suitable color scale, score images are generated. This was shown to provide a useful method for visualizing differences and similarities between pixels of the ion images. From these pixels, spectra that reflect chemical composition can be found in the image and correlations in the localization of the lipid molecules of interest can be observed. This is then used to identify peaks for further analysis. In this paper it was also shown that, for consecutive analyses following 10 keV Ar_{2500}^+ sputtering, different biomolecules are affected differentially by Ar_{2500}^+ sputtering. Significant changes in signal intensities between consecutive analyses were observed for high mass molecules including intact lipids.

In paper IV, ToF-SIMS imaging was used to investigate the effects of orally administrated methylphenidate on the lipid structure of *Drosophila* brain. ToF-SIMS imaging was carried out using a recently designed high energy 40 keV Ar_{4000}^+ gas cluster ion gun which demonstrated improved sensitivity for intact lipids in the fly brain compared to the 40 keV C_{60}^+ primary ion gun. In addition, correlation of ToF-SIMS and SEM imaging on the same fly brain showed that there is specific localization that is related to biological functions of various biomolecules. Different lipids distribute in different parts of the brain - central brain, optical lobes, and proboscis - depending on the length of carbon chain and saturation level of fatty acid branches. Interestingly, data analysis using image PCA, peak intensity comparison, and SIMS ion images shows that methylphenidate has significant actions on a variety of biomolecules, especially the elevated amount of diacylglycerides, phosphatidylethanolamine, and phosphatidylinositol in the fly brains. A significant decrease of phosphatidylcholine levels was observed. Not only were

their abundances changed but also their localizations in the brain varied. This lays the groundwork for an understanding of lipid effects on exocytosis where these lipids have been shown to increase or decrease the rate of exocytosis events depending on the shapes of the lipids. The ToF-SIMS imaging approach clearly visualizes the effects of methylphenidate on the chemical structure of the fly brain and might be much more significant.

In paper V, laser desorption ionization mass spectrometry was used to image brain lipids in *Drosophila*. Different sample preparation methods, including sublimation with organic matrices and surface modification with gold nanoparticles, were examined in the aspects of sample profiling and imaging. Recrystalization with trifluoroacetic acid following matrix deposition was also applied to increase the incorporation of biomolecules with matrix resulting in efficient ionization. The fly brain profiles obtained from different sample preparations were significantly different demonstrating that they can be used to provide complementary chemical compositional information, particularly the small metabolites, diacylglycerides, phosphatidylcholines, and triacylglycerides, of the fly brain. Furthermore, MS imaging appears to enhanced with gold nanoparticle modification showing its potential for cellular and subcellular imaging. The imaging protocol developed here with both MALDI and SALDI provides the best and most diverse lipid chemical images of the fly brain to date with LDI.

In paper VI, I used ToF-SIMS to study the chemical anatomy of *C. elegans* using three-dimensional (3D) and 2-dimensional (2D) approaches on the entire worm and worm sections, respectively. Sample preparation was developed including embedding, frozen sectioning, and freeze-drying. I carried out 3D imaging using the high energy 40 keV Ar_{4000}^+ gas cluster ion gun, which greatly benefited entire animal analysis in terms of cleaning the sample surface, preserving the nature of subsurface, and maintaining molecular signals. For the 2D imaging the 40 keV C_{60}^+ gun was used, offering detailed structural information of the worm section at approximately 1 μm spatial resolution. Significant changes in the chemical distribution were observed along the depth of the worm. In addition, correlation between 2D and 3D ion images showed different molecular structures across the worm, possible localization of the nerve ring and the cuticle, and the fluid containing space inside the worm. I concluded that ToF-SIMS imaging with 2D and 3D approaches, and correlation between the two, will provide very useful anatomical information on the chemical level to worm research in the future.

ACKNOWLEDGEMENTS

These past five years have been an incredible journey for me bringing a great deal of memories and experiences. I have been growing up a lot both professionally and personally. I have had opportunities to meet and interact with many great people. Their talents and excitement in science and their great personalities influenced me significantly. Therefore, I would like to acknowledge some people who have been important to me during this period.

To my supervisor John Fletcher, thank you for taking me as your Ph.D. student. Your great knowledge and expertise helped me incredibly to develop in SIMS imaging and science. Thank you for always being happy and willing to provide scientific guidance when I need. Every student feels happy to have you as a supervisor.

To Professor Andrew Ewing, thank you for believing in my ability and giving me the opportunity to pursue my Ph.D. at the start. Your excitement in "everything" inspires me a lot in my work and helped me develop confidence and grow up in science.

To my second supervisor Peter Sjövall, many thanks for your excellent consultantation and guidance and for always being willing to help despite of the work distance.

To my examiners, Margareta Wedborg and Stefan Hulth, thank you for your supports and being available when I needed.

To Per, thank you for your guidance on the ToF-SIMS instrument, and PCA software. You are an excellent scientist and lab manager.

To all the co-authors of the papers, Ingela Lanekoff, Jörg Hanrieder, Carina Berglund, Amir Mohammadi, Masoumeh Dowlatshahi, and Manish Rauthan, thank you for all the helpful discussions. It is nice to work with you. I have learned a lot from you. Wish you all success and many papers published.

Many thanks to friends that helped me out sometime in my lab work especially at the beginning, Ingela Lanekoff - for CE-MS instrument, Nick Kuklinski - for *Drosophila* culturing, and Tina Angerer - for the J105 instrument.

To Sanna, my office mates, thank you for some fun chatting time in the office. Thanks for listening when I wanted to talk.

To all friends and colleagues in the group and related groups in the past and present, Tina, Ingela, Nick, Carina, Lisa, Mike, Jenny, Maria, Joakim, Gulnara, Yuqing Lin, Jörg, Raphaël, Jun, Jackie, Mellisa, Soodabeh, Kubra, Hoda, Neda, Jelena, Amir, Johan, Lorenz, Åsa, Sanna, Masoumeh, Anna, Xianchan, Yuanmo, Lin Ren, Sara, Mai, and Mary, thank you for all the discussions in group meetings, and social group activities.

To all friends on the 4th floor and Eliza, thank you for fun chats and nice times in coffee and lunch breaks.

To Amir and Masoumeh, thank you for your friendships and support. You are the friends and colleagues that everyone wants to have.

To Andy and all friends in the Tang Soo Do group, thank you for all the fun classes and social activities. You have added more energy and joy to my life during this time.

To all my Vietnamese friends in the choir - my second family in Sweden, thank you everyone for so many fun and enjoyable times.

To Chunxie and Bethmini, thank you for always being best friends. Thanks for all great memories we have had together.

To my family, thank you mom and dad! You have made me feel I am the best daughter in this world. You are the biggest strength and support in my life. Thanks to my brothers Tin and Tri, you have made me feel comfortable and easy to be here because of your doing well and taking care of our parents.

To Mr Monkey, my life has changed to another chapter since I got to know you. Thank you for always being around giving me strength and confidence, and for being supportive with care and love!!!

REFERENCES

1. Lodish, H.; Berk, A.; Zipursky, S. L.; Matsudaira, P.; Baltimore, D.; Darnell, J., Overview of Neuron Structure and Function. In *Molecular Cell Biology*, 4 ed.; Lodish, H.; Berk, A.; Zipursky, S. L.; Matsudaira, P.; Baltimore, D.; Darnell, J., Eds. W. H. Freeman and Company: New York, 2000.
2. Savtchenko, L. P.; Rusakov, D. A., The Optimal Height of The Synaptic Cleft. *Proceedings of the National Academy of Sciences of the United States of America* **2007,** *104* (6), 1823-1828.
3. Fischbach, G. D., Mind and Brain. *Scientific American* **1992,** *267*, 48-57.
4. Morell, P.; Quarles, R. H., The Myelin Sheath. In *Basic Neurochemistry: Molecular, Cellular and Medical Aspects*, 6 ed.; Siegel, G. J.; Agranoff, B. W.; Albers, R. W.; Fisher, S. K.; Uhler, M. D., Eds. American Society for Neurochemistry: Philadelphia, 1999.
5. Purves, D.; Augustine, G. J.; Fitzpatrick, D.; Katz, L. C.; LaMantia, A. S.; McNamara, J. O.; Williams, S. M., Neurotransmitters. In *Neuroscience*, 2 ed.; Purves, D.; Augustine, G. J.; Fitzpatrick, D.; Katz, L. C.; LaMantia, A. S.; McNamara, J. O.; Williams, S. M., Eds. Sinauer Associates: Sunderland (MA), 2001.
6. Siegel, A.; Sapru, H. N., Essential Neuroscience. 2 ed.; Lippincott Williams & Wilkins: 2010.
7. Werkman, T. R.; Glennon, J. C.; Wadman, W. J.; McCreary, A. C., Dopamine Receptor Pharmacology: Interactions with Serotonin Receptors and Significance for the Aetiology and Treatment of Schizophrenia. *CNS & Neurological Disorders Drug Targets* **2006,** *5* (1), 3-23.
8. Webster, R. A., Neurotransmitter Systems and Function: Overview. In *Neurotransmitters, Drugs and Brain Function* Webster, R. A., Ed. John Wiley& Sons Ltd: 2001; pp 1-32.
9. The Official Web Site of The Nobel Prizes. http://www.nobelprize.org/.
10. Webster, R. A., Dopamine (DA). In *Neurotransmitters, Drugs and Brain Function*, 2 ed.; Webster, R. A., Ed. John Wiley & Sons, Ltd: 2001; pp 137-161.
11. Iversen, S. D.; Iversen, L. L., Dopamine: 50 years in perspective. *Trends in Neuroscience* **2007,** *30* (5), 188-93.
12. Barnes, N. M.; Sharp, T., A review of central 5-HT receptors and their function. *Neuropharmacology* **1999,** *38* (8), 1083–1152.
13. Ichikawa, J.; Meltzer, H. Y., R(+)-8-OH-DPAT, a Serotonin1A Receptor Agonist, Potentiated S(-)-Sulpiride-Induced Dopamine Release in Rat Medial Prefrontal Cortex and Nucleus Accumbens But Not Striatum. *The Journal of Pharmacology and Experimental Therapeutics* **1999,** *291* (3), 1227–1232.
14. Stanford, S. C., 5-Hydroxytryptamine. In *Neurotransmitters, Drugs and Brain Function*, 2 ed.; Webster, R. A., Ed. John Wiley & Sons, Ltd: 2001; pp 187-209.
15. Frazer, A.; Hensler, J. G., Serotonin. In *Basic Neurochemistry: Molecular, Cellular and Medical Aspects*, 6 ed.; Siegel, G. J.; Agranoff, B. W.; Albers, R. W.; Fisher, S. K.; Uhler, M. D., Eds. Lippincott-Raven: Philadelphia, 1999.
16. Olsen, R. W.; DeLorey, T. M., GABA and Glycine. In *Basic Neurochemistry: Molecular, Cellular and Medical Aspects*, 6 ed.; Siegel, G. J.; Agranoff, B. W.; Albers, R. W.; Fisher, S. K.; Uhler, M. D., Eds. Lippincott-Raven: Philadelphia, 1999.
17. Nathanson, J. A.; Greengard, P., Octopamine-Sensitive Adenylate Cyclase: Evidence for a Biological Role of Octopamine in Nervous Titssue. *Science* **1973,** *180* (4083), 308-310.

18. Roeder, T.; Seifert, M.; Kahler, C.; Gewecke, M., Tyramine and octopamine: antagonistic modulators of behavior and metabolism. *Archives of insect biochemistry and physiology* **2003,** *54* (1), 1-13.
19. Saudou, F.; Amlaiky, N.; Plassat, J. L.; Borrelli, E.; Hen, R., Cloning and characterization of a Drosophila tyramine receptor. *EMBO Journal* **1990,** *9* (11), 3611-3617.
20. Roeder, T., Octopamine in Invertebrates. *Progress in neurobiology* **1999,** *59* (5), 533-561.
21. Roeder, T., Tyramine and Octopamine: Ruling Behavior and Metabolism. *Annual review of entomology* **2005,** *50*, 447-477.
22. Alkema, M. J.; Hunter-Ensor, M.; Ringstad, N.; Horvitz, H. R., Tyramine Functions independently of octopamine in the Caenorhabditis elegans nervous system. *Neuron* **2005,** *46* (2), 247-60.
23. Lange, A. B., Tyramine: From Octopamine Precursor to Neuroactive Chemical in Insects. *General and comparative endocrinology* **2009,** *162* (1), 18-26.
24. Saraswati, S.; Fox, L. E.; Soll, D. R.; Wu, C. F., Tyramine and Octopamine Have Opposite Effects On The Locomotion of Drosophila Larvae. *Journal of neurobiology* **2004,** *58* (4), 425-41.
25. McClung, C.; Hirsh, J., Stereotypic Behavioral Responses to Free-base Cocaine and The Development of Behavioral Sensitization in Drosophila. *Current Biology* **1998,** *8*, 109-112.
26. Wick, M. M.; Mul, A., Synthesis and Biologic Evaluation N-Acetyldopamine in Experimental of the Dopamine Analog Leukemia in Mice. *Journal of National Cancer Institute* **1981,** *66* (2), 351-354.
27. Aonuma, H.; Watanabe, T., Octopaminergic System in The Brain Controls Aggressive Motivation in The Ant, Formica Japonica. *Acta biologica Hungarica* **2012,** *63 Suppl 2*, 63-68.
28. Solanto, M. V., Neuropsychopharmacological mechanisms of stimulant drug action in attention-deficit hyperactivity disorder: a review and integration. *Behavioural Brain Research* **1998,** *94*, 127-152.
29. Kollins, S. H.; MacDonald, E. K.; Rush, C. R., Essessing the abuse potential of methylphenidate in nonhuman and human subjects. *Pharmacology Biochemistry Behavior* **2001,** *68*, 611-627.
30. Chen, N.; Reith, M. E. A., Structure and Function of The Dopamine Transporter. *European Journal of Pharmacology* **2000,** *405*, 329-339.
31. Huang, X.; Gu, H. H.; Zhan, C. G., Mechanism for Cocaine Blocking the Transport of Dopamine: Insights from Molecular Modeling and Dynamics Simulations. *Journal of Physical Chemistry B* **2009,** *113*, 15057–15066.
32. Huang, X.; Zhan, C. G., How Dopamine Transporter Interacts With Dopamine: Insights From Molecular Modeling and Simulation. *Biophysical journal* **2007,** *93* (10), 3627-39.
33. Beuming, T.; Kniazeff, J.; Bergmann, M. L.; Shi, L.; Gracia, L.; Raniszewska, K.; Newman, A. H.; Javitch, J. A.; Weinstein, H.; Gether, U.; Loland, C. J., The binding sites for cocaine and dopamine in the dopamine transporter overlap. *Nature neuroscience* **2008,** *11* (7), 780-9.
34. Website of Genetic Science Learning Center. http://learn.genetics.utah.edu.
35. Volkow, N. D., Is Methylphenidate Like Cocaine? *Archives of General Psychiatry* **1995,** *52* (6), 456.
36. Grabowski, J.; Roache, J. D.; Schmitz, J. M.; Rhoades, H.; Creson, D.; Korszun, A., Replacement Medication for Cocaine Dependence: Methylphenidate. *Journal of Clinical Psychopharmacology* **1997,** *17* (6), 485-488.
37. Schmitz, F.; Scherer, E. B.; Machado, F. R.; da Cunha, A. A.; Tagliari, B.; Netto, C. A.; Wyse, A. T., Methylphenidate induces lipid and protein damage in prefrontal cortex, but not in cerebellum, striatum and hippocampus of juvenile rats. *Metabolic brain disease* **2012,** *27* (4), 605-12.

38. Charach, G.; Kaysar, N.; Rabinovich, A.; Argov, O.; Weintraub, M., MPH and Dyslipidemia. *Current Directions in ADHD and Its Treatment* **2012,** (9), 185-192.
39. Charach, G.; Kaysar, N.; Grosskopf, I.; Rabinovich, A.; Weintraub, M., Methylphenidate has positive hypocholesterolemic and hypotriglyceridemic effects: new data. *Journal of clinical pharmacology* **2009,** *49* (7), 848-51.
40. Pandey, U. B.; Nichols, C. D., Human disease models in Drosophila melanogaster and the role of the fly in therapeutic drug discovery. *Pharmacological reviews* **2011,** *63* (2), 411-36.
41. Botas, J., Drosophila Researchers Focus on Human Disease. *Nature Genetics* **2007,** *39* (5), 589-591.
42. Wolf, F. W.; Heberlein, U., Invertebrate models of drug abuse. *Journal of neurobiology* **2003,** *54* (1), 161-78.
43. Kraut, R., Roles of sphingolipids in Drosophila development and disease. *Journal of neurochemistry* **2011,** *116* (5), 764-78.
44. Kliman, M.; Vijayakrishnan, N.; Wang, L.; Tapp, J. T.; Broadie, K.; McLean, J. A., Structural mass spectrometry analysis of lipid changes in a Drosophila epilepsy model brain. *Molecular bioSystems* **2010,** *6* (6), 958-66.
45. Berglund, E. C.; Makos, M. A.; Keighron, J. D.; Phan, N.; Heien, M. L.; Ewing, A. G., Oral administration of methylphenidate blocks the effect of cocaine on uptake at the Drosophila dopamine transporter. *ACS chemical neuroscience* **2013,** *4* (4), 566-74.
46. Phan, N. T.; Hanrieder, J.; Berglund, E. C.; Ewing, A. G., Capillary electrophoresis-mass spectrometry-based detection of drugs and neurotransmitters in Drosophila brain. *Analytical chemistry* **2013,** *85* (17), 8448-54.
47. Phan, N. T.; Fletcher, J. S.; Ewing, A. G., Lipid structural effects of oral administration of methylphenidate in Drosophila brain by secondary ion mass spectrometry imaging. *Analytical chemistry* **2015,** *87* (8), 4063-71.
48. Scholz, H.; Ramond, J.; Singh, C. M.; Heberlein, U., Functional Ethanol Tolerance in Drosophila. *Neuron* **2000,** *28*, 261-271.
49. Teleman, A. A.; Ratzenböck, I.; Oldham, S., Drosophila: A Model for Understanding Obesity and Diabetic Complications. *Experimental Clinical Endocrinology Diabetes* **2012,** *120* (04), 184-185.
50. Helfand, S. L.; Rogina, B., Genetics of Aging in The Fruit Fly, Drosophila Melanogaster. *Annual review of genetics* **2003,** *37*, 329-48.
51. Llorens, J. V.; Navarro, J. A.; Martinez-Sebastian, M. J.; Baylies, M. K.; Schneuwly, S.; Botella, J. A.; Molto, M. D., Causative role of oxidative stress in a Drosophila model of Friedreich ataxia. *FASEB Journal* **2007,** *21* (2), 333-44.
52. Zhang, X.; Smith, D. L.; Meriin, A. B.; Engemann, S.; Russel, D. E.; Roark, M.; Washington, S. L.; Maxwell, M. M.; Marsh, J. L.; Thompson, L. M.; Wanker, E. E.; Young, A. B.; Housman, D. E.; Bates, G. P.; Sherman, M. Y.; Kazantsev, A. G., A Potent Small Molecule Inhibits Polyglutamine Aggregation in Huntington's Disease Neurons and Suppresses Neurodegeneration In Vivo. *Proceedings of the National Academy of Sciences of the United States of America* **2005,** *102* (3), 892-7.
53. Model Organism Encyclopedia of DNA Elements-Educational Supplement. http://modencode.sciencemag.org/drosophila/introduction.
54. Adams, M. D., The Genome Sequence of Drosophila Melanogaster. *Science* **2000,** *287*, 2185-2195.
55. Bernards, A.; Hariharan, I. K., Of flies and men — studying human disease in Drosophila. *Current Opinion in Genetics & Development* **2001,** *11*, 274-278.
56. Yeh, E.; Gustafson, K.; Boulianne, G. L., Green Fluorescent Protein As a Vital Marker and Reporter of Gene Expression in Drosophila. *Proceedings of the National Academy of Sciences of the United States of America* **1995,** *92*, 7036-7040.
57. Heisenberg, M., Fly Brains. In *eLS*, John Wiley & Sons, Ltd: 2001.

58. Waddell, S.; Quinn, W. G., What Can We Teach Drosophila? What Can They Teach Us? *TRENDS in Genetics* **2001,** *17* (12), 719-726.
59. Huang, C.; Wang, P.; Xie, Z.; Wang, L.; Zhong, Y., The differential requirement of mushroom body alpha/beta subdivisions in long-term memory retrieval in Drosophila. *Protein & cell* **2013,** *4* (7), 512-9.
60. Fahrbach, S. E., Structure of The Mushroom Bodies of The Insect Brain. *Annual review of entomology* **2006,** *51*, 209-32.
61. Wolff, T.; Iyer, N. A.; Rubin, G. M., Neuroarchitecture and neuroanatomy of the Drosophila central complex: A GAL4-based dissection of protocerebral bridge neurons and circuits. *The Journal of comparative neurology* **2015,** *523* (7), 997-1037.
62. Hanesch, U.; Fischbach, K. F.; Heisenberg, M., Neuronal architecture of the central complex in Drosophila melanogaster. *Cell Tissue Research* **1989,** *257*, 343-366.
63. Tanaka, N. K.; Endo, K.; Ito, K., Organization of antennal lobe-associated neurons in adult Drosophila melanogaster brain. *The Journal of comparative neurology* **2012,** *520* (18), 4067-130.
64. Stocker, R. F.; Schorderet, M., Cobalt Filling of Sensory Projections from Internal and External Mouthparts in Drosophila. *Cell Tissue Research* **1981,** *216*, 513-523.
65. Nichols, C. D., Drosophila melanogaster neurobiology, neuropharmacology, and how the fly can inform central nervous system drug discovery. *Pharmacology & therapeutics* **2006,** *112* (3), 677-700.
66. O'Kane, C. J., Drosophila as a Model Organism for the Study of Neuropsychiatric Disorders. Hagan, J. J., Ed. Springer Heidelberg: New York, 2011.
67. Mao, Z.; Davis, R. L., Eight different types of dopaminergic neurons innervate the Drosophila mushroom body neuropil: anatomical and physiological heterogeneity. *Frontiers in neural circuits* **2009,** *3*, 5.
68. Liu, X.; Krause, W. C.; Davis, R. L., GABAA receptor RDL inhibits Drosophila olfactory associative learning. *Neuron* **2007,** *56* (6), 1090-102.
69. Wilson, R. I.; Laurent, G., Role of GABAergic inhibition in shaping odor-evoked spatiotemporal patterns in the Drosophila antennal lobe. *The Journal of Neuroscience* **2005,** *25* (40), 9069-79.
70. Busch, S.; Selcho, M.; Ito, K.; Tanimoto, H., A map of octopaminergic neurons in the Drosophila brain. *The Journal of comparative neurology* **2009,** *513* (6), 643-67.
71. Nagaya, Y.; Kutsukake, M.; Chigusa, S. I.; Komatsu, A., A trace amine, tyramine, functions as a neuromodulator in Drosophila melanogaster. *Neuroscience letters* **2002,** *329*, 324-328.
72. Kuklinski, N. J.; Berglund, E. C.; Engelbreksson, J.; Ewing, A. G., Determination of salsolinol, norsalsolinol, and twenty-one biogenic amines using micellar electrokinetic capillary chromatography-electrochemical detection. *Electrophoresis* **2010,** *31* (11), 1886-1893.
73. Karlson, P.; Sekeris, C. E., NADA as Sclerotizing Agent of Insect Cuticle. *Nature Letters* **1962,** *195*, 183-184.
74. Riddle, D. L.; Blumenthal, T.; Meyer, B. J.; Priess, J. R., The Biological Model. In *C. elegans II*, 2 ed.; Riddle, D. L.; Blumenthal, T.; Meyer, B. J.; Priess, J. R., Eds. Cold Spring Harbor Laboratory Press: Cold Spring Harbor (NY), 1997.
75. Rauthan, M.; Pilon, M., The Mevalonate Pathway in C. Elegans. *Lipids in health and disease* **2011,** *10*, 243-254.
76. Jafari, G.; Burghoorn, J.; Kawano, T.; Mathew, M.; Morck, C.; Axang, C.; Ailion, M.; Thomas, J. H.; Culotti, J. G.; Swoboda, P.; Pilon, M., Genetics of extracellular matrix remodeling during organ growth using the Caenorhabditis elegans pharynx model. *Genetics* **2010,** *186* (3), 969-82.

77. Leung, M. C.; Williams, P. L.; Benedetto, A.; Au, C.; Helmcke, K. J.; Aschner, M.; Meyer, J. N., Caenorhabditis Elegans: An Emerging Model in Biomedical and Environmental Toxicology. *Toxicological Sciences* **2008,** *106* (1), 5-28.
78. Consortium, T. C. e. S., Genome Sequence of the Nematode C. elegans: A Platform for Investigating Biology. *Science* **1998,** *282* (5396), 2012-2018.
79. Kaletta, T.; Hengartner, M. O., Finding function in novel targets: C. elegans as a model organism. *Nature Reviews - Drug Discovery* **2006,** *5* (5), 387-98.
80. Frank, C. A.; Baum, P. D.; Garriga, G., HLH-14 is a C. elegans achaete-scute protein that promotes neurogenesis through asymmetric cell division. *Development* **2003,** *130* (26), 6507-18.
81. The online review of C. elegans Biology. http://www.wormbook.org.
82. http://www.people.ku.edu/~erikl/wormexplain.html.
83. Meer, G. V.; Voelker, D. R.; Feigenson, G. W., Membrane lipids: where they are and how they behave. *Nature Reviews - Molecular Cell Biology* **2008,** *9* (2), 112-24.
84. Fahy, E.; Subramaniam, S.; Murphy, R. C.; Nishijima, M.; Raetz, C. R.; Shimizu, T.; Spener, F.; van Meer, G.; Wakelam, M. J.; Dennis, E. A., Update of the LIPID MAPS comprehensive classification system for lipids. *Journal of lipid research* **2009,** *50 Suppl*, S9-14.
85. Farooqui, A. A.; Horrocks, L. A., Phospholipid Metabolism in Brain. In *Glycerophospholipids in the Brain: Phospholipases A2 in Neurological Disorders*, Springer Science+Business Media, LLC: New York, 2007.
86. Farooqui, A. A.; Horrocks, L. A.; Farooqui, T., Glycerophospholipids in brain: their metabolism, incorporation into membranes, functions, and involvement in neurological disorders. *Chemistry and Physics of Lipids* **2000,** *106*, 1-29.
87. Piomelli, D.; Astarita, G.; Rapaka, R., A neuroscientist's guide to lipidomics. *Nature Reviews - Neuroscience* **2007,** *8* (10), 743-54.
88. Ostrowski, S. G.; Van Bell, C. T.; Winograd, N.; Ewing, A. G., Mass spectrometric imaging of highly curved membranes during Tetrahymena mating. *Science* **2004,** *305* (5680), 71-3.
89. Paolo, G. D.; Moskowitz, H. S.; Gipson, K.; Wenk, M. R.; Voronov, S.; Obayashi, M.; Flavell1, R.; Fitzsimonds, R. M.; Ryan, T. R.; Camilli, P. D., Impaired PtdIns(4,5)P2 synthesis in nerve terminals produces defects in synaptic vesicle traffickin. *Nature* **2004,** *431*, 415-422.
90. Brown, D. A.; London, E., Functions of Lipid Rafts in Biological Membranes. *Annual Review of Cell Developmental Biology* **1998,** *14*, 111-136.
91. Berg, J. M.; Tymoczko, J. L.; Stryer, L., Triacylglycerols Are Highly Concentrated Energy Stores. In *Biochemistry*, 5 ed.; W H Freeman: New York, 2002.
92. Khan, W. A.; Blobe, G. C.; Hannun, Y. A., Arachidonic Acid and Free Fatty Acids As Second Messengers and The Role of Protein Kinase C. *Cellular Signalling* **1995,** *7* (3), 171-184.
93. Fitzgerald, L. W.; Ortiz, J.; Hamedani, A. G.; Nestler, E. J., Drugs of Abuse and Stress Increase the Expression of GluRl and NMOARI Glutamate Receptor Subunits in the Rat Ventral Tegmental Area: Common Adaptations among Cross-Sensitizing Agents. *Journal of Neuroscience* **1996,** *16* (1), 274-282.
94. Swanson, C. J.; Baker, D. A.; Carson, D.; Worley, P. F.; Kalivas, P. W., Repeated Cocaine Administration Attenuates Group I Metabotropic Glutamate Receptor-Mediated Glutamate Release and Behavioral Activation: A Potential Role for Homer. *Journal of Neuroscience* **2001,** *21* (22), 9043-9052.
95. Sang, N.; Chen, C., Lipid signaling and synaptic plasticity. *The Neuroscientist : a review journal bringing neurobiology, neurology and psychiatry* **2006,** *12* (5), 425-34.
96. Ohanian, J.; Liu, G.; Ohanian, V.; Heagerty, A. M., Lipid Second Messengers Derived From Glycerolipids and Sphingolipids, and Their Role in Smooth Muscle Function. *Acta Physiologica Scandinavica* **1998,** *164*, 533-548.
97. Hannun, Y. A.; Cowart, L. A., The Role of Ceramide in Cell Regulation. Dennis, E. A., Ed. Elsevier Inc: USA, 2003.

98. Blusztajn, J. K.; Zeisel, S. H.; Wurtman, R. J., Synthesis of Lecithin (Phosphatidylcholine) From Phosphatidylethanolamine in Bovine Brain. *Brain Research* **1979,** *179*, 319-327.
99. Birner, R.; Bürgermeister, M.; Schneiter, R.; Daum, G., Roles of Phosphatidylethanolamine and of Its Several Biosynthetic Pathways in Saccharomyces cerevisiae. *Molecular Biology of the Cell* **2001,** *12*, 997-1007.
100. Infante, J. P., Rate-limiting Steps in The Cytidine Pathway For The Synthesis of Phosphatidylcholine and Phosphatidylethanolamine. *Biochemical Journal* **1977,** *167*, 847-849.
101. Binaglia, L.; Goracci, G.; Porcellati, G.; Roberti, R.; Woelk, H., The Synthesis of Choline and Ethanolamine Phosphoglycerides in Neuronal and Glial Cells of Rabbit in Vivo. *Journal of neurochemistry* **1973,** *21* (5), 1067-1082.
102. Thompton, W.; Strickland, K. P.; Rossiter, R. J., Biosynthesis of Phosphatidylinositol in Rat Brain. *Biochemical Journal* **1963,** *87*, 136-142.
103. Tolias, K. F.; Cantley, L. C., Pathways for phosphoinositide synthesis. *Chemistry and Physics of Lipids* **1999,** *98*, 69-77.
104. Toker, A., The Synthesis and Cellular Roles of Phosphatidylinositol 4,5-bisphosphate. *Current Opinion in Cell Biology* **1998,** *10*, 254-261.
105. Bloomquist, B. T.; Shortridge, R. D.; Schneuwly, S.; Perdew, M.; Montell, C.; Steller, H.; Rubin, G.; Pak, W. L., Isolation of a putative phospholipase c gene of drosophila, norpA, and its role in phototransduction. *Cell* **1988,** *54* (5), 723-733.
106. Li, Z.; Agellon, L. B.; Allen, T. M.; Umeda, M.; Jewell, L.; Mason, A.; Vance, D. E., The ratio of phosphatidylcholine to phosphatidylethanolamine influences membrane integrity and steatohepatitis. *Cell metabolism* **2006,** *3* (5), 321-31.
107. Cui, Z.; Houweling, M., Phosphatidylcholine and cell death. *Biochimica et biophysica acta* **2002,** *1585*, 87-96.
108. Schwarz, E.; Prabakaran, S.; Whitfield, P.; Major, H.; Leweke, F. M.; Koethe, D.; McKenna, P.; Bahn, S., High Throughput Lipidomic Profiling of Schizophrenia and Bipolar Disorder Brain Tissue Reveals Alterations of Free Fatty Acids, Phosphatidylcholines, and Ceramides. *Journal of proteome research* **2008,** *7*, 4266–4277.
109. Kaddurah-Daouk, R.; McEvoy, J.; Baillie, R.; Zhu, H.; J, K. Y.; Nimgaonkar, V. L.; Buckley, P. F.; Keshavan, M. S.; Georgiades, A.; Nasrallah, H. A., Impaired plasmalogens in patients with schizophrenia. *Psychiatry research* **2012,** *198* (3), 347-52.
110. Matsumoto, J.; Sugiura, Y.; Yuki, D.; Hayasaka, T.; Goto-Inoue, N.; Zaima, N.; Kunii, Y.; Wada, A.; Yang, Q.; Nishiura, K.; Akatsu, H.; Hori, A.; Hashizume, Y.; Yamamoto, T.; Ikemoto, K.; Setou, M.; Niwa, S., Abnormal phospholipids distribution in the prefrontal cortex from a patient with schizophrenia revealed by matrix-assisted laser desorption/ionization imaging mass spectrometry. *Analytical and bioanalytical chemistry* **2011,** *400* (7), 1933-43.
111. Burgess, J. R.; Stevens, L.; Zhang, W.; Peck, L., Long-chain Polyunsaturated Fatty Acids in Children With Attention-deficit Hyperactivity Disorder. *The American Journal of Clinical Nutrition* **2000,** *71 (Suppl)*, 327S–30S.
112. Ross, B. M.; Seguin, J.; Sieswerda, L. E., Omega-3 fatty acids as treatments for mental illness: which disorder and which fatty acid? *Lipids in health and disease* **2007,** *6*, 21.
113. Kidd, P. M., Omega-3 DHA and EPA for Cognition, Behavior, and Mood: Clinical Findings and Structural-Functional Synergies with Cell Membrane Phospholipids. *Alternative Medicine Review* **2007,** *12* (3), 207-227.
114. Germano, M.; Meleleo, D.; Montorfano, G.; Adorni, L.; Negroni, M.; Berra, B.; Rizzo, A. M., Plasma, red blood cells phospholipids and clinical evaluation after long chain omega-3 supplementation in children with attention deficit hyperactivity disorder (ADHD). *Nutritional neuroscience* **2007,** *10* (1-2), 1-9.
115. Lipton, P., Ischemic Cell Death in Brain Neurons. *Physiological Review* **1999,** *79* (4), 1431-1568.

116. Shanta, S. R.; Choi, C. S.; Lee, J. H.; Shin, C. Y.; Kim, Y. J.; Kim, K. H.; Kim, K. P., Global changes in phospholipids identified by MALDI MS in rats with focal cerebral ischemia. *Journal of lipid research* **2012,** *53* (9), 1823-31.
117. Lim, W. L.; Martins, I. J.; Martins, R. N., The involvement of lipids in Alzheimer's disease. *Journal of genetics and genomics* **2014,** *41* (5), 261-74.
118. Farooqui, A. A.; Ong, W. Y.; Horrocks, L. A., Biochemical Aspects of Neurodegeneration in Human Brain: Involvement of Neural Membrane Phospholipids and Phospholipases A2. *Neurochemical research* **2004,** *29* (11), 1961-1977.
119. Rabel, S.; Stobaugh, J., Applications of Capillary Electrophoresis in Pharmaceutical Analysis. *Pharm Res* **1993,** *10* (2), 171-186.
120. Li, S. F. Y., Capillary Electrophoresis—Principles, Practice and Applications. Elsevier: Amsterdam, 1992.
121. Lapos, J. A.; G., E. A., Electrophoretic Separation–Based Sensors. In *A century of Separation Science*, Issaq, H. J., Ed. Marcel Dekker, Inc.: New York, 2002.
122. Kuklinski, N. J.; Berglund, E. C.; Engelbrektsson, J.; Ewing, A. E., Biogenic Amines in Microdissected Brain Regions of Drosophila melanogaster Measured with Micellar Electrokinetic Capillary Chromatographys Electrochemical Detection. *Analytical chemistry* **2010,** *82*, 7729–7735.
123. Omiatek, D. M.; Dong, Y.; Heien, M. L.; Ewing, A. G., Only a Fraction of Quantal Content is Released During Exocytosis as Revealed by Electrochemical Cytometry of Secretory Vesicles. *ACS chemical neuroscience* **2010,** *1* (3), 234-245.
124. Piyankarage, S. C.; Featherstone, D. E.; Shippy, S. A., Nanoliter hemolymph sampling and analysis of individual adult Drosophila melanogaster. *Analytical chemistry* **2012,** *84* (10), 4460-6.
125. Nandi, P.; Lunte, S. M., Recent Trends in Microdialysis Sampling Integrated with Conventional and Microanalytical Systems for Monitoring Biological Events: A Review. *Analytica Chimica Acta* **2009,** *651* (1), 1-14.
126. Soga, T.; Ohashi, Y.; Ueno, Y.; Naraoka, H.; Tomita, M.; Nishioka, T., Quantitative Metabolome Analysis Using Capillary Electrophoresis Mass Spectrometry. *Journal of proteome research* **2003,** *2*, 488-494.
127. Rejtar, T.; Hu, P.; Juhasz, P.; Campbell, J. M.; Vestal, M. L.; Preisler, J.; Karger, B. L., Off-Line Coupling of High-Resolution Capillary Electrophoresis to MALDI-TOF and TOF/TOF MS. *Journal of proteome research* **202,** *1*, 171-179.
128. Taylor, H. E., Figures of Merit. In *Inductively Coupled Plasma-Mass Spectrometry*, Taylor, H. E., Ed. Academic Press: San Diego, 2001; pp 149-160.
129. Profrock, D.; Leonhard, P.; Prange, A., Determination of sulfur and selected trace elements in metallothionein-like proteins using capillary electrophoresis hyphenated to inductively coupled plasma mass spectrometry with an octopole reaction cell. *Analytical and bioanalytical chemistry* **2003,** *377* (1), 132-9.
130. Fleurbaaij, F.; Heemskerk, A. A.; Russcher, A.; Klychnikov, O. I.; Deelder, A. M.; Mayboroda, O. A.; Kuijper, E. J.; van Leeuwen, H. C.; Hensbergen, P. J., Capillary-electrophoresis mass spectrometry for the detection of carbapenemases in (multi-)drug-resistant Gram-negative bacteria. *Analytical chemistry* **2014,** *86* (18), 9154-61.
131. Hoffmann, d. E.; Stroobant, V., Ion Source. In *Mass Spectrometry: Principles and Applications*, 3 ed.; John Wiley & Sons Ltd.: England, 2007.
132. Sigmund, P., Sputtering by Ion Bombardment: Theoretical Concepts. In *Sputtering by Particle Bombardment I*, Behrisch, R., Ed. Springer Berlin Heidelberg: 1981.
133. Sigmund, P., Theory of Sputtering. I. Sputtering Yield of Amorphous and Polycrystalline Targets. *Physical Review* **1969,** *184* (2), 383-416.
134. Vickerman, J. C.; Briggs, D., *ToF-SIMS: Surface Analysis by Mass Spectrometry*. IM Pulication: 2013.

135. Postawa, Z.; Czerwinski, B.; Winograd, N.; Garrison, B. J., Microscopic Insights into the Sputtering of Thin Organic Films on Ag{111} Induced by C60 and Ga Bombardment. *The Journal of Physical Chemistry B* **2005,** *109*, 11973-11979.
136. Rzeznik, L.; Czerwinski, B.; Garrison, B. J.; Winograd, N.; Postawa, Z., Molecular dynamics simulations of sputtering of organic overlayers by slow, large clusters. *Applied Surface Science* **2008,** *255* (4), 841-843.
137. Fletcher, J. S.; Conlan, X. A.; Jones, E. A.; Biddulph, G.; Lockyer, N. P.; Vickerman, J. C., TOF-SIMS Analysis Using C60. Effect of Impact Energy on Yield and Damage. *Analytical chemistry* **2006,** *78*, 1827-1831.
138. Gnaser, H., Cs Incorporation in Semiconductors During Low-energy Bombardment: A Dynamic Computer Simulation Study. *Nuclear Instruments and Methods in Physics Research Section B: Beam Interactions with Materials and Atoms* **2009,** *267* (17), 2808-2816.
139. Kozole, J.; Willingham, D.; Winograd, N., The Effect of Incident Angle on The C(60) Bombardment of Molecular Solids. *Applied Surface Science* **2008,** *255* (14), 1068-1070.
140. Czerwinski, B.; Rzeznik, L.; Paruch, R.; Garrison, B. J.; Postawa, Z., Effect of impact angle and projectile size on sputtering efficiency of solid benzene investigated by molecular dynamics simulations. *Nuclear Instruments and Methods in Physics Research Section B: Beam Interactions with Materials and Atoms* **2011,** *269* (14), 1578-1581.
141. Bozack, M. J.; Swanson, L. W.; Bell, A. E., Materials Considerations in Liquid Metal Ion Source Development. *Le Journal de Physique Colloques* **1986,** *47* (C2), C2-95-C2-100.
142. Delcorte, A.; Garrison, B. J., Sputtering Polymers with Buckminsterfullerene Projectiles: A Coarse-Grain Molecular Dynamics Study. *The Journal of Physical Chemistry C* **2007,** *111*, 15312-15324.
143. Appelhans, A. D.; Delmore, J. E., Comparison of Polyatomic and Atomic Primary Beams for Secondary Ion Mass Spectrometry of Organics. *Analytical chemistry* **1989,** *61*, 1087-1093.
144. Kollmer, F., Cluster primary ion bombardment of organic materials. *Applied Surface Science* **2004,** *231-232*, 153-158.
145. Touboul, D.; Kollmer, F.; Niehuis, E.; Brunelle, A.; Laprevote, O., Improvement of biological time-of-flight-secondary ion mass spectrometry imaging with a bismuth cluster ion source. *Journal of the American Society for Mass Spectrometry* **2005,** *16* (10), 1608-18.
146. Fletcher, J. S.; Lockyer, N. P.; Vickerman, J. C., C60, Buckminsterfullerene: its impact on biological ToF-SIMS analysis. *Surface and Interface Analysis* **2006,** *38*, 1393-1400.
147. Schiffer, Z. J.; Kennedy, P. E.; Postawa, Z.; Garrison, B. J., Molecular Dynamics Simulations Elucidate the Synergy of C60and Low-Energy Ar Cobombardment for Molecular Depth Profiling. *The Journal of Physical Chemistry Letters* **2011,** *2* (20), 2635-2638.
148. Ninomiya, S.; Nakata, Y.; Honda, Y.; Ichiki, K.; Seki, T.; Aoki, T.; Matsuo, J., A fragment-free ionization technique for organic mass spectrometry with large Ar cluster ions. *Applied Surface Science* **2008,** *255* (4), 1588-1590.
149. Rabbani, S. N.; Barber, A.; Fletcher, J. S.; Lockyer, N. P.; Vickerman, J. C., Enhancing secondary ion yields in time of flight-secondary ion mass spectrometry using water cluster primary beams. *Analytical chemistry* **2013,** *85* (12), 5654-8.
150. Angerer, T. B.; Blenkinsopp, P.; Fletcher, J. S., High Energy Gas Cluster Ions For Organic and Biological Analysis By Time-of-Flight Secondary Ion Mass Spectrometry. *International Journal of Mass Spectrometry* **2014**.
151. Rudenauer, F. G., Spatially Multidimensional Secondary Ion Mass Spectrometry Analysis. *Analytica Chimica Acta* **1994,** *297*, 197-230.
152. McDonnell, L. A.; Heeren, R. M., Imaging mass spectrometry. *Mass spectrometry reviews* **2007,** *26* (4), 606-43.

153. Steinhauser, M. L.; Lechene, C. P., Quantitative imaging of subcellular metabolism with stable isotopes and multi-isotope imaging mass spectrometry. *Seminars in cell & developmental biology* **2013,** *24* (8-9), 661-7.
154. Fletcher, J. S.; Vickerman, J. C., A New SIMS Paradigm for 2D and 3D Molecular Imaging of Bio-systems. *Analytical and bioanalytical chemistry* **2010,** *396* (1), 85-104.
155. Angerer, T. B.; Fletcher, J. S., 3D Imaging of TiO2nanoparticle accumulation inTetrahymena pyriformis. *Surface and Interface Analysis* **2014**, n/a-n/a.
156. Fletcher, J. F.; Rabbani, S.; Henderson, A.; Blenkinsopp, P.; Thompson, S. P.; Lockyer, n. P.; Vickerman, J. C., A New Dynamic in Mass Spectral Imaging of Single Biological Cells. *Analytical chemistry* **2008,** *80*, 9058–9064.
157. Kurczy, M. E.; Piehowski, P. D.; Parry, S. A.; Jiang, M.; Chen, G.; Ewing, A. G.; Winograd, N., Which is more important in bioimaging SIMS experiments-The sample preparation or the nature of the projectile? *Applied Surface Science* **2008,** *255* (4), 1298-1304.
158. Cannon, D. M.; Michaeleen, J.; Pacholski, L.; Winograd, N.; Ewing, A. E., Molecule Specific Imaging of Freeze-Fractured, Frozen-Hydrated Model Membrane Systems Using Mass Spectrometry. *Journal of the American Chemical Society* **2000,** *122*, 603-610.
159. Passarelli, M. K.; Winograd, N., Lipid imaging with time-of-flight secondary ion mass spectrometry (ToF-SIMS). *Biochimica et biophysica acta* **2011,** *1811* (11), 976-90.
160. Lanekoff, I.; Phan, N. T.; Van Bell, C. T.; Winograd, N.; Sjovall, P.; Ewing, A. G., Mass spectrometry imaging of freeze-dried membrane phospholipids of dividing Tetrahymena pyriformis. *Surface and Interface Analysis* **2013,** *45* (1), 211-214.
161. Roddy, T. P.; Cannon, D. M.; Ostrowski, S. G.; Ewing, A. G.; Winograd, N., Proton Transfer in Time-of-Flight Secondary Ion Mass Spectrometry Studies of Frozen-Hydrated Dipalmitoylphosphatidylcholine. *Analytical chemistry* **2003,** *75*, 4087-4094.
162. Bich, C.; Vianello, S.; Guérineau, V.; Touboul, D.; De La Porte, S.; Brunelle, A., Compatibility between TOF-SIMS lipid imaging and histological staining on a rat brain section. *Surface and Interface Analysis* **2013,** *45* (1), 260-263.
163. Hanrieder, J.; Malmberg, P.; Lindberg, O. R.; Fletcher, J. S.; Ewing, A. G., Time-of-flight secondary ion mass spectrometry based molecular histology of human spinal cord tissue and motor neurons. *Analytical chemistry* **2013,** *85* (18), 8741-8.
164. Jerigova, M.; Biro, C.; Kirchnerova, J.; Chorvatova, A.; Chorvat, D., Jr.; Lorenc, D.; Velic, D., Chemical Imaging of Cardiac Cell and Tissue by Using Secondary Ion Mass Spectrometry. *Molecular imaging and biology* **2011,** *13* (6), 1067-76.
165. Brulet, M.; Seyer, A.; Edelman, A.; Brunelle, A.; Fritsch, J.; Ollero, M.; Laprévote, O., Lipid Mapping of Colonic Mucosa by Cluster TOF-SIMS Imaging and Multivariate Analysis in cftr Knockout Mice. *Journal of lipid research* **2010,** *51* (10), 3034-3045.
166. Kurczy, M. E.; Piehowski, P. D.; Van Bell, C. T.; Heien, M. L.; Winograd, N.; Ewing, A. G., Mass spectrometry imaging of mating Tetrahymena show that changes in cell morphology regulate lipid domain formation. *Proceedings of the National Academy of Sciences of the United States of America* **2010,** *107* (7), 2751-6.
167. Fletcher, J. S.; Rabbani, S.; Henderson, A.; Lockyer, N. P.; Vickerman, J. C., Three-dimensional mass spectral imaging of HeLa-M cells-sample preparation, data interpretation and visualisation. *Rapid Communications in Mass Spectrometry* **2011,** *25* (7), 925-932.
168. Brison, J.; Robinson, M. A.; Benoit, D. S.; Muramoto, S.; Stayton, P. S.; Castner, D. G., TOF-SIMS 3D imaging of native and non-native species within HeLa cells. *Analytical chemistry* **2013,** *85* (22), 10869-10877.
169. Sjovall, P.; Greve, T. M.; Clausen, S. K.; Moller, K.; Eirefelt, S.; Johansson, B.; Nielsen, K. T., Imaging of distribution of topically applied drug molecules in mouse skin by combination of time-of-flight secondary ion mass spectrometry and scanning electron microscopy. *Analytical chemistry* **2014,** *86* (7), 3443-52.

170. Steinhauser, M. L.; Bailey, A. P.; Senyo, S. E.; Guillermier, C.; Perlstein, T. S.; Gould, A. P.; Lee, R. T.; Lechene, C. P., Multi-isotope Imaging Mass Spectrometry Quantifies Stem Cell Division and Metabolism. *Nature* **2012,** *481* (7382), 516-9.
171. Zhang, D. S.; Piazza, V.; Perrin, B. J.; Rzadzinska, A. K.; Poczatek, J. C.; Wang, M.; Prosser, H. M.; Ervasti, J. M.; Corey, D. P.; Lechene, C. P., Multi-isotope imaging mass spectrometry reveals slow protein turnover in hair-cell stereocilia. *Nature* **2012,** *481* (7382), 520-4.
172. Legin, A. A.; Schintlmeister, A.; Jakupec, M. A.; Galanski, M.; Lichtscheidl, I.; Wagner, M.; Keppler, B. K., NanoSIMS combined with fluorescence microscopy as a tool for subcellular imaging of isotopically labeled platinum-based anticancer drugs. *Chemical Science* **2014,** *5* (8), 3135.
173. Cillero-Pastor, B.; Eijkel, G.; Kiss, A.; Blanco, F. J.; Heeren, R. M., Time-of-flight secondary ion mass spectrometry-based molecular distribution distinguishing healthy and osteoarthritic human cartilage. *Analytical chemistry* **2012,** *84* (21), 8909-16.
174. Tian, H.; Wucher, A.; Winograd, N., Molecular imaging of biological tissue using gas cluster ions. *Surface and Interface Analysis* **2014,** *46* (1), 115-117.
175. Karas, M.; Bachmann, D.; Bahr, U.; Hillenkamp, F., Matrix Assisted Ultraviolet Laser Desorption of Non Volatile Compounds *International Journal of Mass Spectrometry and Ion Processes* **1987,** *78*, 53-68.
176. Jurchen, J. C.; Rubakhin, S. S.; Sweedler, J. V., MALDI-MS imaging of features smaller than the size of the laser beam. *Journal of the American Society for Mass Spectrometry* **2005,** *16* (10), 1654-1659.
177. Luxembourg, S. L.; Mize, T. H.; McDonnell, L. A.; Heeren, R. M. A., High-Spatial Resolution Mass Spectrometric Imaging of Peptide and Protein Distributions on a Surface. *Analytical chemistry* **2004,** *76*, 5339-5344.
178. Zavalin, A.; Todd, E. M.; Rawhouser, P. D.; Yang, J.; Norris, J. L.; Caprioli, R. M., Direct imaging of single cells and tissue at sub-cellular spatial resolution using transmission geometry MALDI MS. *Journal of Mass Spectrometry* **2012,** *47* (11), 1473-81.
179. Guenther, S.; Koestler, M.; Schulz, O.; Spengler, B., Laser spot size and laser power dependence of ion formation in high resolution MALDI imaging. *International Journal of Mass Spectrometry* **2010,** *294* (1), 7-15.
180. Schwartz, S. A.; Reyzer, M. L.; Caprioli, R. M., Direct tissue analysis using matrix-assisted laser desorption/ionization mass spectrometry: practical aspects of sample preparation. *Journal of Mass Spectrometry* **2003,** *38* (7), 699-708.
181. Chughtai, K.; Heeren, R. M., Mass spectrometric imaging for biomedical tissue analysis. *Chemical Review* **2010,** *110* (5), 3237-77.
182. Vermillion-Salsbury, R. L.; Hercules, D. M., 9-Aminoacridine As a Matrix for Negative Mode Matrix-assisted Laser Desorption/ionization. *Rapid Communication Mass Spectrometry* **2002,** *16*, 1575-1581.
183. Zaima, N.; Hayasaka, T.; Goto-Inoue, N.; Setou, M., Matrix-assisted laser desorption/ionization imaging mass spectrometry. *International journal of molecular sciences* **2010,** *11* (12), 5040-55.
184. Thomas, A.; Chaurand, P., Advances in tissue section preparation for MALDI imaging MS. *Bianalysis* **2014,** *6* (7), 967-982.
185. Yang, J.; Caprioli, R. M., Matrix sublimation/recrystallization for imaging proteins by mass spectrometry at high spatial resolution. *Analytical chemistry* **2011,** *83* (14), 5728-5734.
186. Poetsch, A.; Schlüsener, D.; Florizone, C.; Eltis, L.; Menzel, C.; Rögner, M.; Steinert, K.; Roth, U., Improved Identification of Membrane Proteins by MALDI-TOF MS/MS Using Vacuum Sublimated Matrix Spots on an Ultraphobic Chip Surface. *Journal of Biomolecular Techniques* **2008,** *19* (2), 129–138.

187. Chiang, C. K.; Chen, W. T.; Chang, H. T., Nanoparticle-based mass spectrometry for the analysis of biomolecules. *Chemical Society reviews* **2011,** *40* (3), 1269-1281.
188. McLean, J. A.; Stumpo, K. A.; Russell, D. H., Size-Selected (2-10 nm) Gold Nanoparticles for Matrix Assisted Laser Desorption Ionization of Peptides. *Journal of the American Chemical Society Communications* **2005,** *127*, 5304-5305.
189. Goto-Inoue, N.; Hayasaka, T.; Zaima, N.; Kashiwagi, Y.; Yamamoto, M.; Nakamoto, M.; Setou, M., The detection of glycosphingolipids in brain tissue sections by imaging mass spectrometry using gold nanoparticles. *Journal of the American Society for Mass Spectrometry* **2010,** *21* (11), 1940-3.
190. Su, C. L.; Tseng, W. L., Gold Nanoparticles as Assisted Matrix for Determining Neutral Small Carbohydrates through Laser Desorption/Ionization Time-of-Flight Mass Spectrometry. *Analytical chemistry* **2007,** *79*, 1626-1633.
191. Son, J.; Lee, G.; Cha, S., Direct analysis of triacylglycerols from crude lipid mixtures by gold nanoparticle-assisted laser desorption/ionization mass spectrometry. *Journal of the American Society for Mass Spectrometry* **2014,** *25* (5), 891-4.
192. Chiang, C. K.; Chiang, N. C.; Lin, Z. H.; Lan, G. Y.; Lin, Y. W.; Chang, H. T., Nanomaterial-based Surface-assisted Laser Desorption/ionization Mass Spectrometry of Peptides and Proteins. *Journal of the American Society for Mass Spectrometry* **2010,** *21* (7), 1204-7.
193. Tanaka, K.; Waki, H.; Ido, Y.; Akita, S.; Yoshida, Y.; Yoshida, T., Protein and Polymer Analyses up to mlz 100 000 by Laser Ionization Time-of-flight Mass Spectrometry. *Rapid Communication Mass Spectrometry* **1988,** *2* (8), 151-153.